**NTNU – Trondheim**
Norwegian University of
Science and Technology

# Investigation of a Concept for Simultaneous Reliquefaction of Boil-Off-Gas and Vaporization of LNG for Marine Atmospheric LNG Fuel Tanks

Arrigo Battistelli

Master of Energy and Environmental Engineering
Submission date: June 2014
Supervisor: Petter Nekså, EPT

Norwegian University of Science and Technology
Department of Energy and Process Engineering

# Abstract

The aim of this thesis is to design and optimize a heat pump process to reliquefy Boil-Off-Gas from Liquefied Natural Gas (LNG) cryogenic tanks, and simulataneously vaporize LNG at high pressure. The process is meant for use onboard LNG fuelled ship different from LNG carriers, equipped with LNG fuel tanks at atmospheric pressure and 2-strokes engines with high pressure gas injection, which is considered the most efficient propulsion arrangement for medium-large vessels.

The study is based on a patented concept from the norwegian company LNG New Technlogies, within the thesis this concept is evolved to a more complex process layout, its distinctive features are low temperature suction of the heat pump refrigerant compressor, absence of heat discharge to the environment and condensation of the Boil-Off-Gas via recirculation of subcooled LNG. Four different operating scenarios of the process are simulated with the commercial software HYSYS® , the results of the simulations are presented in the form of case studies, sensitivity analyses, thermodynamic diagrams and tables, and analized in detail. A number of modifications to the selected layout are evaluated, e.g. Boil-Off-Gas feed to the Auxiliary engine and compressor intercooling. Based on the simulation results a preliminary selection of the process equipment is outlined, with focus on the refrigerant compressor.

The results prove that the proposed heat pump process can effectively refrigerate the LNG tank if the ship is operating in the normal mode or at half of the main engine load, however at lower engine loads, especially when the main engine is shut down, the system can not produce the required refrigeration effect. In this scenario the excess Boil-Off-Gas would be fed to the Auxiliary engines, or in the worst case burnt in Gas Combustion Units. The heat pump efficiency for the normal operation is 2-3 times higher than for commercial on-board Boil-Off-Gas reliquefaction processes, but the maximum reliquefaction capacity is intrinsically lower. The operating parameters of the compressor suggest the use of a reciprocating oil-free compressor with cryogenic material specifications, this is considered the most non-conventional and costly unit of the process.

# Acknowledgments

This Master thesis was written in the spring of 2014 at the Energy and Process Engineering faculty of the Norwegian University of Science and Technology NTNU during the second year of a double degree program (TIME) with the italian university Politecnico di Milano.
I would like to thank first my academic supervisor Petter Nekså for his valuable assistance and experienced mentoring throughout the course of the thesis, and my research advisors Kjell Kolsaker and Dag Stenersen for their great availability and their constructive criticism at every meeting. Special thanks go to the process engineer Jørn Magnus Jonas of the company LNG New Technologies that inspired the concept of the thesis and closely followed its development contributing with his precious industrial knowledge, as well as his colleagues Andreas Norberg and Kjetil Sjølie Strand for their contribution and for hosting me in the company's office in a pleasant and friendly enviroment.
I would also like to thank the professor Paolo Chiesa of Politecnico di Milano for accepting the role of co-supervisor and monitoring the status of the work. The NTNU and Sintef researchers Rahul Anantharaman, Lars Nord and Rajesh Kempegowda helped me and other students with process simulations by offering voluntary software training lectures. The master student Joseph DiRenzo helped me in the initial stage of my work by sharing his rich literature collection on the topic.
Finally I am grateful to my family ad friends for their moral and material support, in particular to Alfredo and Alberto Battistelli for reading parts of my thesis and to Tina Bautovic for her lovely care.

# Contents

# Chapter 1

# Introduction

Liquefied Natural Gas (LNG) is becoming a competitive marine fuel due to the introduction of stricter environmental standards for marine emissions, and the market for LNG fuelled ships is expected to grow from local short-sea market to deep-sea shipping on a global scale. The recent orders for large LNG fuelled ships reveal the existence of a growing market and the need for more advanced and efficient technological solutions for LNG fuel systems, propulsion systems and handling of LNG Boil-Off-Gas (BOG) generated from heat transfer through the cryogenic tank insulation (heat leak).
The technical literature and the market players seem to have identified the most efficient design for large LNG fuelled ships in the combination of atmospheric fuel tanks and 2-strokes low speed gas diesel engines with gas injection at high pressure (ME-GI). Both systems are established and commercially available technologies, however their combination poses the practical challenge of BOG handling that is still not fully resolved, due to the high pressure required by the ME-GI engine.

Many manufacturers and technology providers are currently developing high pressure Fuel Gas Supply System arrangements, but it is still not clear how these will provide a reliable and efficient solution to the BOG issue. The Norwegian company LNG New Technologies patented the concept for a heat pump system that should extracts heat from the cryogenic tanks and discharge it to the vaporizing high pressure LNG directed to the ME-GI engine, thereby controlling the BOG generation in the tank.

The purpose of this thesis is to test different process layouts and operation modes of the above mentioned heat pump concept, to assess and optimize its performance by means of computer simulations, to suggest an optimal configuration and indicate what kind of process equipment would be needed.

The background to the work is described in the 2nd chapter of the thesis, which includes an overview of the LNG fuelled ship market, descriptions of the key technologies involved, namely gas engines, cryogenic tanks, BOG handling methods such as reliquefaction cycles and finally the state of the art of fuel supply solutions for ME-GI engines applications. Chapter 3 is dedicated to the description of the proposed heat pump process in its layout details, and to the definition of a specific scenario as a basis for the calculations. Chapter 4 presents the computer simulations executed with the commercial software HYSYS®, starting from the model structure and inputs to the simulation results presentation and discussion. Finally, chapter 5 outlines a preliminary selection of process equipment on the basis of the simulation results, with particular emphasis on the heat pump refrigerant compressor.

# Chapter 2

# Background

## 2.1 LNG as ship fuel

### 2.1.1 Motivations for LNG as a ship fuel

LNG has been used as a fuel for propulsion on LNG Carriers (LNGC) since 1964, after the introduction of the first LNG fuelled vessel (non-LNGC) in 2000 the last decade has seen LNG becoming a competitive fuel for marine transport, mainly due to the introduction of restrictions in the international environmental regulations on marine emissions that favour LNG compared to more conventional and polluting marine fuels.
LNG marine projects certainly demand a higher investment cost than conventional projects, related to the tank and fuel gas system, but some savings can be expected on fuel cost according to the fuel pricing scenarios [1, 2], however as fuel price prediction is critical in a long term project the savings associated with emission regulations are currently the main drive for LNG projects in the shipping industry.

The most influential international regulation is the "MARPOL 73/78", outlined by the International Maritime Organization (IMO) in a diplomatic conference in 1973 and expanded since then with six annexes [2, 3]. The last MARPOL Annex VI sets limits for $NO_x$ and $SO_x$ emissions from exaust gas, differentiating from open sea and selected coastal areas denominated Emission Control Areas (ECA). Figure 2.1 illustrates how the regulations are getting more stringent in the decade 2010-2020, especially in the ECAs. The current global status of the ECAs is illustrated in Figure 2.2.

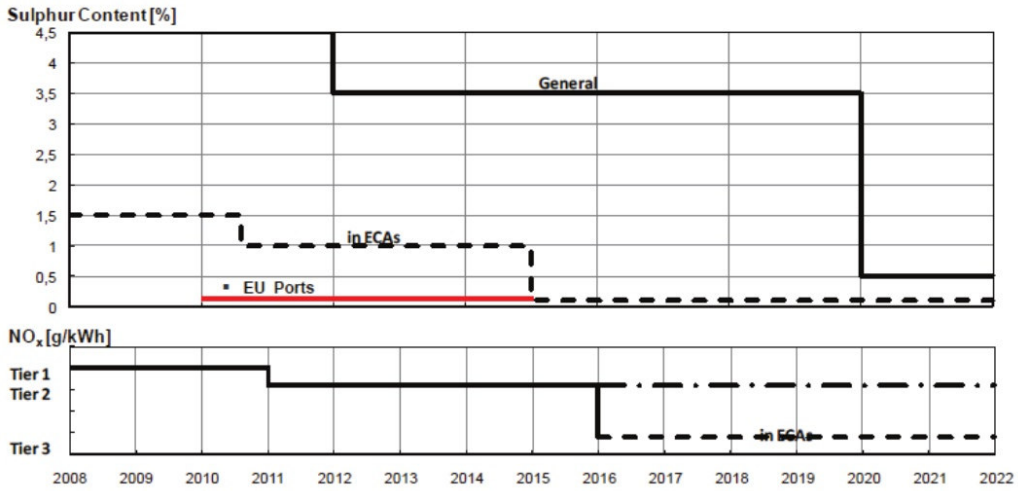


Figure 2.1: Implementation schedule for Revised MARPOL Annex VI [4, p.2]

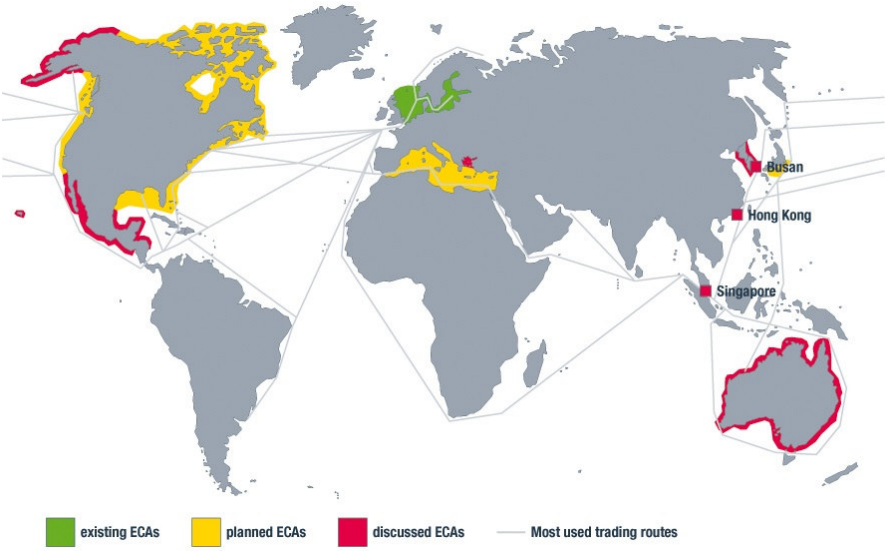


Figure 2.2: Emission Control Areas [5]

In this context LNG is seen as a viable alternative to the conventional more polluting fuels such as Marine Diesel Oil (MDO) and Heavy Fuel Oli (HFO), for an increasing number of shipping segments.

### 2.1.2 Ship propulsion alternatives

To date ship propulsion is largely dominated by diesel engines that replaced steam turbines in the course of the 20$^{th}$ century, less frequently ships are driven by gas turbines, almost only LNG Carriers are still driven by steam turbines due to the flexibility in the fuel mix.

Diesel engines can be classified by the shaft speed: low, medium or high (the latter being limited to very small vessels), or by the number of strokes: 2-strokes (always low speed) or 4-strokes (usually medium speed) [6]. Figure 2.3 relates the thermal efficiency of commercial ship propulsion technologies with the installed power, it results that diesel low speed engines are the most efficient, followed by medium speed engines, gas turbine cycles and lastly steam turbines.

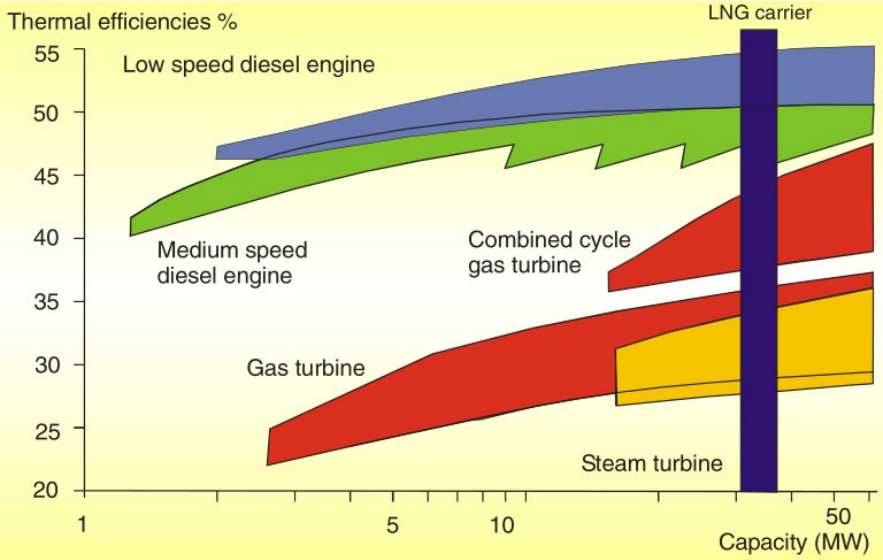


Figure 2.3: Typical thermal efficiency of prime movers [7, p.244]

All of the options listed above are suitable for LNG Carriers propulsion, some of them also for LNG fuelled ships (non-LNGC). Figure 2.4 has been created to offer a more detailed overview of the main propulsion alternatives for LNG fuelled ships and LNG Carriers, mapping the various technology by type of fuel used. The three vertical boxes in the background indicate the possible fuel modes of the machine, for instance steam turbines cover the three fuel modes meaning that the steam boiler can burn either only natural gas, or a mixture of gas and fuel oil, or only fuel oil (MDO/HFO); low speed engines on the other hand cover only the second two modes since they can not run on pure natural gas and require at least a minimum amount of pilot fuel oil.

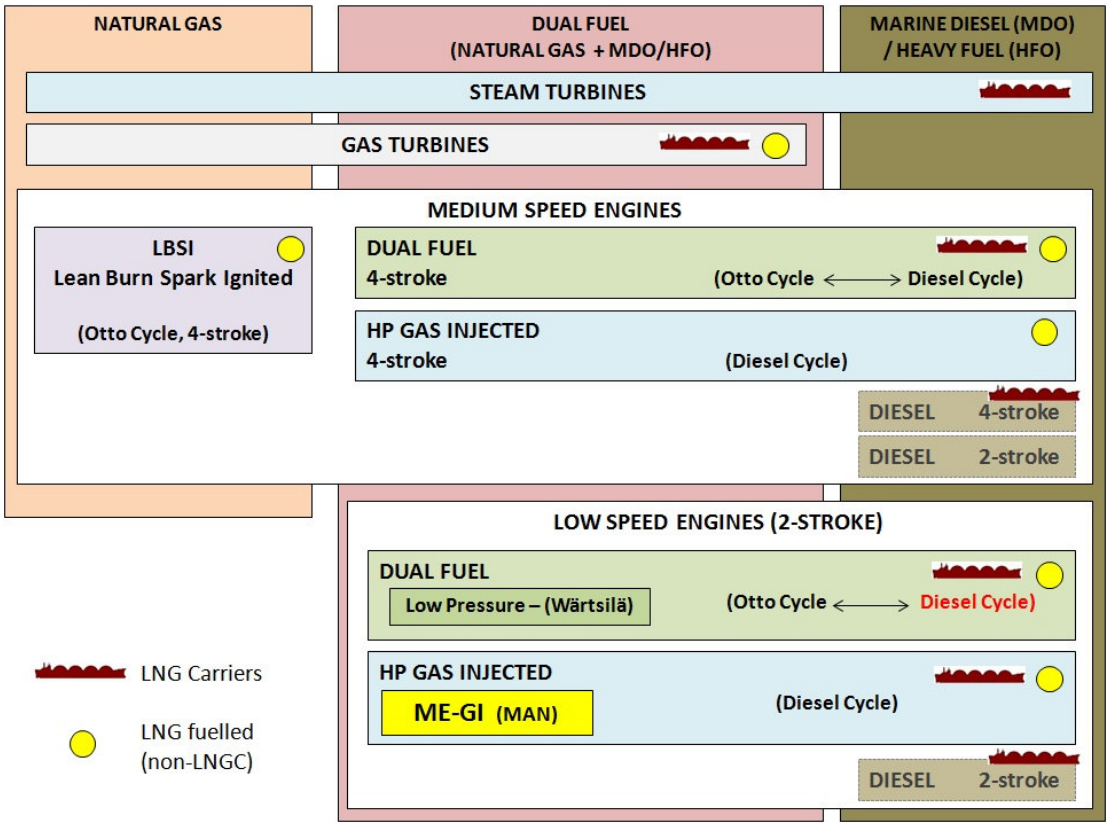


Figure 2.4: Ship propulsion alternatives for Natural Gas fuelled ships and Carriers sorted by type of fuel [8, 7, 9, 10, 4, 6, 11, 12, 13, 14]

The most attractive propulsion alternatives for LNG fuelled ships are reciprocating engines working in dual fuel mode, most of these machine can run on natural gas with a variable amount of fuel oil and easily switch to fuel oil mode if required. In the current state of the art of small LNG fuelled vessels mainly 4-strokes medium speed engines are employed of the types Dual Fuel and LBSI. The shaft speed of these type of engines is too high for the propeller optimum operation, therefore the power transmission normally goes through a gear or through electric generators (Figures 2.6 and 2.5).

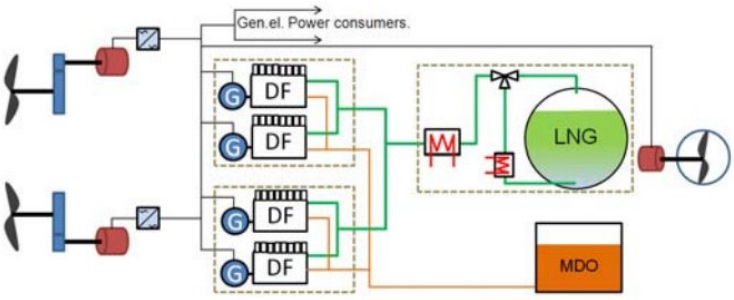


Figure 2.5: Platform supply vessel, Dual fuel Diesel-Electric propulsion [8]

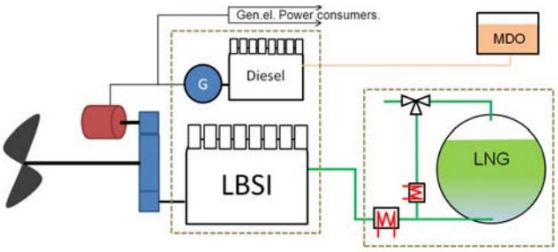


Figure 2.6: Ro-Ro ship, Pure LNG operation, Diesel-Mechanical propulsion, with Diesel backup engine [8]

In addition to the superior thermal efficiency, another advantage of low speed engines is that they can match the optimum propeller speed and be directly coupled to the propeller without a reduction gear and without the need for electric generators [15]. Among those the High Pressure Gas Injected engines have high efficiency at all loads thanks to the thermal properties of the Diesel cycle [8], MAN Diesel & Turbo is the world leading producer of this type of machines that are gaining popularity in the market of medium-large gas fuelled ships under the name of "ME-GI" engines.
The main disadvantage of ME-GI engines is that the high pressure required for gas injection introduces complications and safety concerns in the design of the Fuel Gas Supply System, to overcome this the competitor company Wartsila offers a low pressure dual fuel 2-stroke solution, renouncing to the properties of the Diesel cycle in favor of the Otto cycle.

The present thesis aims to develop a system specifically fitted to a ME-GI engine propelled vessel.

### 2.1.3 LNG fuelled ships

As of today a number of different categories of ships are being built or designed for LNG propulsion, the primary distinction for LNG fuelled ships divides them in two groups:

- LNG Carriers (LNGC);
- LNG fuelled ships (other than LNG Carriers).

The first ships to use LNG as a fuel were LNG Carriers, since 1964. All of the early LNG Carriers were driven by steam turbines, fuelled by marine Heavy Fuel Oil (HFO) and LNG BOG from the cargo tanks [16], in the 1980's started the development of more efficient internal combustion engines systems for LNGC [8, p.2], in 2006 Slow Speed Diesel engines with BOG reliquefaction systems entered the market, together with Dual Fuel engines and electric propulsion [16, p.3].

In 2000 the first LNG fuelled ship (non-LNGC) started sailing in the norwegian coast [17], since then a number of small ferries and vessels for short-sea routes came into service mostly in Norway [3, p.3] [8, p.2]. Most of the early LNG fuelled vessels were car/passenger ferries, Platform Support Vessels (PSV) and similar short-sea vessels, in the recent years also tankers, cargo vessels and tug boats went into operations.
As of today the last confirmed orders include chemical tankers, cargo vessels as well as Ro-Ro vessels, bulk carriers and container ships [18]. The motivation to power these types of ships with LNG could be related to maximise the savings in ECA zones, as a matter of fact ship

traffic analyses indicate that small and medium Ro-Ro vessels, tankers, bulk carriers and container vessels spend considerable time sailing in ECA zones [3, p.5], [19, p.26], . In particular it can be observed that fuel cost accounts for the highest share of the running cost for container vessels among the main shipping segments [20, 21] and the industry is showing a particular interest in developing large LNG fuelled container vessels for international shipping routes [1, 22].

For the scope of this thesis, the most relevant difference between LNG Carriers and other LNG fuelled ships is the ratio between the tank size and the power of the propulsion system. This parameter is important when it comes to analyzing and comparing BOG handling alternatives, as the tank size can be considered proportional to the heat leak in the tank and to the BOG flowrate, while the propulsion power is proportional to the fuel consumption of LNG or BOG. It can be observed in Figure 2.7 that the ratio between the LNG tank volume and the installed main engine power is much higher for LNGC, due to the fact that the cargo volume in a LNGC contributes to the total LNG volume and BOG generation.

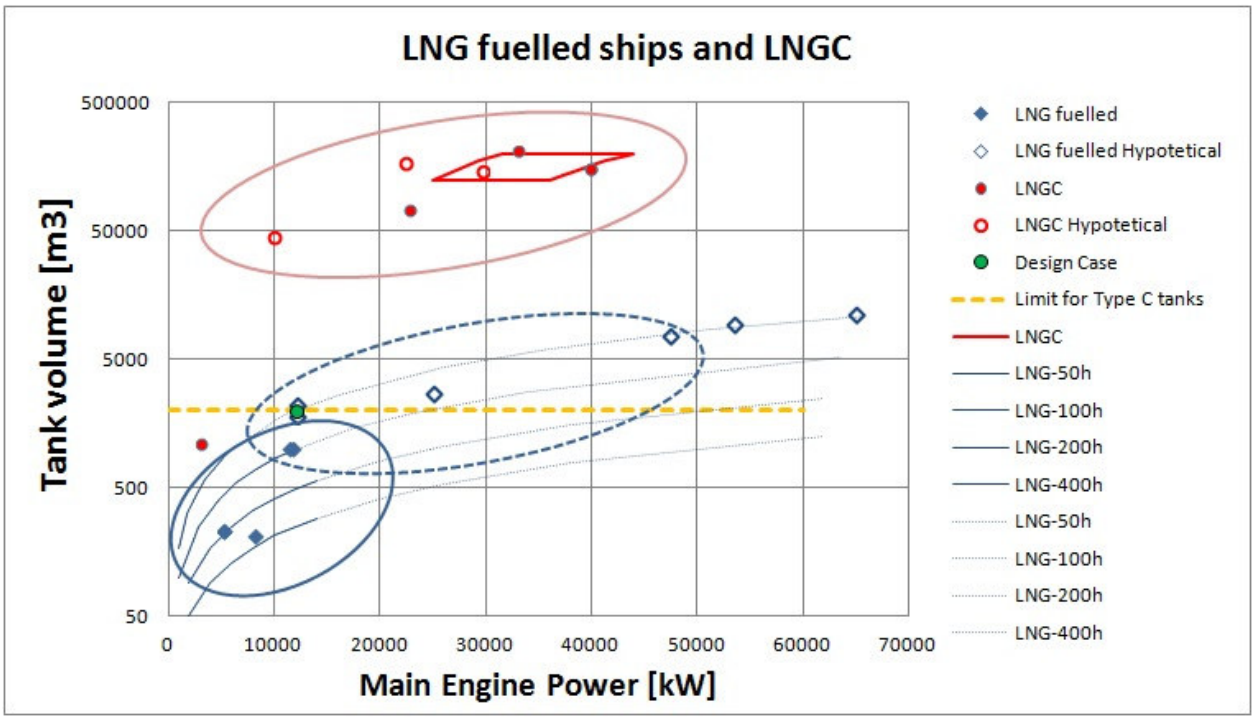


Figure 2.7: Comparison between LNGC and other LNG fuelled vessels, the blue lines indicate constant ratio between the LNG tank volume and the main engine power, [23, p.9], [24, 25, 26]

## 2.2 Tank types

LNG on ships is stored in cryogenic insulated tanks at the temperature of -160 to -162℃. LNG marine tanks have been classified by the IMO in three categories:

- Type A and Membrane tanks
  characterized by complete secondary barrier;
- Type B tanks
  characterized by partial secondary barrier, they typically have a self-supporting structure;
- Type C tanks
  characterized by absence of secondary barrier, they are in most cases smaller pressurized tanks.

The first LNG tanks for ships were developed for the cargo on LNG Carriers. Since the LNG fuel on LNGCs is taken directly from the cargo tanks a dedicated LNG fuel tank is not needed, however with the introduction of LNG fuelled ships also dedicated LNG fuel tanks had to be developed.
Currently type C pressurized tanks are the only used for the small existing LNG fuelled ships (non-LNGC) [18]. The advantage of this type of tank is that they can operate at a pressure up to 8 barg, this allows the gas to accumulate in the tank atmosphere for some time before this pressure is reached. The main disadvantages of Type C tanks are the large amount of deadspace and the tank capacity limits (currently in the order of 500 $m^3$) [27, p.13].

It is expected that other types of tanks than Type C will be taken in consideration for larger volumes of LNG fuel [27], for example Germanischer Lloyds estimates that for container ships with LNG volumes larger than 2000-3000 $m^3$ large type B prismatic tanks would be preferable to small Type C tanks due to lower specific costs [1, p.9]. If Type A and B are utilized as fuel tanks in LNG fuelled ships the maximum pressure of about 1.7 bara will provide very little buffer capacity for containing the BOG generated by the heat leak, as a consequence a different BOG handling approach will be needed.

## 2.3 BOG handling

LNG Boil Off Gas (BOG) is generated in any type of LNG tank due to the heat flow from the enviroment to the cryogenic tank, this flammable gas rich in Nitrogen and Methane accumulates in the tank atmosphere above the LNG liquid level at a temperature usually higher than the bulk liquid, causing the tank pressure to steadily increase in time. The generation and accumulation

of BOG must be controlled to make sure that the tank pressure stays within the limits, in particular a too high pressure could lead to damages to the tank structure.
Depending on the type of tank and the application different BOG handling methods are used alone or in combinations:

- BOG containment in pressurized Type C tanks;
- BOG "flaring" in Gas Combustion Units (GCU);
- BOG as a fuel for ship propulsion;
- BOG as a fuel for Auxiliary engines;
- BOG reliquefaction;
- BOG venting (as a last resource).

As discussed BOG containment is currently the only BOG handling method for LNG fuelled ships non-LNGC, this is an efficient and simple method but its viability is limited to modest tank size for short-sea shipping with frequent bunkering.
Gas Combustion Units are used on LNG Carriers to dispose of the excess BOG when it exceeds the fuel consumption or the reliquefaction capacity, in these reactors the gas is burned and the exhaust vented to the atmosphere, this system is the on board equivalent of flaring.
BOG was used in the first LNGCs as a fuel for propulsion and burned with HFO in steam turbine boilers, recently more advanced and efficient propulsion system have been developed for LNGC where the BOG is burned alone or in a mixture with other marine fuels for propelling the ship. Figure 2.8) collects the technologies for LNGC propulsion with respect to utilization of BOG.

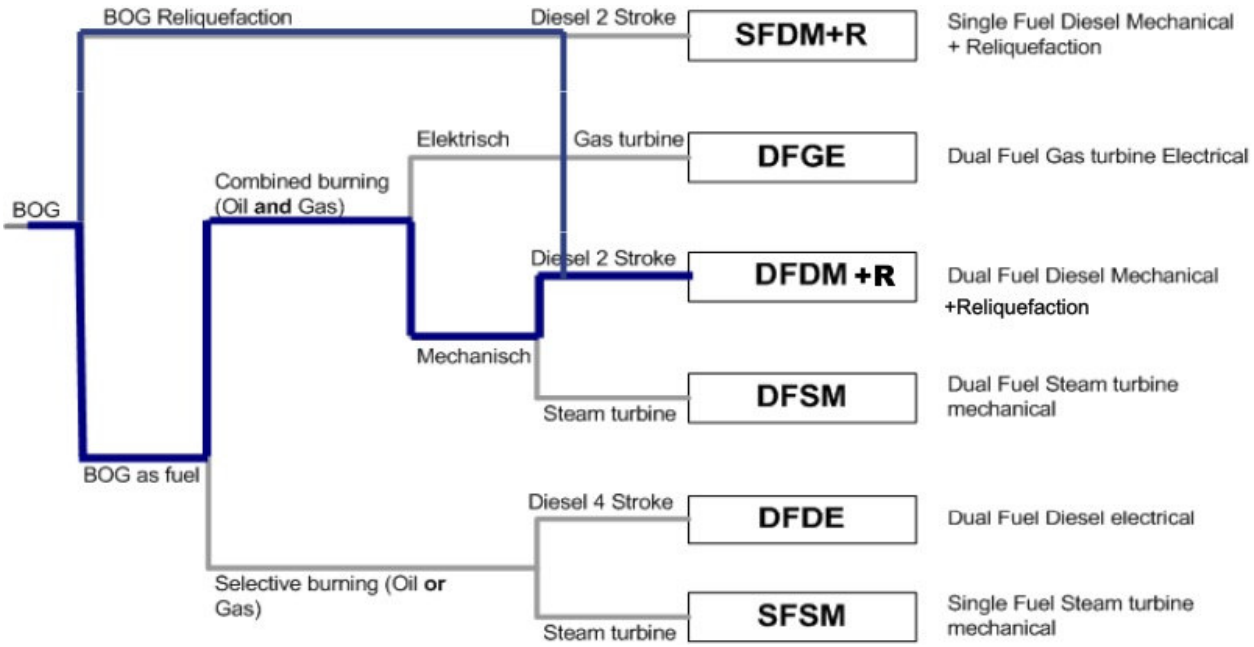


Figure 2.8: Propulsion systems for LNG Carriers [9, p.5], the highlighted alternative refers to low speed 2 stroke gas injected diesel engines integrated with a high pressure BOG compressor and a reliquefaction cycle

BOG can be used for electric power production if the vessel is equipped with a set of Dual Fuel 4-stroke Diesel Auxiliary engines, however due to the variability of the Auxiliary power demand on a ship a parallel system would be needed to handle the BOG under all operating scenarios.

### 2.3.1 BOG reliquefaction on LNGC

On board processes for BOG reliquefaction have been developed for LNG Carriers, the first plant was built in 2000 and since then a number of different technology became available on the market (Table 2.1).

Table 2.1: Main technologies for reliquefaction of BOG on LNG carriers [13]

| Plant model | Manufacturer | Work Cycle | Year | Reliq. Capacity [kg/h] | Power [kW] | spec work [kWh/kg] |
|---|---|---|---|---|---|---|
| LNG Jamal | Osaka Gas | Brayton | 2000 | 3000 | 3000 | 1 |
| TGE | Tractebel | Brayton | 2004 | 6250 | 5030 | 0.75 |
| Mark I | HGS | Brayton | 2006 | 6000 | 5800 | 0.96 |
| EcoRel | Cryostar | Brayton | 2008 | 7000 | 6000 | 0.86 |
| Mark III | HGS | Brayton | 2008 | 7000 | 5500 | 0.78 |
| Mark III Laby-GI | HGS | Brayton | 2009 | | | |
| TGE Laby-GI | Tractebel | Cascade | 2009 | | | |

The most common process for on board reliquefaction is the Nitrogen Brayton refrigeration cycle, produced by several manufacturers with different layouts. Alternatives to the Brayton cycle are the Ethylene/Propylene cascade process produced by Tractebel Gas Engineering (TGE) and Burckhardt Compression [28, p.24] and the mixed refrigerant MiniLNG plant developed by Sintef.

### Nitrogen Brayton cycle

The main manufacturer of Brayton processes for on board BOG reliquefaction is Hamworthy (recently bought by Wartsila). The first version of the Hamworthy process, also known as Moss process, or Hamworthy Mark I, is shown in Figure 2.9, in this process the BOG from the tank is compressed to about 4.5 bar by a two stage centrifugal compressor and reliquefied in the plate fin heat exchanger in the cold box. The cooling medium is pure Nitrogen which is compressed from 13.5 to 57 bar by a centrifugal 3 stage compressor coupled with a single stage turbo expander [13],[7, p.270].

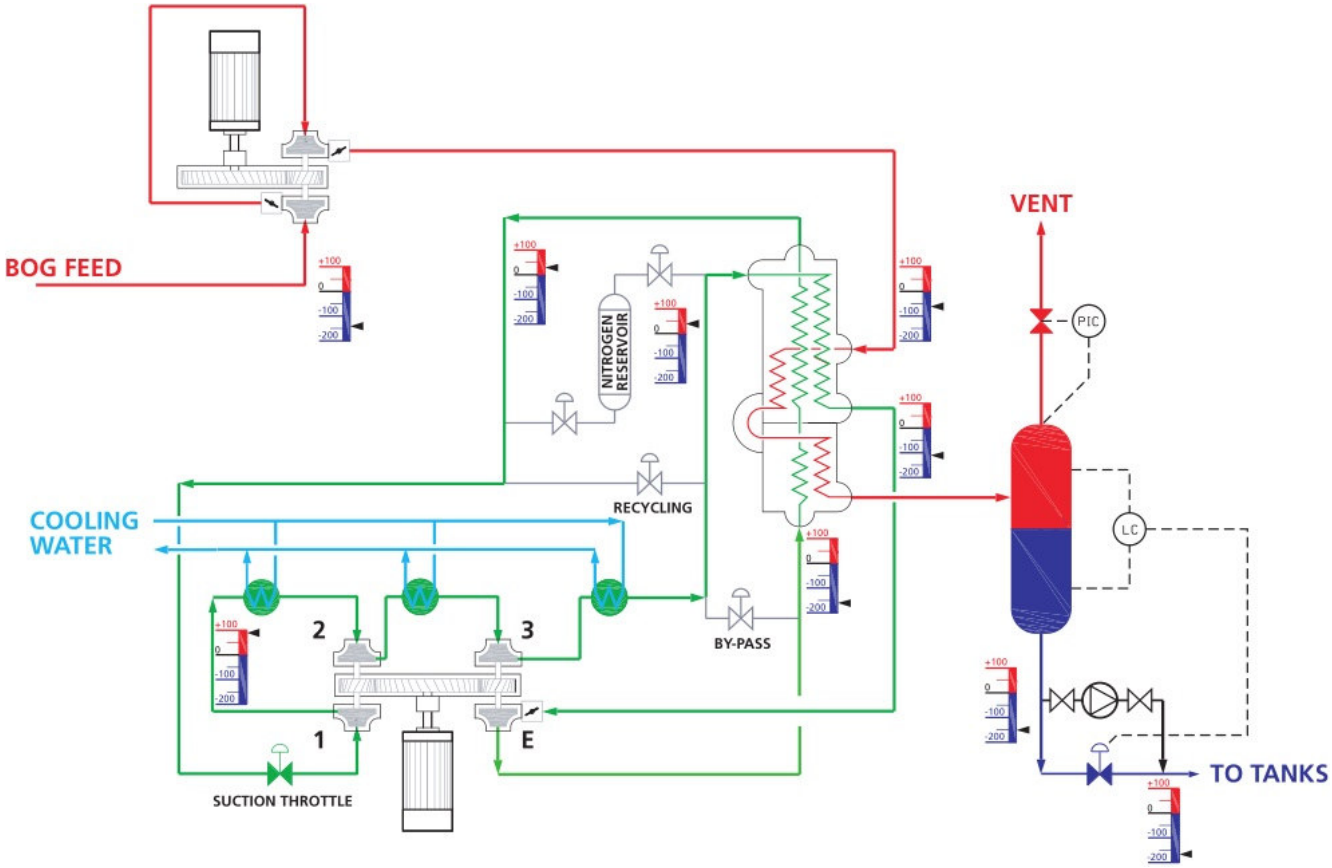


Figure 2.9: Hamworthy 1st generation BOG Reliquefaction System (Mark I) [29, p.5]

A more recent version of this system is the Hamworthy Mark III cycle in Figure 2.10 with the main difference that the tank BOG is preheated by HP warm Nitrogen before entering the compressor, as a consequence 3 stages with intercooling are required to compress the BOG to its reliquefaction pressure, with the advantage that part of the compression heat can be discharged to the seawater, thereby increasing the overall efficiency [29, p.6]

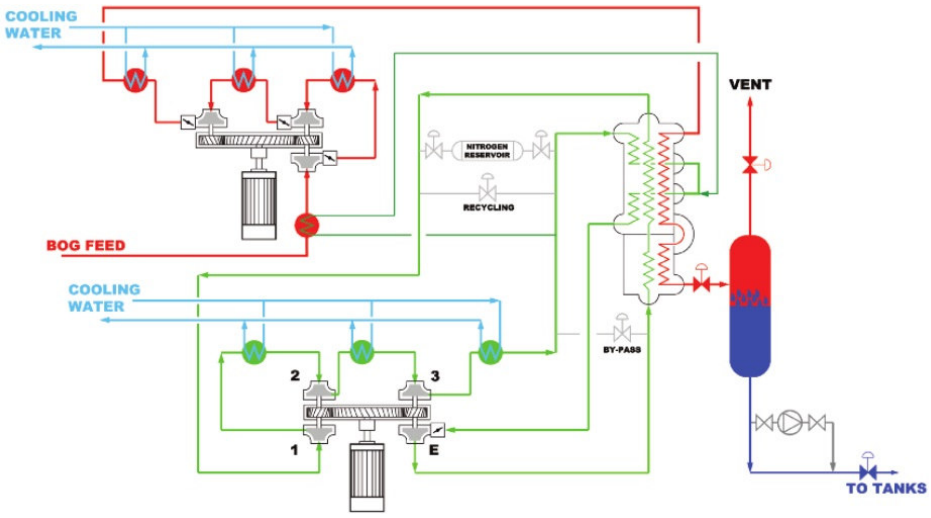


Figure 2.10: Hamworthy 3rd generation BOG Reliquefaction System (Mark III) [29, p.6]

The Cryostar's EcoRel process is a different version of a Brayton cycle with distinct heat exchangers of which one internal recuperative Nitrogen heat exchanger, two separate heat exchanger for BOG desuperheating and liquefaction and one BOG compressor cryogenic intercooler. It can be observed that while Hamworthy moves the BOG compression to the warm temperatures to take advantage of seawater intercooled stages, Cryostar choses to maintain a cold BOG compression (at about 4.8 bar) using the Nitrogen for the intercooling, in parallel with the BOG desuperheating.

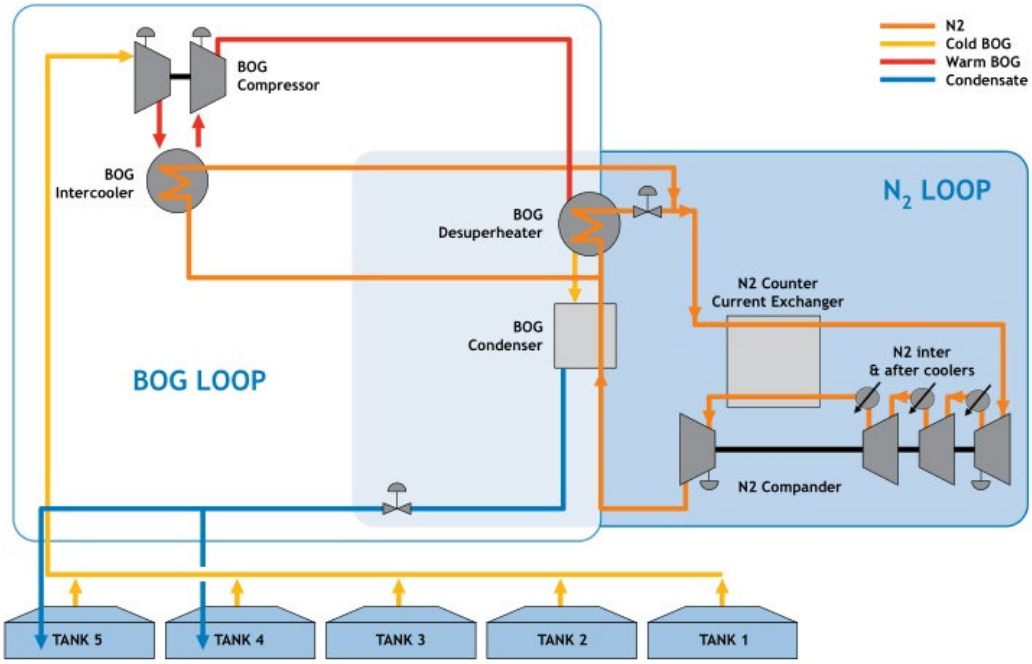


Figure 2.11: Cryostar EcoRel reliquefaction process for LNG Carriers [30, p.5]

### Mini LNG

The Mini LNG system is a mixed refrigerant process that has been developed and tested in the Sintef laboratories in Trondheim, and operated on a small LNGC since 2009 [31]. In this plant configuration the tank BOG is compressed by a oil-free labyrinth compressor to the pressure of 18bara (max 22bara) and above ambient temperature. The warm gas is then cooled by a seawater aftercooler and a Propylene precooling cycle to the temperature of -35℃ , before entering the heat exchanger where it is desuperheated, liquefied and subcooled against the Mixed Refrigerant. At this point the subcooled liquid is throttled to tank pressure [32, p.145]. A full scale Mini LNG plant has been installed on a Multigas Carrier by I.M. Skaugen SE, with a capacity of 20 tonnes LNG/day [33] and a energy consumption of 0.7 kWh/kg of reliquefied LNG [34]. The lower value of energy consumption of 0.47 kWh/kg in Table 2.2, is due to the fact that the Propylene compressor work is not included in the calculations [34].

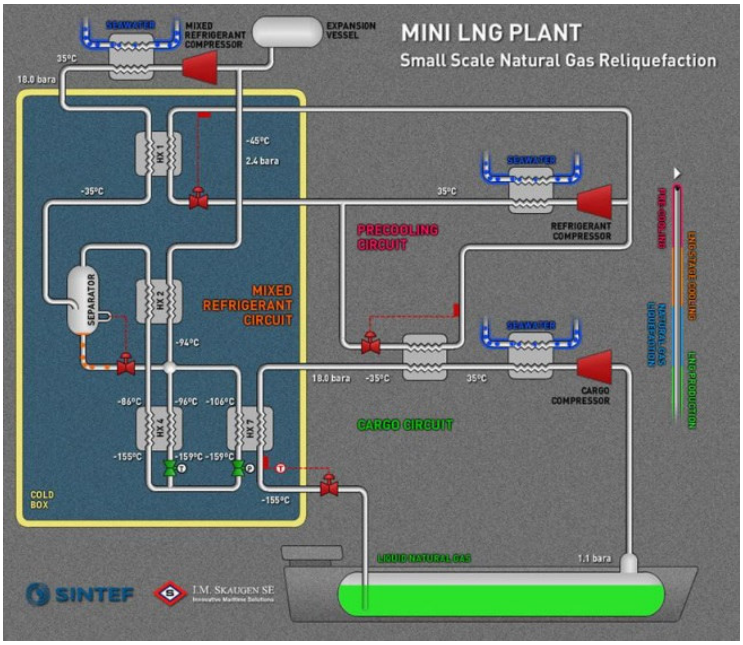

Figure 2.12: SINTEF Mini LNG Process, PFD [31, p.34]

Table 2.2: SINTEF Mini LNG Process, main parameters [31, p.35]

**BOG NG with 89 mol% CH4, 11 mol% N2 (18 bara)**

| | |
|---|---|
| Boil-off gas liquefaction capacity | 20 tonnes/d |
| LNG exit temperature (before throttling to tank) | -155 °C |
| MR (at first vapour-liquid separator inlet) and NG pre-cooling temperature | -35 °C |
| Mixed refrigerant compressor pressure ratio | 9.3 - |
| Mixed refrigerant compressor power consumption | 395 kW |
| Estimated compressor isentropic efficiency | 0.65 - |
| Mixed refrigerant actual suction volume | 1520 $m^3/h$ |
| Specific suction volume | 1.8 $m^3$/kg LNG |
| Specific power consumption mini-LNG | 0.47 kWh/kg LNG |

Table 2.3: SINTEF Mini LNG Process, performance [31, p.39]

**Results from full scale tests and simulation model verification**

Including simulation results for future plant operating conditions (corrects for off-design conditions at full scale tests)

| Parameter | Unit | Measured | Simulation | Simulation corrected 1) (dp and leak) | Simulation corrected 2) (precooling t) |
|---|---|---|---|---|---|
| **Liquefaction capacity** | tonnes/d | 14,4 | 14,4 | 17,1 | 18,8 |
| **LNG exit temperature before throttling to tank** | °C | -154,1 | -154,1 | -155 | -155 |
| **MR precooling temperature at vap-liq separtor** | °C | -24,9 | -24,9 | -24,9 | -35 |
| **NG precooling temperature** | °C | -31,7 | -31,7 | -35 | -35 |
| **Refrigerating capacity** | kW | | 70,7 | 84,3 | 93,2 |
| **Volume flow LP MR out of coldbox** | $m^3/h$ | | 1436 | 1512 | 1517 |

To compare the Mini LNG performance to the one of process in this study it is useful to estimate its COP. If the refrigeration duty of 70-93 kW is taken from table 2.3, with a mixed refrigerant compressor work of 395 kW [31, p.35] (precooling refrigerant compressor neglected), the resulting COP is 0.18 to 0.24. If refrigeration duty is computed from the BOG mass flow according to the equation

$$\dot{Q}_{ref} = \dot{m}_{BOG} \cdot \Delta h_{evap} = \frac{20000 kg/day}{24 \cdot 3600} \cdot 517.1 kJ/kg = 119 kW \tag{2.1}$$

then the COP becomes 0.3.

## 2.4 Systems for 2-Strokes Low Speed Engine Propulsion

The objective of this thesis is to develop a system for LNG fuelled ships equipped with 2-stroke low speed gas diesel engines, there are two reasons why the topic has been restricted to this specific scenario. The main reason is that this type of engines are expected to have a bright outlook in the market of medium-large LNG fuelled ships due to the remarkable propulsion efficiency given by the thermal features of the gas diesel cycle and by the possibility of direct coupling to large slow propellers; secondly the BOG handling is particularly critical in this scenario due to the difficulty of feeding it to the engine at high pressure. In summary it is expected that providing an innovative solution for the BOG handling in this scenario would open the way to one of the most efficient propulsion solutions for gas fuelled ships.

In the present chapter the state of the art of ship propulsion systems with 2-stroke gas diesel engines is described, including an overview of the engine technology itself and a series of options for fuel supply that are under development.

### 2.4.1 ME-GI engines

MAN Diesel & Turbo is the world leading manufacturer of large low speed gas diesel engines for ship propulsion, these engines are known by the designation "ME-GI", they are 2-stroke Dual Fuel Elecronically controlled Gas Injected engines, Figure 2.13 shows the typical look and cross section of a ME-GI engine.

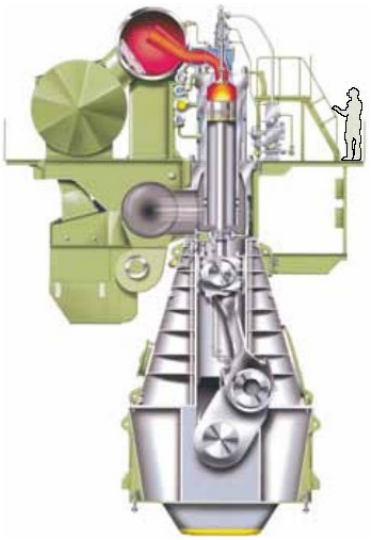

Figure 2.13: Sketch of a ME-GI engine [28, p.5]

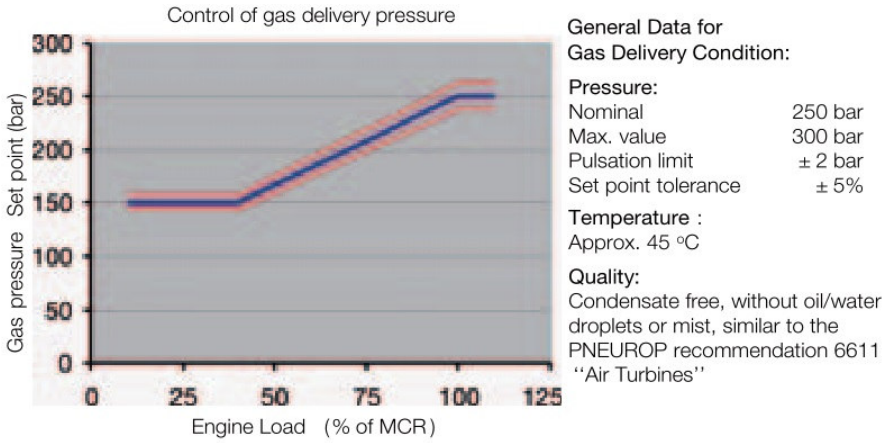


Figure 2.14: Example of ME-GI Gas supply specifications, delivery pressure at varying engine load, for a 250 bar engine feed [35, p.15]

The attribute "Dual Fuel" indicates that the engine can run on fuel-oil alone or on a mixture of fuel-oil and Natural Gas, the amount of injected fuel-oil can be reduced down to a minimum preset of 2-5% of pilot fuel necessary for ignition, meaning that operation with Natural Gas alone is not possible [28]. The main feature of these machines compared to other Dual Fuel engines is that they operate in a standard Diesel cycle, with HP gas injection at the end of compression, thereby gaining the advantages of the Diesel cycle such as absence of limits for knocking and misfiring, possibility to operate at maximum power and Break Mean Effective Pressure (BMEP) and unnecessary de-rating [8]. The thermal efficiency of about 50% of the gas injected Diesel cycle is comparable to the conventional fuel-oil cycle, this value is high and fairly stable at different gas/fuel-oil ratios and at reduced engine load [35].
The detailed description and modelling of the engine is out of the scope of this thesis, yet this machine sets the requirements for the Fuel Gas Supply System and therefore the boundary conditions for a related simulation model. In particular ME-GI engines require gas at 250-300 bar and about 45℃ during normal operation, at reduced load the pressure can be reduced linearly as shown in Figure 2.14.

The two available options for supplying Natural Gas to such high pressure are LNG cryogenic pumps or multistage reciprocating BOG compressors.

### 2.4.2 High Pressure BOG compression

The use of High Pressure (HP) compressors is the most energy intensive alternative but it has the benefit that it offers a solution to the BOG handling problem. Burckhardt Compression and MAN are developing a BOG HP compressor system for LNG Carriers with ME-GI propulsion, in a configuration where the HP Fuel Gas Supply System is integrated with reliquefaction processes (Figure 2.15).

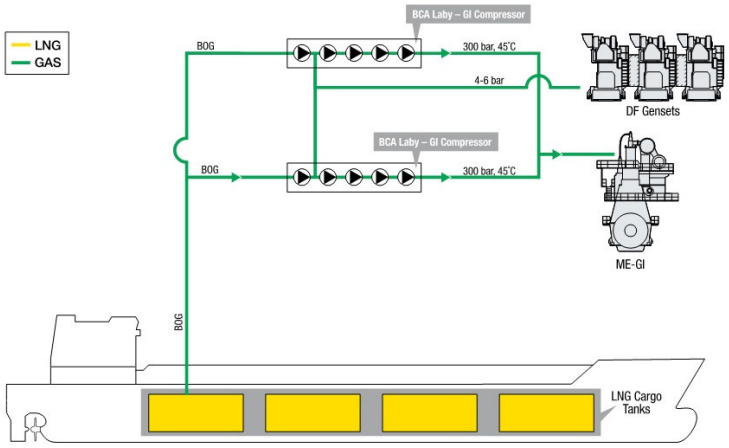


Figure 2.15: ME-GI engine with High Pressure BOG labyrinth compressor (reliquefaction unit not shown) [28, p.6]

#### Integration of HP compressor and reliquefaction processes

Burckhardt Compression and Hamworthy Gas Systems have developed a solution for LNG Carriers that integrates the Laby-GI compressor with the Hamworthy Mark III reliquefaction system. This system shown in Figure 2.16 allows to divert the BOG at 5-6 bar after the second compression stage to the reliquefaction system or to the remaining stages towards the engine according to the mass balance between BOG generation and gas fuel consumption of the ME-GI dual fuel engine [28, p.24],[13, p.8].

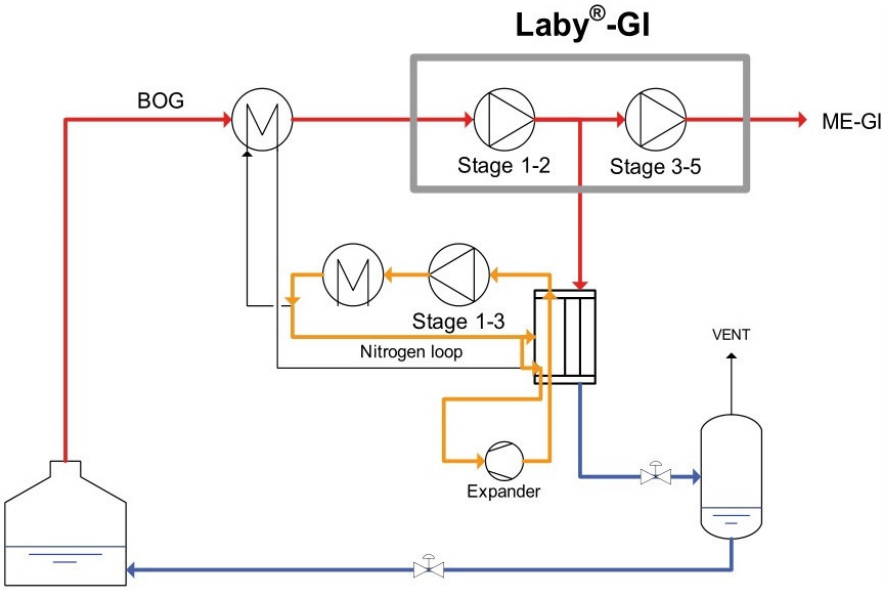


Figure 2.16: BOG Reliquefaction System, HP Compressor [28, p.24]

### 2.4.3 High Pressure LNG Fuel Gas Supply Systems

To avoid the high energy consumption of the HP compressor many companies have focused in developing different technologies to pump the liquid LNG and evaporate it at high pressure, some of those are HGS, TGE, DSME, Cryostar, HHI and MHI [28, p.29].
Cryostar in [28, p.31] identifies the main components of a HP Fuel Gas Supply System (FGSS) for ME-GI engines:

- Reciprocating LNG HP pump with Variable Frequency Drive (VFD);
- Automatic pump control system (to meet engine delivery pressure);
- Buffer volume for pressure pulsations damping.

Figure 2.17 shows this FGSS layout, includes a list of potential BOG handling methods that might be required.

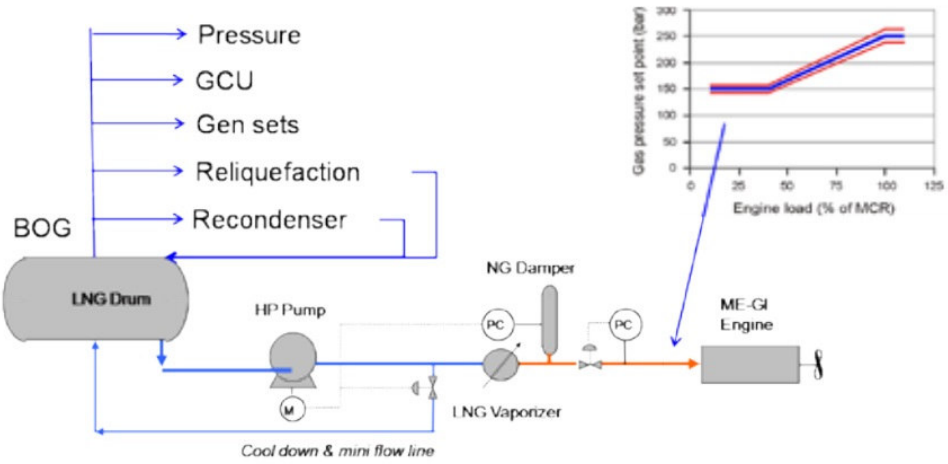


Figure 2.17: FGSS with Cryostar's HP pump solution and BOG handling alternatives [28, p.31]

Hyundai Heavy Industries (HHI) in [36] defines a set of general specifications for HP FGSS for ME-GI engines, the layout suggested in this document is shown in Figure 2.18.

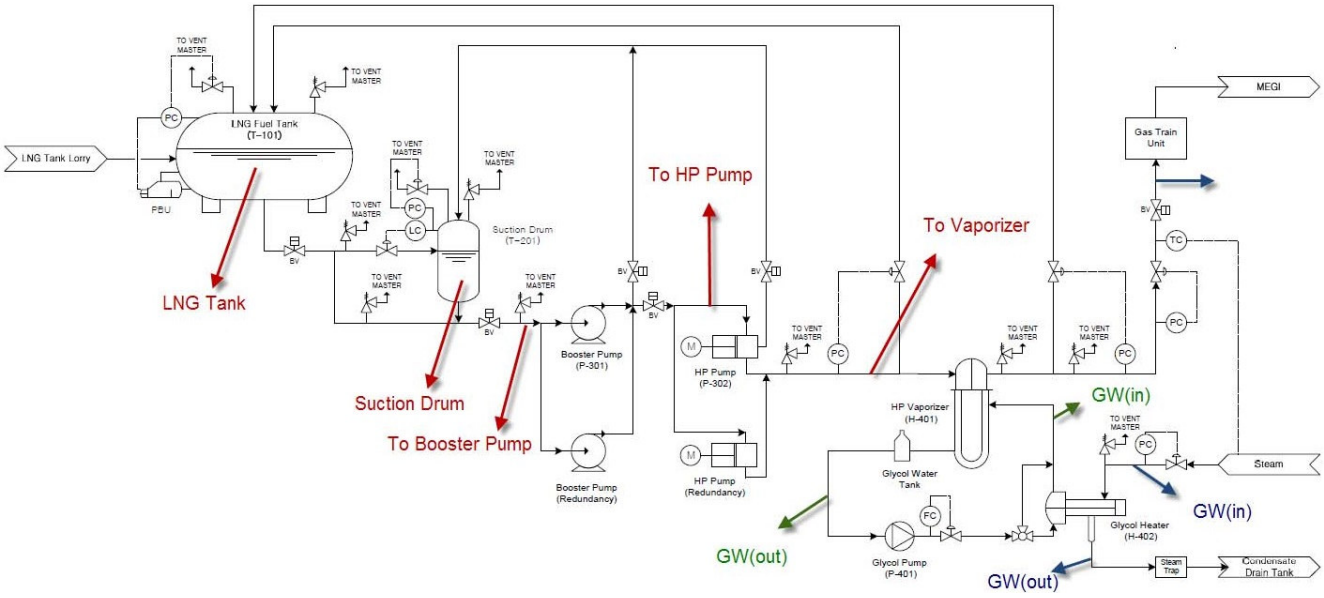


Figure 2.18: PFD of HP Fuel Gas Supply System, for a design flowrate of 0.39kg/s [36, p.20]

This system is designed for LNG fuelled ships (non-LNGC) with a 5.5 barg Type C fuel tank and a fuel consumption of 0.39 kg/s of LNG at 100% engine load, compared to the one in Figure 2.18 this layout does not include a HP buffer tank, but is equipped with a Suction drum and Low Pressure (LP) pumps upstream the HP pumps, these units protect the HP pumps avoiding vapor slip in the pump suction and cavitation. In this configuration the HP vaporizer system is composed by a shell & tube glycol heat exchanger that vaporizes and superheats the LNG to its target temperature, and a glycol closed loop where the fluid is heated by steam generated in

boilers [36].
One example of HP FGSS layout for Type B atmospheric tanks is illustrated in Figure 2.19, this layout differs from Type C applications as it includes a BOG handling system with LP BOG feed to the Auxiliary engines or boiler, and a BOG recondenser. The recondenser is a contactor that mixes LNG pumped at LP (in the subcooled region) with LP superheated BOG in a suitable ratio, the output is saturated liquid that can be fed to the HP pump. This component is frequently used for BOG handling in LNG receiving terminals [37].

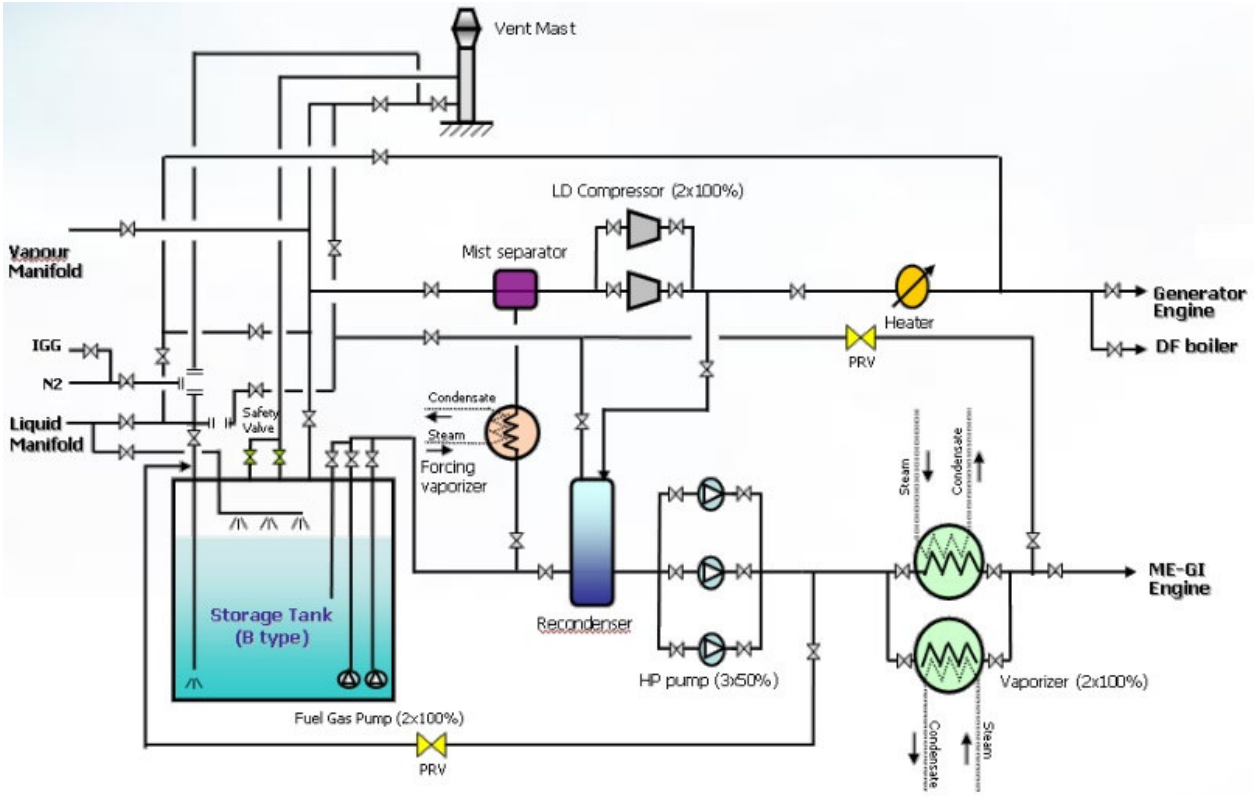


Figure 2.19: PFD of HP Fuel Gas Supply System (250 bar) for Type B tank, equipped with BOG compressor and recondenser (5 bar) [24, p.18]

### Integration of HP Fuel Gas Supply Systems and reliquefaction processes

It is quite correct to state that the subject of the present thesis is a heat integration between the HP FGSS and a BOG reliquefaction process. Examples of such process integration are found in the literature applied to LNGCs.

Hamworthy studied how to optimize its Mark III reliquefaction cycles for ME-GI applications, in the system shown in Figure 2.20 the FGSS is integrated with the reliquefaction cycle through a heat exchanger named "Optimizer", this component is part of the Brayton cycle in parallel with

the "BOG Preheater" and the cold box, and has the function of recovering part of the low temperature exergy of the cold HP LNG stream with a fraction of the HP Nitrogen stream, thereby enhancing the Brayton cycle efficiency.

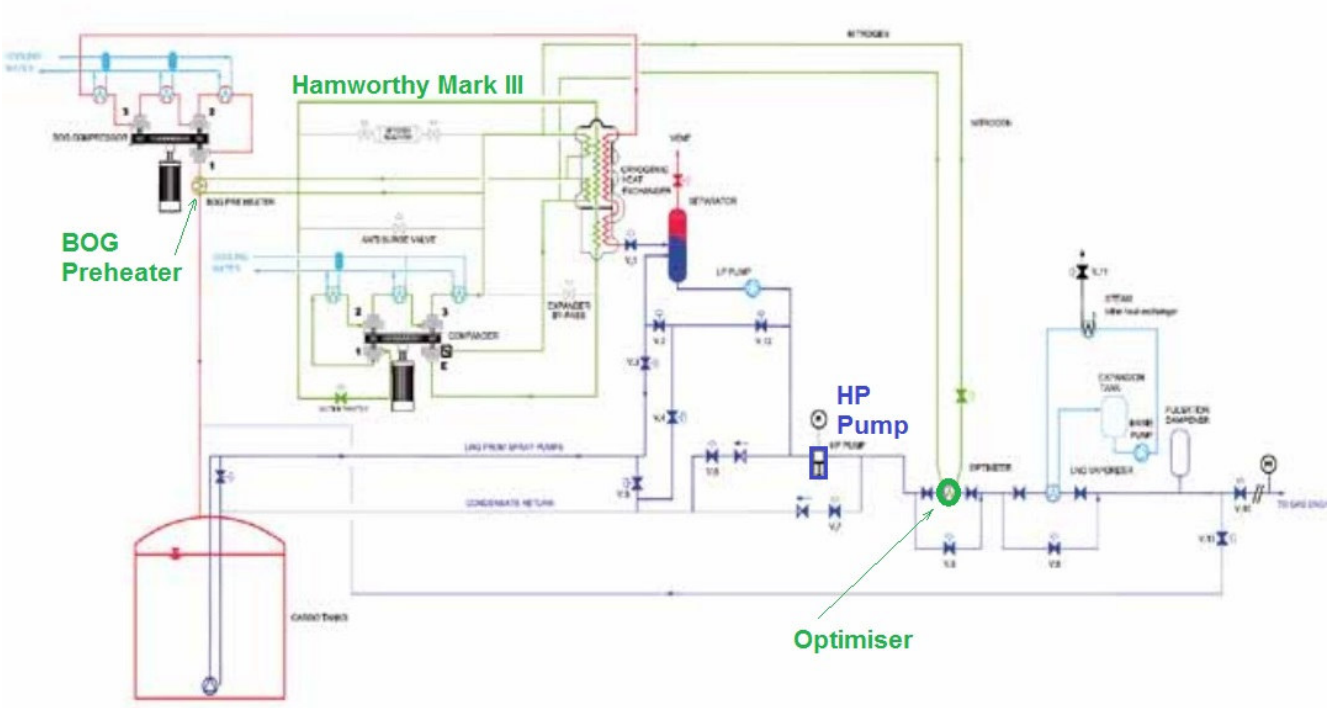


Figure 2.20: Integration of HP FGSS and Hamworthy Mark III reliquefaction cycle, published by MAN in [28, p.19]

Wartsila, that acquired Hamworthy in the beginning of 2012, is also studying this system for applications with HP 2-strokes engines, Figure 2.21 shows a process similar to the one illustrated above, here the BOG compressor is also used to send gas at 5-6 bar to the Auxiliary engines.

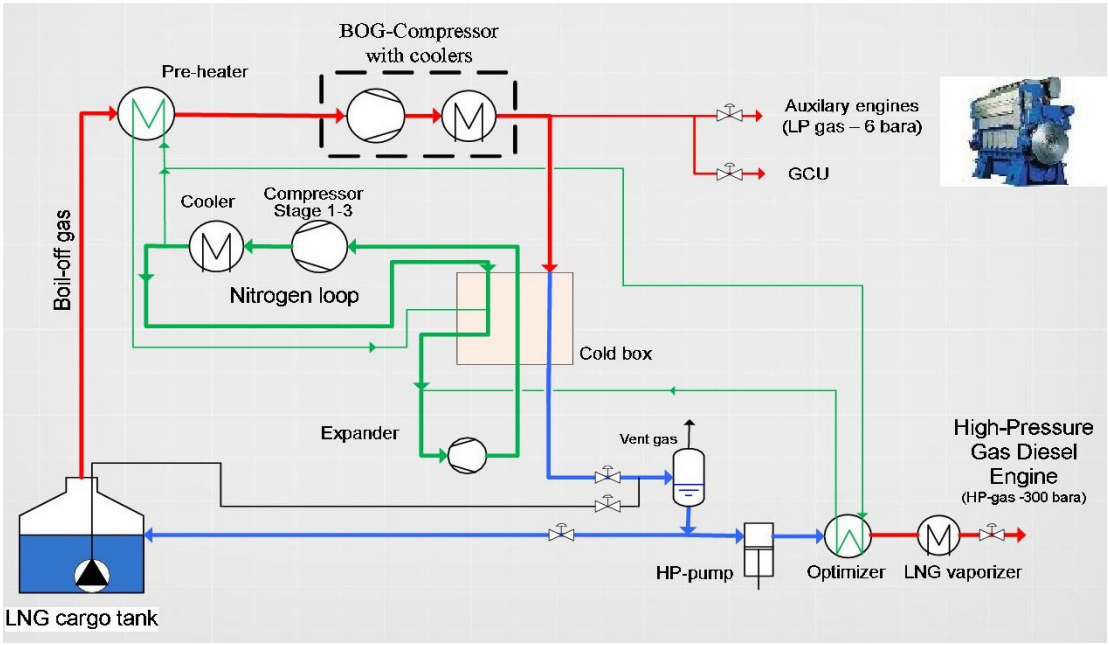


Figure 2.21: Integration of HP FGSS and BOG Reliquefaction System LNGRS (or Hamworthy Mark III), published by Wartsila in [38, p.18]

# Chapter 3

# Heat pump process

The options for integrating BOG handling systems with the HP Fuel Gas Supply System illustrated in the previous chapter are mostly suited for LNG Carriers, and in general consist in modifying a standard reliquefaction process fitting it to the HP FGSS.
On the other hand there are reasons to believe that a different approach could be followed when it comes to LNG fuelled ships instead of LNGCs:

- The amount of BOG generated in LNG fuelled ships is roughly 10-100 times less than for a similar size LNGC (Figure 2.7);
- Standard reliquefaction processes for LNGCs consist of large size plants with considerable reliquefaction capacity;
- Space and process complexity constraints are tighter on a merchant ship than on a LNGC.

The approach of the present thesis was inspired by the norwegian company LNG New Technologies that outlined and patented a process to cool the LNG fuel tank and bunkering pipe of a LNG fuelled ship by means of a refrigerant cycle that uses the heat requirement of the HP cold LNG in the FGSS to drive the process. The patented system illustrated in Figure 3.1 is essentially a heat pump process that transfers heat from the cold fuel tank space (5b) and filling pipe (5a) to the LNG Fuel Supply line (8) directed to the engines. The refrigerant fluid (1) is a inert gas such as Nitrogen subject to compression in (2) and pressure reduction in (4) via throttle valve or expander [39], it can be noted that heat exchangers with external utilities such as seawater, steam or glycol loops are not included in this layout.

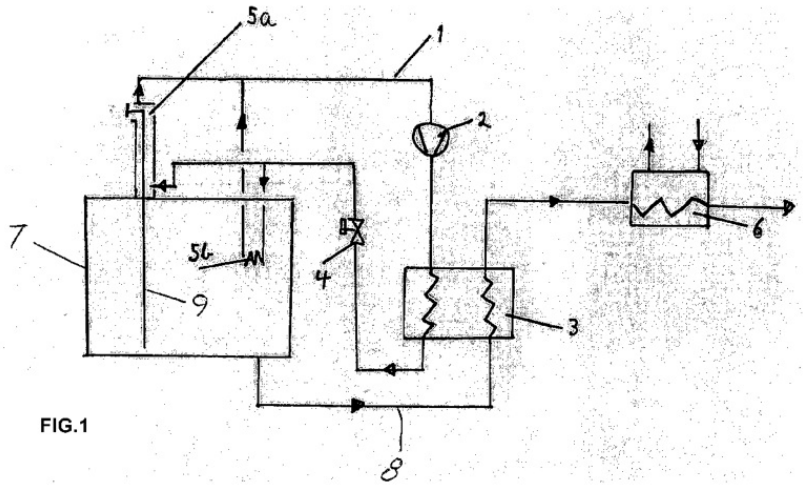


Figure 3.1: Jorn M. Jonas patented heat pump process [39]

The principle of integrating the HP FGSS with the Nitrogen reliquefaction cycle was already investigated by Hamworthy and others as detailed in chapter 2.4.3, the heat pump process as outlined by LNG New Technologies differs from those approaches in the way that it aims to achieve the fullest possible integration between the process streams, until the heat discharge to the environment in the form of external utilities streams is excluded.
In the development of the present thesis, different process layouts than the one suggested by LNG New Technologies were studied but the "philosophy" of full heat integration between the process streams without heat discharge to the enviroment was maintained as a constant feature, with the intention to assess the limitations of this simple and efficient approach.

## 3.1 Process layout

A number of different process layouts have been explored in the course of this thesis, Figure 3.2 illustrates the main configuration that the simulation results reported in this document refer to. The Process Flow Diagram (PFD) is divided in three parts:

- the Fuel Supply lines, that transfer LNG fuel from the cryogenic tank to the main and Auxiliary engines at the prescribed temperature and pressure;
- the Tank Reflux System, that extracts LNG from the tank and recirculates it back at lower temperature;
- the Heat Pump cycle, that transfers the heat from the Tank Reflux System to the Fuel Supply lines, in a closed refrigerant loop.

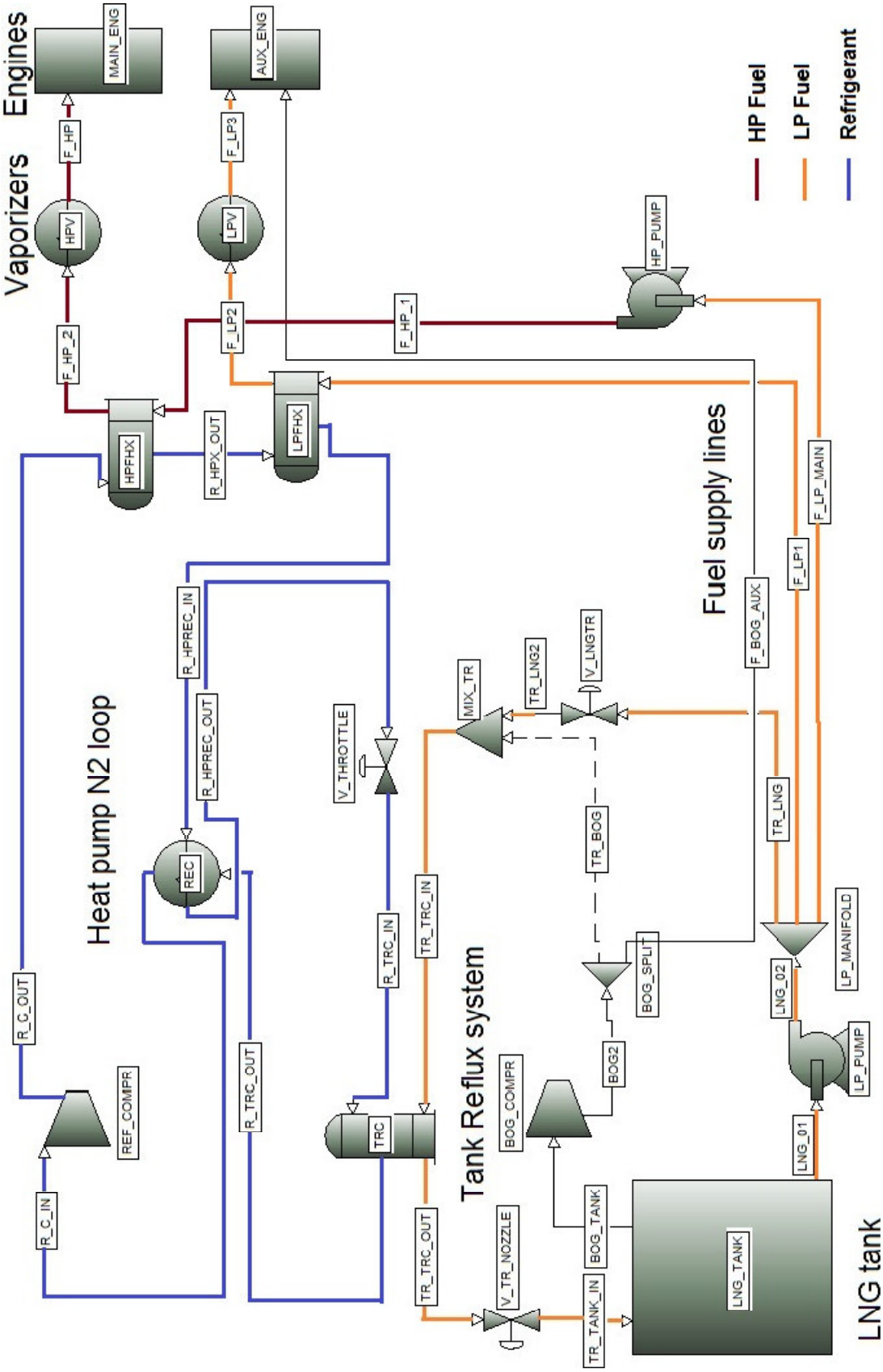


Figure 3.2: Main PFD of the heat pump process

As indicated by the color legend the heat pump loop contains pure Nitrogen refrigerant. The Nitrogen, after being compressed by the Refrigerant Compressor, is cooled by the LNG fuel in the High Pressure Fuel Heat Exchanger (HPFHX) in series with the Low Pressure Fuel Heat Exchanger (LPFHX), following the heat discharge to the Fuel Supply lines it enters the Recuperator (REC) for internal heat exchange. At the Recuperator outlet the refrigerant is throttled to a lower pressure in the two phase region, so it can evaporate in the heat exchanger labeled Tank Reflux Cooler (TRC) providing the necessary cooling duty to the Tank Reflux system. The Fuel Supply lines consist in a HP LNG supply for the main ME-GI engine and a LP LNG supply for the Auxiliary engine, the LP BOG supply to the Auxiliary engine is also included in the PDF (F-BOG-AUX) but it not active in in the simulations. Similarly the Tank Reflux system is fed by LP LNG that is subcooled in the TRC, compressed BOG recirculation in the Tank Reflux system (dotted stream TR-BOG) has been investigated as an alternative to the liquid subcooling.

### 3.1.1 Alternative process layouts

Modest modifications to the layout shown in Figure 3.2 can be considered, two possibilities are illustrated and discussed in the present chapter.

One feature of the process in figure 3.2 is that the same LP Pump is used to feed the Auxiliary engine, the HP Pump, and the Tank Reflux system, this design choice has the advantages that it minimizes the the number of cryogenic machinery items and it allows the pump to operate above the minimum flow specification characteristic of cryogenic pumps (this is related to the fact that the heat leak in the piping and in the pump body might lead to cavitation in the pump if the flow is too low [40]). On the other hand this configuration has one important disadvantage with respect to the efficiency of the process. The LP Pump needs to work with a sendout pressure higher than 6 bara for the Auxiliary engine feed, but the required inlet pressure to the Tank Reflux system only needs to compensate the pressure drop in the piping, in the TRC heat exchanger and in the tank spray system. A Tank Reflux system pressure higher than required would increase the specific work of the LP Pump and therefore the enthalpy of the "TR-LNG" stream, yielding to an increased "energy leak" into the tank.
One way to limit this effect is to use a dedicated cryogenic Pump to recirculate the LNG to the tank ("TR-PUMP" in Figure 3.3, with valve "V-LNG-TR" closed) with a lower sendout pressure determined by the pressure drop in the Tank Reflux system, this option needs to be evaluated comparing the expected gain in efficiency and the added complexity and investment cost of the process, as well as possible operational problems related to the minimum flow specifications of

the LP Pump.

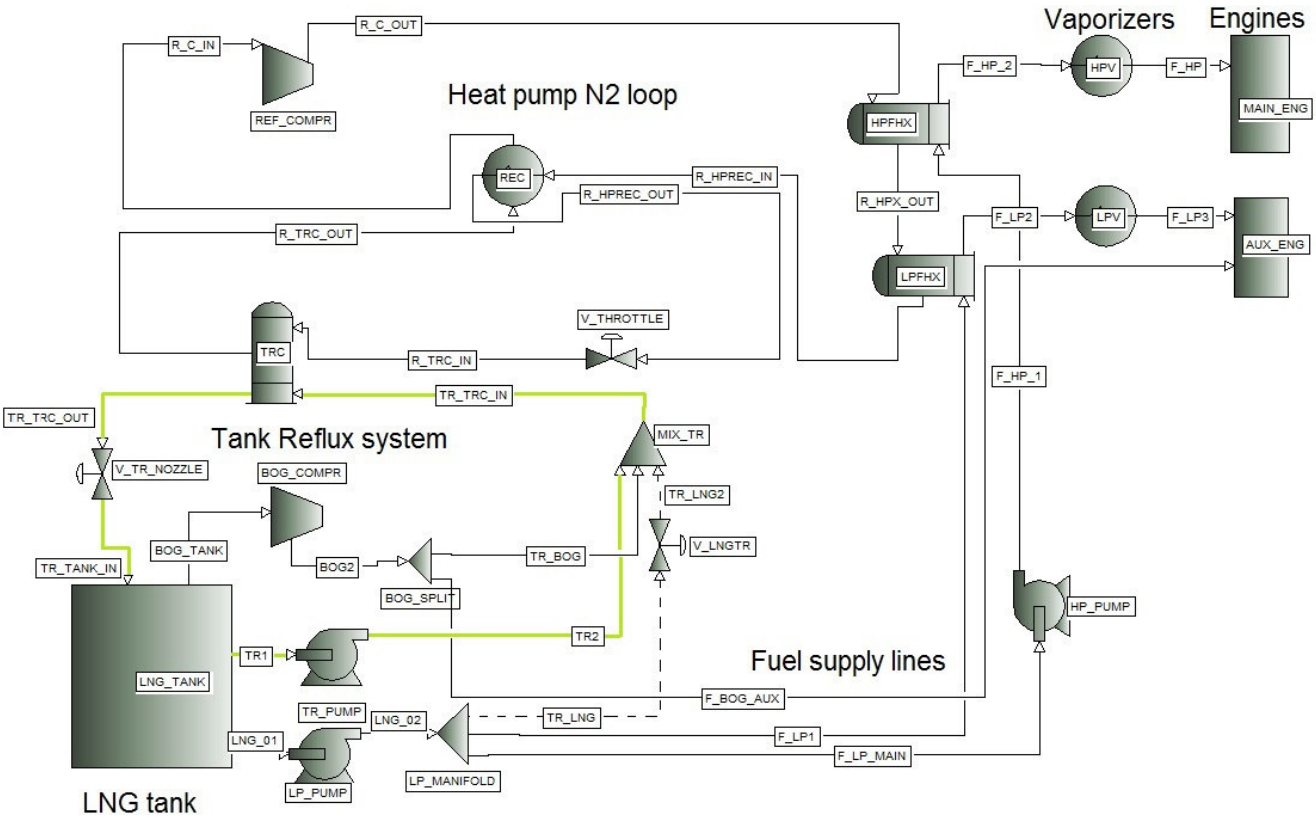


Figure 3.3: PFD: N2 Recuperated loop, with TR dedicated Pump

A second important modification to the process would be to remove the LPFHX and use a BOG Compressor to feed the tank BOG to the Auxiliary engines. This alternative would be interesting if the specific energy consumption for compressing the BOG was low compared to the specific energy consumption of the heat pump process. The advantages of this configuration compared to the one in Figure 3.2 are the following:

- the heat exchanger (LPFHX) can be removed, saving one unit;
- the LP Pump now can work with a much lower outlet pressure, within the limitation of the NPSH required by the HP Pump.

Compared to the layout in Figure 3.3 this layout requires less units and the Tank Reflux system allows the LP Pump to fulfill the minimum flow requirements.

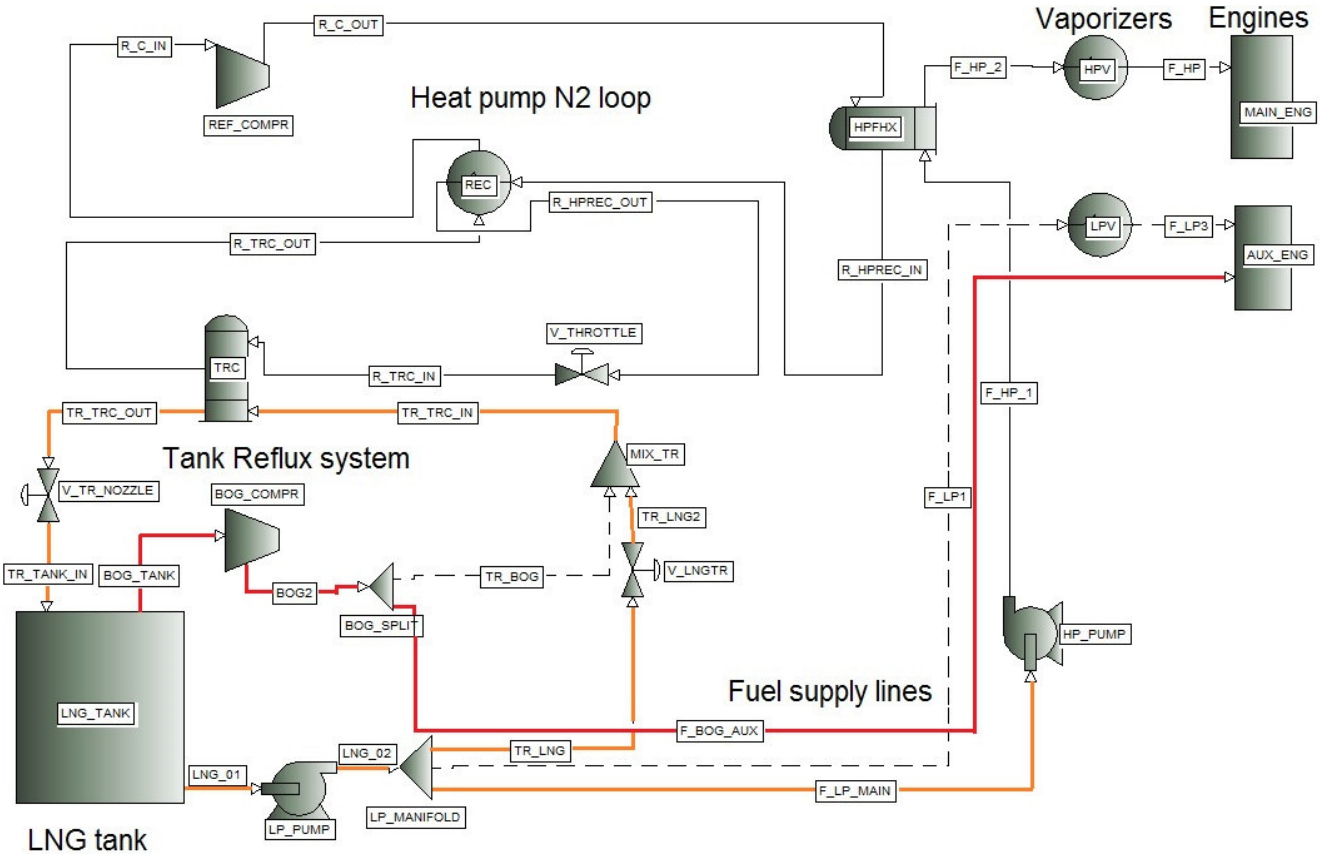


Figure 3.4: PFD: N2 Recuperated loop, with BOG fuelled AUX engine

## 3.2 Selection of a reference case

Since the described heat pump process is based on a full integration with different systems of a LNG fuelled vessel and consequently its performance is expected to be dependent on the proportions between those systems, a particular effort has been dedicated to adopt a realistic and conservative reference case in order to define the boundary conditions for the process.
From the market trends discussed in chapter 2.1.3 it appears that there is a need for new BOG handling systems on medium-large LNG fuelled ships for deep-sea routes that require a fuel tank size larger than 2000-3000 $m^3$ and spend long time in the Emission Control Areas (ECA).
According to these description a generic merchant ships is taken as a reference case, this could correspond to a bulk or chemical carrier, a Ro-Ro vessel or a container vessel.
In order to quantitatively define the reference case, three parameters have been identified as essential to characterize the FGSS and thus set the boundary conditions for the heat pump process, namely:

- the tank volume, used to estimate the average heat leak and set a target for the refrigera-

tion duty;

- the Main engine Power, related to the flowrate of HP fuel in the Fuel Supply system and heat pump heat exchanger (HPFHX);
- the Auxiliary engine Power related to the flowrate of LP fuel in the Fuel Supply system and heat pump heat exchanger (LPFHX).

Taking into accound the market trends the company LNT [40] suggests as a base case for the process design and optimization a medium size ship with the following characteristiscs:

- Tank volume: 2000 $m^3$;
- Main engine power: 10.94 MW;
- Aux engine power: 450 kW.

### 3.2.1 Main engine

It is assumed that the ship is propelled by a single ME-GI main engine with power of 10.94 MW. This value refers to the engine power for driving the propeller under normal ship operation, i.e. the condition at which the ship operates most of the time during voyage, engine manufacturers refer to this parameter as "Service Power", or "Normal Continuous Rating" (NCR), or "continuous Service rating for Propulsion" (SP) [41, p.28]. The NCR is lower than the maximum power that the engine can deliver, for example the NCR is usually 85-90% of the Specified Maximum Continuous Rating (SMCR) that represents the owner's requirement for the continuous operation of the engine. The SMCR has to be lower or equal to the Nominal Maximum Continuous Rating (NMCR) that is a characterstic of the engine corresponding to the mean effective pressure and engine speed limits in the layout diagram [41, p.29].
In order to perform a correct selection of the Main engine and thereby calculate the fuel consuption as accurately as possible, the present section refers to studies conducted by technology suppliers, and catalogues by the engine manufacturer MAN Diesel&Turbo.
The company Samsung Heavy Industries conducted a comparative study of different types of shipping gas engines [24] for A-max (Aframax [42]) oil tankers propulsion, using the ME-GI engine model 6S60ME-GI8.2 [24, p.30], with a NCR of 10,860 kW. This engine corresponds to 6S60ME-C8-GI in the most recent catalogue [43, p.53] in figure B.3. According to the MAN designation in figure B.2 this is a 6 cylinders Super long stroke, 60 cm diameter cylinder, Electronically controlled, Compact, Gas Injected engine.
A second study on different fuel gas supply system for LNG carriers has been carried out by

MAN Diesel&Turbo for smaller size 5 cylinders engine 5S60ME-C82-GI [25], with a SMCR of 10,000 kW at 105rpm, operating at a NCR equal to 81% of the SMCR. This engine is more similar to the new model 5S60ME-C8-GI in figure B.3 in the appendix. In this thesis, with reference to the similar examples reported above, the 6 cylinders 6S60ME-C8-GI engine was selected to supply the NCR of 10,940 kW. As described in table 3.1 the SMCR is a fraction of the NMCR, here 85% [44, p.66], also the NCR is 91% of the SMCR and 77% of the NMCR, which gives a Specific Fuel Consumption (SFC) of about 133.1 g/kWh of gas fuel extracted from the datasheet in figure B.3. This fuel consumption for the design fuel LHV in table 4.5, taking into account the pilot fuel, gives a thermal efficiency of the engine of 53% which is high optimistic value giving a low fuel consumption therefore conservative for the heat pump process operation.

Table 3.1: Main engine features

| Engine | 6S60ME-C8-GI | |
|---|---|---|
| NMCR ("L1") | 14280 | kW |
| SMCR ("M") | 12070 | kW |
| NCR ("S") | 10940 | kW |
| SFC (NG) | 0,133 | kg/kWh |
| SFC (pilot) | 0,006 | kg/kWh |
| mass flow (NG) | 0,404 | kg/s |
| thermal efficiency | 53 | % |

### 3.2.2 Auxiliary engines

Usually 2 or 3 Auxiliary engines are installed on merchant or container vessels for the so called "hotel" consumption, port operations, and other utilities power requirement [6]. The Auxiliary engines' load during normal operation is expected to be modest, and their fuel consumption is also negligible if compared to the main engine's. For this study a Auxiliary engines' power of about 450 kW is chosen as a design value for the normal operation of the ship [40] [25] (Table C.3). It is assumed that the Auxiliary engines are Dual Fuel 4-strokes engines, fuelled by natural gas at about 6 bara, with injection of Diesel pilot fuel for ignition. The Specific Fuel Consumption for the set of Auxiliary engines is expected to be higher than for the main engine, as they are smaller machines working with low pressure, here a SFC of about 0.16 kg/kWh is used to calculate the Auxiliary engine fuel flowrate in table 3.2, [6].

Table 3.2: Auxiliary engines lumped features

| | | |
|---|---|---|
| Number of Engines | 2 - 4 | - |
| Power Installed | 2500-3500 | kW |
| Normal Power | 450 | kW |
| SFC (NG) | 0,160 | kg/kWh |
| SFC (pilot) | 0,005 | kg/kWh |
| mass flow (NG) | 0,020 | kg/s |
| thermal efficiency | 44 | % |

### 3.2.3 Heat leak calculations

The amount of BOG produced in a on board LNG tank depends on several factors, primarily on the type of tank and insulation, but also on the temperatures of the liquid and the tank during filling operations (also called "bunkering" for fuel tanks), the ambient weather conditions and the sea state [45]. An averaged parameter to quantify the production of BOG is the Boil Off Rate (BOR), defined as the percentage of the total LNG volume evaporating daily, from operation practice the BOR for this size of atmospheric tanks varies between 0.18%/day [40] and 0.4%/day [24].

Table 3.3: Calculation of Heat leak for a given tank size

| | | |
|---|---|---|
| Fuel tank size | 2000 | m3 |
| Max tank filling | 95 | % |
| Max Fuel volume | 1900 | m3 |
| BOR | 0,24 | %/day |
| Volume flow (LNG_evap) | 0,19 | m3/h |
| density (LNG) | 457 | kg/m3 |
| mass flow (BOG) | 86,83 | kg/h |
| Heat of vaporization (BOG) | 517,1 | kJ/kg |
| Heat leak | 12,5 | kW |

In this study a BOR of 0.24%/day is assumed [40]. For the selected tank size of 2000 $m^3$ a conservative estimate of the BOG evaporation rate can be obtained by multiplying the BOR with the volume of LNG corresponding to the 95% filled tank, as in equation 3.1, BOG mass flowrate is calculated with the density of 455 $kg/m^3$ calculated with HYSYS for the given composition, as in equation 3.2.

$$\dot{V}_{LNG,ev} = (V_{tank} \cdot 95\%) \cdot BOR \tag{3.1}$$

$$\dot{m}_{BOG} = \rho_{LNG} \cdot \dot{V}_{LNG,ev} \tag{3.2}$$

Assuming that all the heat that leaks into the tank is only absorbed by the phase change of the LNG, the heat leak can be estimated by equation 3.3 [46, p.126].

$$Q_{leak} = \dot{m}_{BOG} \cdot \Delta h_{LNG,ev} \tag{3.3}$$

Evaporation enthalpy is an output of the HYSYS reports for the BOG stream at tank pressure.

To calculate the refrigeration requirement for the system the estimated heat leak has been increased with a engineering factor of 50% obtaining the value of 18 kW (from equation 3.4) that needs to be covered by the refrigeration duty of the heat pump system.

$$Q_{ref} = Q_{leak} \cdot (1 + 0.5) = 18kW \tag{3.4}$$

This value corresponds to a reliquefaction capacity of about 125 kg/h of BOG (0.0348 kg/s) according to equation 3.3.

## 3.3 Refrigerant

The only refrigerant fluid used in the present thesis is pure Nitrogen, the reasons for this choice are:

- Nitrogen changes phase at temperatures that are near to the LNG tank temperature (Figure 3.5);
- Nitrogen is safe, non-flammable, non-polluting, cheap and available, and already used as inerting fluid in on-board LNG processes.

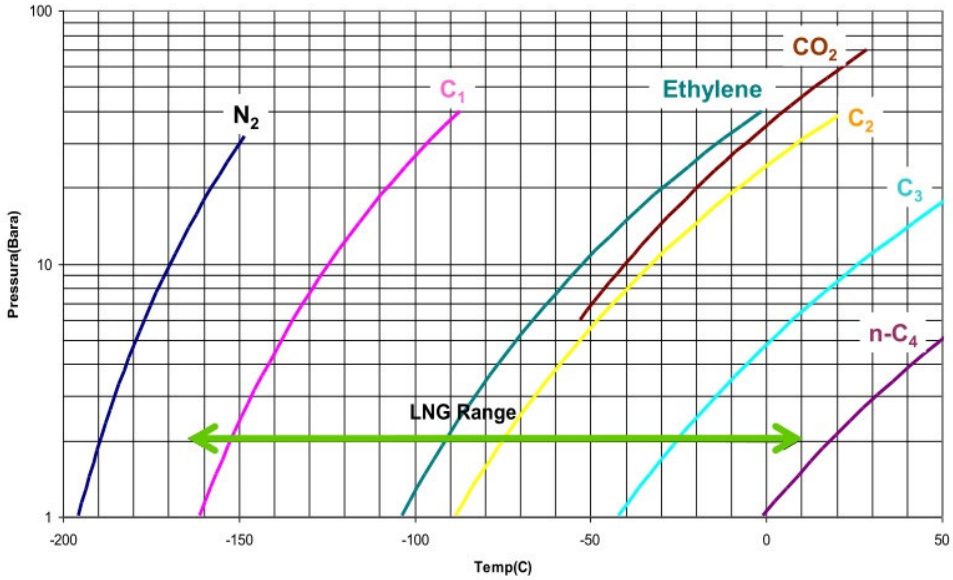


Figure 3.5: Vapor pressure of pure fluids relevant for LNG processes [47]

Other refrigerants could have been considered, in particular pure Methane and mixtures of Nitrogen and Methane. However introducing flammable components in the refrigerant mixture would require many additional safety measures (e.g. double wall ventilated piping, gas dangerous designation for valves, flanges, etc...) and increase the plant complexity. This can be acceptable on a LNG Carrier where gas handling systems already exist and the personnel is trained to oper ate them, but it is probably not desirable when it comes to merchant ships [40]. Partly for this reason, but primarily due to time limitations these options were not investigated in this thesis.

# Chapter 4

# Computer simulations

This chapter presents the structure and the results of a HYSYS® Steady State model that was bult to simulate the performance of the process described in the main Process Flow Diagram in Figure 3.2. The commercial software HYSYS® version 8.3 provided by Aspen has been used, linked to the Aspen Simulation Workbook v8.2® . Results have been extracted in form of text reports and case studies and postprocessed with Excel® and Matlab® to generate plots and tables.

The same HYSYS model was used to simulate the system operation in different scenarios, this model is referred to as "Design" model because it is used to quantitatively define the main equipment characteristics for the design of the process. General equipment performance parameters were specified as inputs of the Design model, examples of these are MITA specifications or constraints for the heat exchangers and constant efficiencies of the rotating machinery. Other parameters related to the size of the equipment (e.g. heat exchanger UA value and flowrates, compressor and pump pressures and flowrates) are outputs of the Design model and were extracted in the form of Case Study plots and reports.

For a more complete analysis also a separate "Off-Design" model could have been built to analyse the part load operation of a defined process where the main equipment sizes are "locked". For example the hypothetical "Off-Design" model would get the heat exchangers' UA values and the compressor and pumps efficiency curves as inputs. Unfortunately due to time limitations the "Off-Design" model was not created in the course of this thesis, the "Design" model instead was run for different scenarios to provide a more complete analysis and to generate outputs that take into account the performance outside the normal operation. It should be clear to the reader that the results of the scenarios different from the normal operation scenario do not represent the operation of the same physical system at reduced load, but rather generate a new design

fit to the new operating conditions.

## 4.1 Model flowsheet

Figure 4.1 shows the HYSYS® model complete flowsheet, that inludes the heat pump loop, the FGSS and the Tank Reflux system, arranged is a similar fashion as the main PFD in Figure 3.2. The engines are not included in the model, but rather define the boudary conditions to the FGSS. The Streams and Unit Operations correspond mostly to actual process piping and equipment, in addition to those the flowsheet contains Adjust and Set operators (green) to manipulate the process variables and Spreadsheet operators to perform calculations. This model can simulate different configurations of pure Nitrogen refrigerant processes activating or deactivating the optional streams or pieces of equipment (Intercooler IC, REC, Expander, BOG Tank Reflux) by changing specifications or stream connections. A number of virtual Tees and Mixers (white) are used to split the connection between two consecutive unit operations in order to provide flexibility for editing the model and also to attribute simple and logical names to the streams in relation to the equipment they flow in or out.

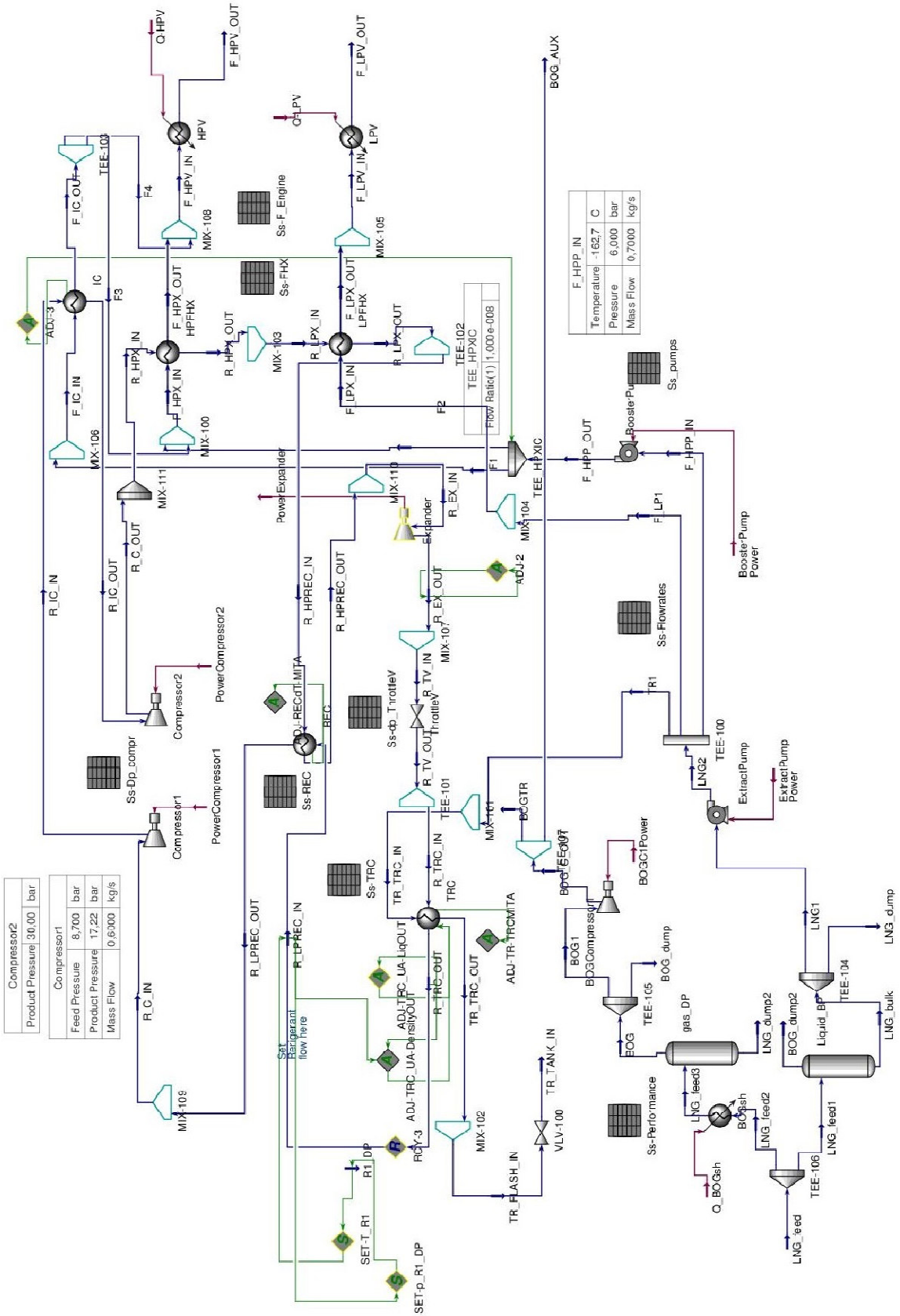


Figure 4.1: HYSYS® model complete flowsheet

### 4.1.1 LNG fuel tank model

The model includes a simple steady state model of the LNG fuel tank, shown in the orange box in Figure 4.2. The function of this part of the flowsheet is not to simulate the real thermodynamics of the cryogenic tank, which is out of the scope of the present thesis and in any case not suitable for a steady state analysis, but merely to provide accurate boundary conditions for the FGSS and for the Tank Reflux system. In other words the tank model is a calculation tool to define the thermodynamic properties of the streams "LNG1" and "BOG1" that are respectively the suction of the LNG LP pump and the suction of the BOG compressor.

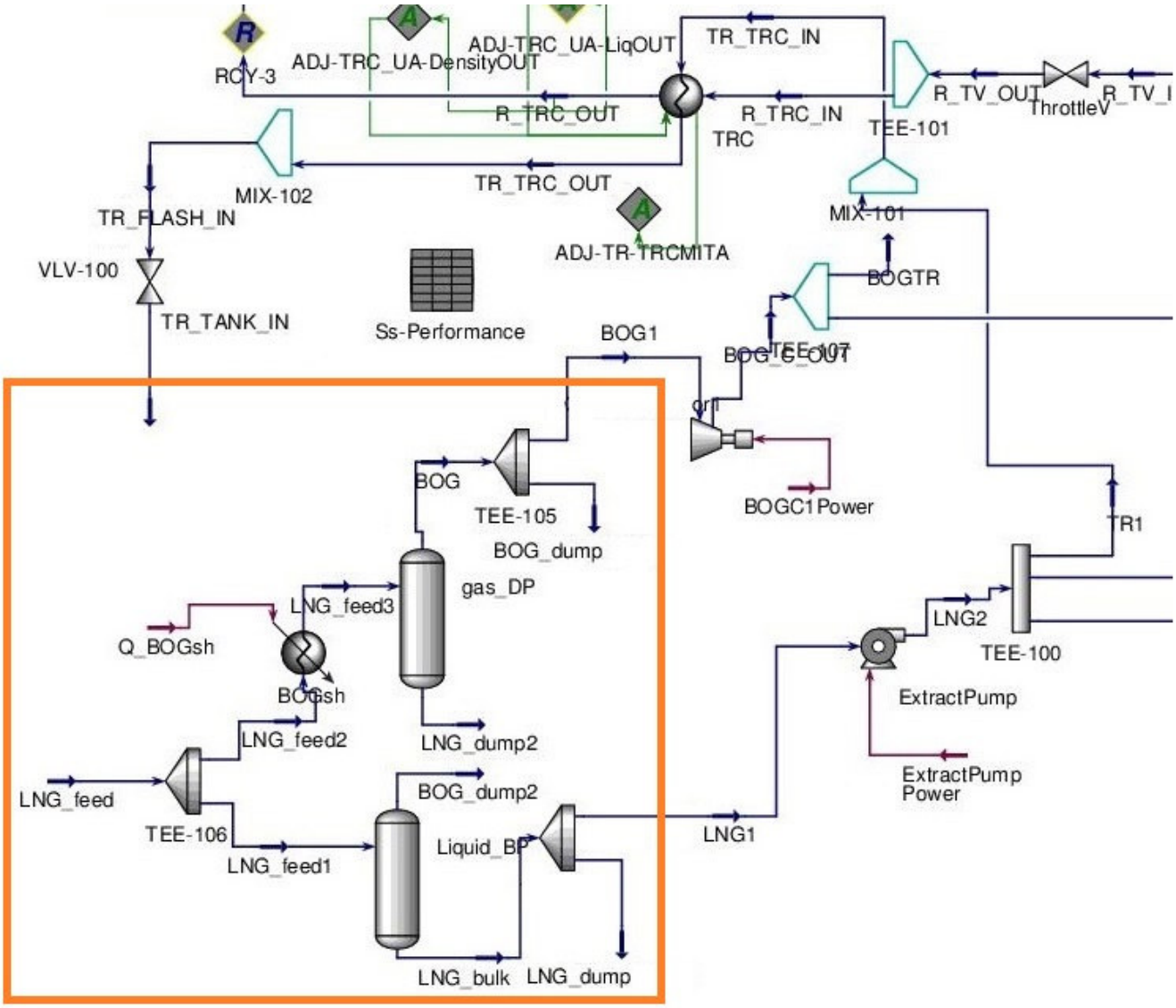


Figure 4.2: Hysys tank model PFD

In this model the LNG composition is defined in the stream "LNG-feed" which feeds the

whole fuel system, here also the pressure and temperature of the bulk liquid in the tank are specified. Part of this stream is directed to the separator "Liquid-BP" where saturated LNG liquid is separated and extracted with in specified flowrate defined by the inputs to the simulation. A second fraction of the "LNG-feed" stream is superheated to a slightly higher temperature corresponding to the tank atmosphere (BOG) temperature in equilibrium with a thin liquid layer on the gas liquid interface [34], it is possible to set the superheat of the BOG to zero in the "BOGsh" specifications, if the BOG is assumed to be in thermal equilibrium with the bulk liquid. The two phases of the superheated stream are also separated and a specified amount of BOG is extracted from the gas phase.
This model gives different compositions for the LNG and BOG that are extracted from the tank, as can be seen in table 4.1 and in the phase envelopes in figure 4.3, it is possible to tune the "LNG-feed" composition and temperature and the degree of BOG superheat to get realistic values of the bulk LNG and BOG composition and temperature. In this case the compositions and phase envelopes of the "LNG-feed" and "LNG1" streams are identical because the "LNG-feed" stream is saturated at the specified conditions.

Table 4.1: LNG and BOG composition at 1.04 bara

| Mole % | LNG-feed | LNG (-161.5 C) | BOG (-160 C) |
|---|---|---|---|
| N2 | 0,22 | 0,22 | 0,81 |
| C1 | 91,21 | 91,21 | 99,17 |
| C2 | 5,95 | 5,95 | 0,02 |
| C3 | 1,95 | 1,95 | 0,00 |
| n-C4 | 0,33 | 0,33 | 0,00 |
| i-C4 | 0,33 | 0,33 | 0,00 |
| C5 | 0,01 | 0,01 | 0,00 |

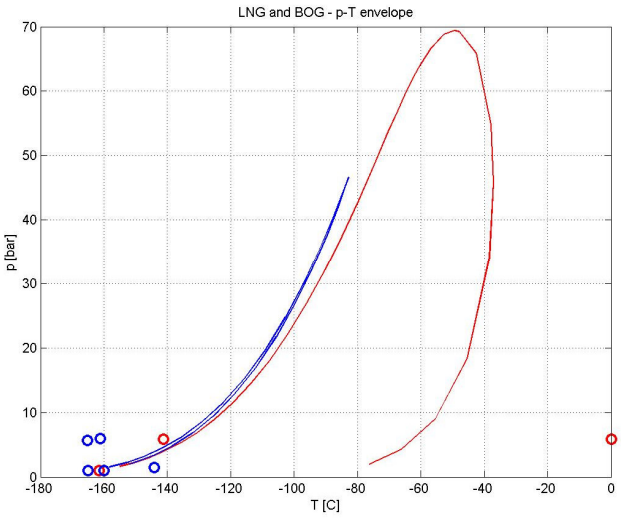


Figure 4.3: Fuel phase envelopes from HYSYS in the pressure-temperature diagram, LNG (red) and BOG (blue)

## 4.2 Design model structure

Even after understanding and defining the process structure and layout still a considerable part of the modelling work is left, that is the process of translating the system into a consistent and stable numerical model. It has been observed for the present case that, even though the model

flowsheet does not count a very large number of components, the tight integration between the various parts of the process can increase the calculation effort and undermine the model convergence, in particular in the circumstances where logical operators (like "Adjust" and "Recycle" [48]) compete with each other or with equipment specifications. In this chapter "Adjust" indicates a logical operator that varies one process variable to fullfill a specification that is to equalize a second variable to a target value, the "Recycle" instead is a non-sequential iterative operator that matches two consecutive streams and is used to resolve closed loops [48].
In order to solve convergence problems a considerable effort has been dedicated to achieving an effective placement of logical operators and a correct definition of constraints and specification. It was found that forcing a sequential solution of the flowsheet (ie. solving the flowsheet in the direction of the flow, from upstream to downstream) gives more stable and convergent model, to achieve this the heat pump loop was solved without the Recycle operator as described in the following "logical sequence":

- Fully define the heat pump loop feed stream "R-LPREC-IN": composition, pressure, vapor fraction (or superheat), flowrate;
- Adjust the REC Low Pressure side temperature increase to match the REC MITA ("AJD-RECdT-MITA");
- Input the heat pump high pressure value (Refrigerant Compressor outlet pressure);
- Calculate the throttle valve pressure drop to compensate compressors and heat exchangers pressure differences;
- Adjust the LNG reflux ("TR-LNG") flowrate to match TRC MITA ("ADJ-TR-TRCMITA");
- Adjust the TRC heat exchanger UA value so that its outlet matches the loop feed stream ("ADJ-TRC-UA-DensityOUT");
- Thanks to the previous operation the loop is consistent and one can now ignore the Recycle operator ("RCY-3").

The input parameters of the Adjust operators are shown in tables 4.2 and 4.3 for the Case Study and for the Sensitivity Analysis respectively, mode relaxed tolerances on the MITA were adopted in the Case Studies to enhance the convergence of the model, the tolerance on the density of the TRC outlet heat pump stream was not relaxed because the operator fullfills the energy balance of the system.

Table 4.2: Adjust settings for Case Studies

| Name | Control Variable | Min | Max | Step | Specification | Value | Tolerance |
|---|---|---|---|---|---|---|---|
| ADJ-TR-TRCMITA | TR mass flow [kg/s] | 1 | 9 | 0.3 | TRC MITA [C] | 9 | 4 |
| ADJ-RECdT-MITA | REC LP side $\Delta$T [C] | 5 | 60 | 4 | REC MITA [C] | 6 | 1 |
| ADJ-TRC-UA-DensityOUT | TRC UA [MJ/C-h] | 1.5 | 70 | 1 | density [kg/m$^3$] | feed | 0.1 |

Table 4.3: Adjust settings for Sensitivity Analysis

| Name | Control Variable | Min | Max | Step | Specification | Value | Tolerance |
|---|---|---|---|---|---|---|---|
| ADJ-TR-TRCMITA | TR mass flow [kg/s] | 1 | 9 | 0.3 | TRC MITA [C] | 5.5 | 0.5 |
| ADJ-RECdT-MITA | REC LP side $\Delta$T [C] | 5 | 60 | 4 | REC MITA [C] | 5.2 | 0.2 |
| ADJ-TRC-UA-DensityOUT | TRC UA [MJ/C-h] | 1.5 | 70 | 1 | density [kg/m$^3$] | feed | 0.1 |

Still under this settings it can occurr that the Adjust operators "ADJ-TR-TRCMITA" and "ADJ-TRC-UA-DensityOUT" compete and ruin the convergence of the model, probably due to the fact that they both influence the performance of the TRC heat exchanger. When this happened the convergency was restored either by relaxing the tolerance on the TRC MITA or by constraining the range of variation of the TRC UA value.

## 4.3 Inputs to Design Model

This chapter lists the assumptions and the numerical inputs to the HYSYS Design model. The Equation Of State used in all the simulations is the cubic Peng Robinson, which is a standard choice for non-polar real hydrocarbon mixtures [49], [50, p.51]. The LNG composition was calculated from a database of compositions from different production plants in the world (Table 4.4), the average adjusted composition that was used in this study is reported in Table 4.5, where Butane is split between Normal and Iso Butane. As previously shown in Table 4.1 this composition was specified in the virtual feed stream "LNG-feed" in the fuel tank model.

Table 4.4: Typical LNG Composition form major export terminals, in Volume % [8, p.6]

| Plant | Country | $C_1$ | $C_2$ | $C_3$ | $C_4$ | $C_{5+}$ | $N_2$ | LHV (MJ/kg) | Methane N (-) |
|---|---|---|---|---|---|---|---|---|---|
| Arzew | (ALG) | 87.4 | 8.6 | 2.4 | 0.05 | 0.02 | 0.35 | 49.11 | 72.7 |
| Bintulu | (MAS) | 91.23 | 4.3 | 2.95 | 1.4 | 0 | 0.12 | 49.35 | 70.4 |
| Bonny | (NGR) | 90.4 | 5.2 | 2.8 | 1.5 | 0.02 | 0.07 | 49.35 | 69.5 |
| Das | (UAE) | 84.83 | 13.39 | 1.34 | 0.28 | 0 | 0.17 | 49.26 | 71.2 |
| Badak | (INA) | 91.09 | 5.51 | 2.48 | 0.88 | 0 | 0.03 | 49.48 | 72.9 |
| Kenai | (USA) | 99.8 | 0.1 | 0 | 0.1 | 0 | 0.1 | 50.02 | 98.2 |
| Lumut | (BRU) | 89.4 | 6.3 | 2.8 | 1.3 | 0.05 | 0.05 | 49.36 | 69.5 |
| Point | (TRI) | 96.2 | 3.26 | 0.42 | 0.07 | 0.01 | 0.01 | 49.91 | 87.4 |
| Ras | (QAT) | 90.1 | 6.47 | 2.27 | 0.6 | 0.03 | 0.25 | 49.32 | 73.8 |
| Skikda | (ALG) | 91.5 | 5.64 | 1.5 | 0.5 | 0.01 | 0.85 | 48.97 | 77.3 |
| Withnell | (AUS) | 89.02 | 7.33 | 2.56 | 1.03 | 0 | 0.06 | 49.36 | 70.6 |
| Snohvit | (NOR) | 91.9 | 5.3 | 1.9 | 0.2 | 0 | 0.6 | 49.20 | 78.3 |
| Average | - | 91.07 | 5.95 | 1.95 | 0.66 | 0.01 | 0.22 | 49.39 | 75.98 |

Table 4.5: LNG composition for the Design model, properties calculated with HYSYS at the reference tank conditions -161.5℃, 1.04 bara.

| Property | Value | UOM |
|---|---|---|
| $N_2$ | 0,22 | mole% |
| $C_1$ | 91,21 | |
| $C_2$ | 5,95 | |
| $C_3$ | 1,95 | |
| n-$C_4$ | 0,33 | |
| i-$C_4$ | 0,33 | |
| $C_5$ | 0,01 | |
| LHV | 49,33 | MJ/kg |
| density | 456,3 | kg/$m^3$ |

The specifications for the process equipment, modeled by HYSYS Unit Operations, are listed in Table 4.6.

Table 4.6: Unit Operations inputs to the Design model

| Unit Operation | Property | Value | UOM |
|---|---|---|---|
| LP Pump | efficiency | 75 | % |
| HP Pump | efficiency | 65 | % |
| Refrigerant Compressor | polytropic efficiency | 75 | % |
| BOG Compressor | polytropic efficiency | 70 | % |
| All HXs | MITA | 5 | ℃ |
| All HXs | pressure drop | 0.3 | bar |
| HX: LPFHX | pressure drop | 0.1 | bar |
| HX: TRC | outlet liquid fraction | 10 | % |

The first part of the table reports the efficiencies of the rotating machinery, the second part describes the specifications of the process Heat Exchangers (HXs). The Minimum Internal Temperature Approach (MITA) of all the process heat exchangers is set to be 5℃, this is a conservative value for a cryogenic process where pinch temperature differences can be as low as 1-3℃[51, p.215], [52]. A costant pressure drop of 30 kPa (0.3 bar) was attributed to all heat exchangers, except for the LPFHX that was assumed to be smaller. Finally the liquid fraction of the low pressure evaporating Nitrogen stream ("R-TRC-OUT") at the outlet of the TRC heat exchanger was specified with an arbitrary value of 10%, this value together with the pressure and flowrate fully defines the stream properties, therefore this can be considered the anchor point of the thermodynamic cycle.

Table 4.7 reports the input properties of some process streams that represent the boundary conditions to the model, since the heat pump cycle is only integrated with the FGSS and with the Tank Reflux System, the only boundary conditions are the LNG fuel tank conditions and the ship engines' feed requirements.

Table 4.7: Stream input properties

| Stream | Property | Value | UOM |
|---|---|---|---|
| LNG (fuel tank) | Temperature | -161,5 | ℃ |
| LNG (fuel tank) | pressure | 1,04 | bara |
| BOG (fuel tank) | Temperature | -160 | ℃ |
| LP Fuel (AUX) | pressure | 6 | bara |
| HP Fuel (MAIN) | pressure | 300 | bara |
| Fuel (MAIN+AUX) | Temperature | 45 | ℃ |

The tank is assumed to be slightly above atmospheric pressure, and the BOG almost in thermal equilibrium with the bulk LNG, regarding the engine feed the pressure and temperature

correspond to the specifications of ME-GI engines and 4-stroke gas diesel generators discussed in the previous chapters.

## 4.4 Design Model Simulation Results

Four cases were simulated with the Design model for normal operation (D-100%NCR) for part load operation (D-50%NCR and D-20%NCR) and for idle or harbour operation (D-0%NCR-100%AUX), as shown in the matrix in Figure 4.4.

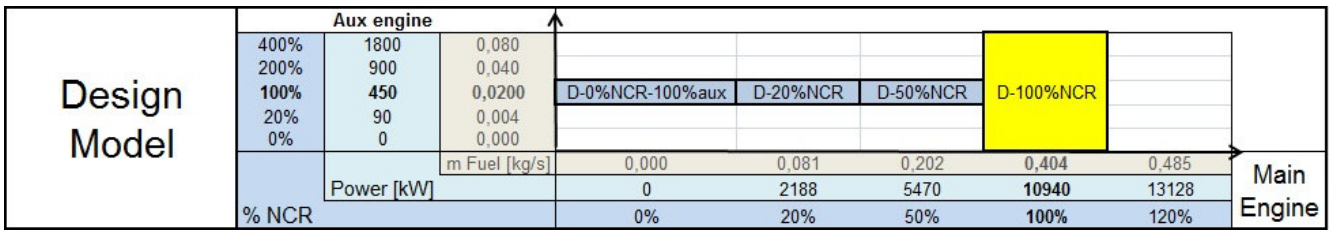


Figure 4.4: Simulation scenarios for the Design model

The horizontal axis of the matrix indicates the main engine power in kW and as a fraction of the Normal Continuous Rating (NCR), as well as the corresponding fuel consumption, the vertical axis shows the corresponding values for the set of Auxiliary engines. The four scenarios differ mainly for the main engine power and consequently for the fuel flowrate, in the part load cases the fuel flowrate is scaled down proportionally with the engine power assuming a constant thermal efficiency, which is a conservative assumption for the heat pump process. For simplicity the Auxiliary engine load was kept constant at the normal value and the effect of a Auxiliary load variation was studied in the sensitivity analyses.

### 4.4.1 Normal operation scenario: D - 100% NCR

Figure 4.5 is a performance map for the normal operation case (100%NCR), generated from Hysys Case Study tables postprocessed with Matlab. The map shows the values of some selected performance parameters of the system varying the heat pump higher pressure on the vertical axis, and the refrigerant mass flow on the horizontal axis. As the low pressure side of the heat pump cycle is kept constant to 9 bara (8.7 bara compressor suction) the compressor outlet pressure on the vertical axis is also proportional to its pressure ratio.

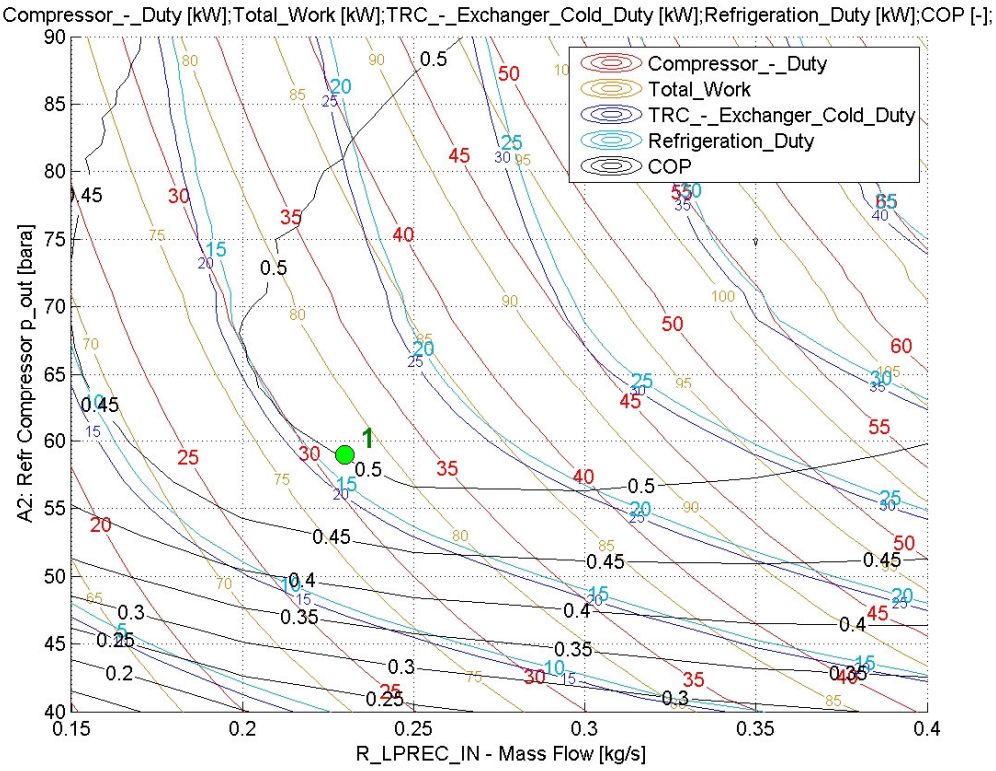


Figure 4.5: D-100%NCR: Performance map

It can be observed that the refrigerant compressor's work increases with increasing pressure ratio and mass flow, this adds to the other fairly constant power requirements of the Fuel Gas Supply System (here LP Pump and HP Pump) giving the total work. The duty of the heat pump evaporator (TRC heat exchanger) is also plotted and increases similarly as the compressor's work. The effective refrigeration duty is calculated from a energy balance on the tank (discussed in Appendix D.1) with the equation

$$\dot{Q}_{Ref} = m_{TR} \cdot (h_{LNG} - h_{TR\_TANK\_IN}) = m_{TR} \cdot (\Delta h_{TRC} - \Delta h_{LPP}) \tag{4.1}$$

this value is close to the TRC duty, but slightly lower due to the LP Pump (LPP) work input to the recirculation stream (TR-LNG).
The COP, calculated as

$$COP = \frac{\dot{Q}_{Refrigeration}}{\dot{W}_{RefCompressor}} \tag{4.2}$$

varies in the range 0.2 to 0.6 for the examined conditions, and drops rapidly when the high pressure is lower than 45-50 bara. For a target refrigeration requirement of 18 kW (from Equation 3.4) the system needs to be operated with a high pressure greater than 40-45 bara for

an acceptable COP, since the pure Nitrogen refrigerant's critical pressure equals 33.96 bar the present system constitutes a supercritical heat pump.
The constant COP lines show that there is a maximum COP for a given refrigeration duty, in other words if the refrigeration effect is held constant varying compressor pressure ratio and flowrate there exist a "optimum" value of the pressure ratio that minimizes the compressor's work. The same behaviour has been extensively studied for $CO_2$ transcritical heat pumps [53, 54, 55, 56] showing that the shape of the isotherms and of the compression path determine the existence of a optimum pressure for heat rejection in the supercritical region.

Based on the performance map above the near optimum operation point D-100%NCR has been selected in the maximum COP region for the specified cooling requirement and marked with a green dot in Figure 4.5. The main system parameters for this conditions are reported in the following Table 4.8 and in Figures 4.6 to 4.3.
Comparing the refrigeration duty and the COP from the table 4.8 and the performance map one can notice that the map underestimates the refrigeration duty by about 2 kW for the point examined, this is due to the fact that the tolerance on the adjust "ADJ-TR-TRCMITA" was relaxed to enhance the case studies convergence, therefore the flowrate of the LNG recirculation stream TR-LNG is mostly larger than required by the MITA constraint, giving a extra LP pump work of about 2 kW as energy input to the tank.

Table 4.8: D-100%NCR: Process Equipment mass and energy balance

| Equipment | Duty [kW] | m Ref [kg/s] | m Fuel [kg/s] | LP [bara] | HP [bara] |
|---|---|---|---|---|---|
| LP Pump | 3.08 | | 2.12 | 1.04 | 6.00 |
| HP Pump | 40.17 | | 0.40 | 6.00 | 300.90 |
| Ref Compr | 31.64 | 0.23 | | 8.70 | 59.00 |
| BOG Blower | 0.63 | | 0.02 | 1.04 | 1.50 |
| Total Work | 75.52 | | | | |
| HPFHX | 51.77 | 0.23 | 0.40 | 59.00 | 300.60 |
| LPFHX | 1.29 | 0.23 | 0.02 | 6.00 | 58.70 |
| REC | 11.62 | 0.23 | | 9.00 | 58.60 |
| TRC | 21.44 | 0.23 | 1.70 | 6.00 | 9.30 |
| Cooling Duty | 18.70 | | | | |
| COP | 0.59 | | | | |

Figure 4.6 shows the heat pump cycles in the Temperature-Duty diagram, where duty is calculated multiplying the refrigerant's enthalpy and mass flowrate. The red curves refer to the LNG tank, fuel streams and recirculation stream for the heat pump heat exchangers, each LNG curve is shifted along the horizontal axis to be aligned with the correspondent refrigerant curve

so that the plot can be read also as a cooling curve plot for each heat exchanger.

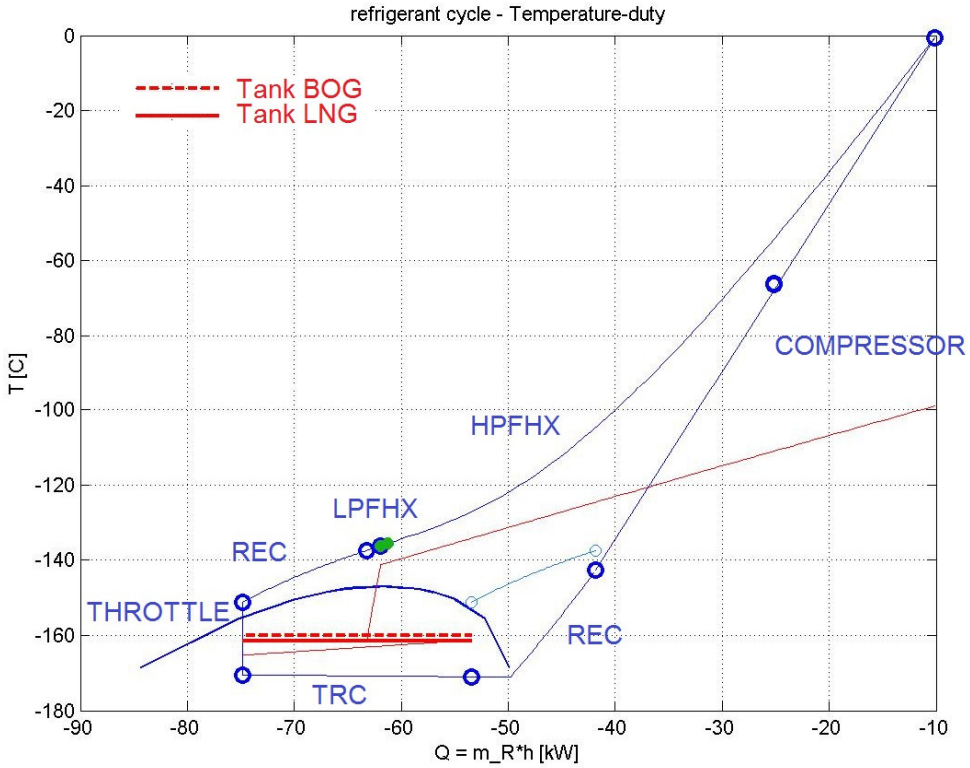


Figure 4.6: D-100%NCR: Refrigerant Temperature-Duty diagram

The diagram shows that the cold Nitrogen gas is compressed (in two consecutive stages without intercooling) and enters the HPFHX still below ambient temperature where it is cooled by the HP LNG, the green dots at the cold end of the HPFHX show the specified 5°C pinch point. The Nitrogen in the dense phase is further cooled in the LPFHX and in the recuperator (REC) before being throttled to the lower pressure inside the two-phase dome, here the fluid at 9 bar and -170°C evaporates with the heat from the subcooling LNG in the Tank Reflux system, after that it enters the REC that evaporates the 10% residual liquid and superheats the gas to the compressor's feed temperature.

Figures 4.7 and 4.8 show respectively the cycle in the pressure enthalpy diagram and the heat exchangers' temperature difference curves.

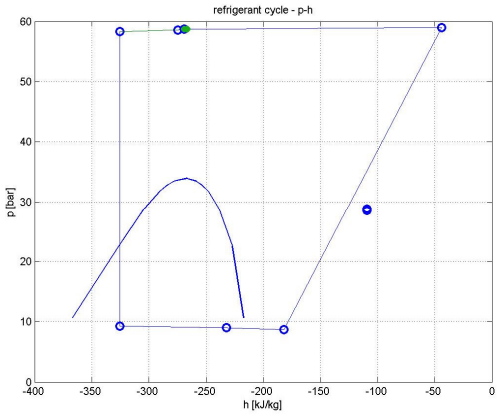


Figure 4.7: (D-100%NCR: Refrigerant cycle in the pressure - enthalpy diagram

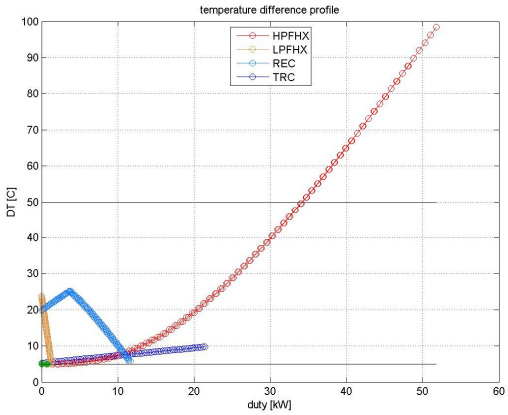


Figure 4.8: D-100%NCR: Temperature difference profile for process HX

The HPFHX is pinched at the cold end meaning that it is possible to decrease the LNG fuel flowrate at least by a small amount without changing the shape of the cycle, as confirmed by the sensitivity analysis in Figure D.68. The REC heat exchanger has a pinch at the hot end which sets a superior limit to the compressor's inlet temperature, if a warmer compressor's inlet is desired heat must be provided by another stream or in a different configuration.

The refrigeration duty of 18.7 kW corresponds to a reliquefaction capacity of of about 125 kg/h (Table 3.3), giving a energy consumption of 910-995 kJ/kg of reliquefied BOG inside the tank (0.25-0.28 kWh/kg) (the higher value includes the LP Pump energy consumption).

### 4.4.2 Sensitivity Analysis on the normal operation scenario: D - 100% NCR

Sensitivity Analyses (also called Parametric Studies) have been carried out on the design model for the normal operation scenario (D-100%NCR) to understand which parameters influence the performance of the cycle and where a more accurate estimate of the equipment properties is needed. Several parameters were varied in a range containing the normal value and the response of selected dependent variables relevant for the system performance was monitored.
In Figures D.64 to D.73 in the appendix Sensitivity Analyses are shown for each different parameter, Figure 4.9 below shows a summary of all the Analyses, the horizontal axis reports the percent variation of the parameters from the normal value while the vertical axis shows the percent variation of the COP for each Analysis.

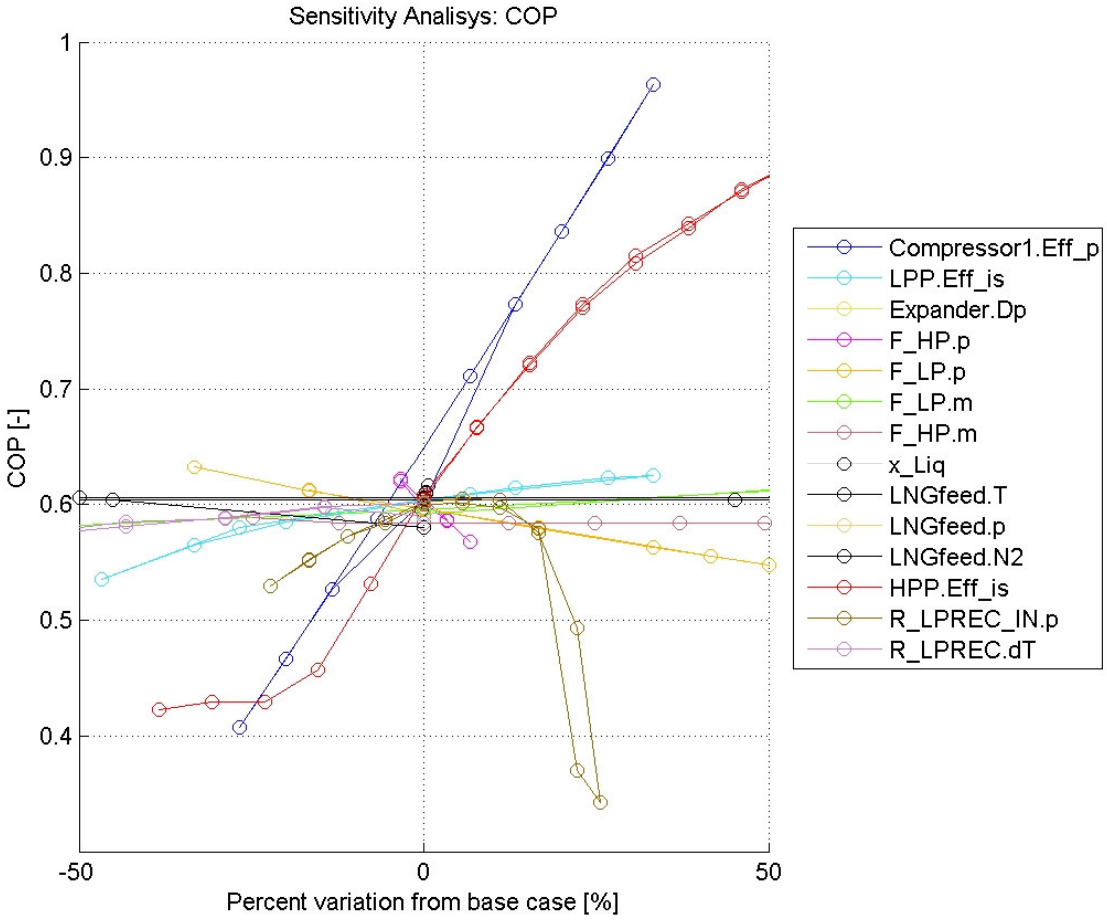


Figure 4.9: D-100%NCR: COP Sensivity for different parameters

It can be observed from Figure 4.9 that the most sensitive parameters for the COP are the following:

- HP Pump efficiency (Figure D.64);
  The HP LNG at the outlet of the HP pump is causing a process pinch in the HPFHX, this means that the temperature of the LNG at the inlet of the heat exchanger limits the amount of heat that can be extracted from the HP Nitrogen, and consequently the cooling capacity of the process. If the efficiency of the HP pump is reduced the temperature of the HP LNG increases and the perfomance of the system drops drastically. It is therefore important to assume a reasonable and conservative value of the efficiency of the HP Pump.

- Refrigerant Compressor efficiency (Figure D.62);
  As obvious the power requirement is affected by the compressor efficiency but not the refrigeration duty (a higher Nitrogen inlet temperature to the HPFHX can be handled by

the heating HP fuel), it is therefore less crucial to estimate the compressor efficiency accurately.

- TRC evaporation pressure (Figure 4.10).
  A higher evaporation pressure gives a lower compressor pressure ratio and work, at the same time if the evaporation temperature is too high the TRC heat exchanger will have to extract heat from the LNG under a small temperature difference and will require a higher LNG flowrate (TR-LNG) and a correspondently higher LP pump work. As the LNG recirculation stream (TR-LNG) is flashed back to the tank the LP pump work constitutes a energy input to the tank, therefore it is to be subtracted to the TRC duty to get the effective refrigeration effect (tank energy balance). For this reason an eccessive LNG recirculation flowrate reduces the refrigeration duty and the COP. In this configuration the LNG that is recirculated to the tank (TR-LNG) is delivered by the LP Pump at 6 bara and flashed back to the tank. If a dedicated pump was to be utilized only for the recirculation stream TR-LNG there would be no need to have a pressure as high as 6 bara, and the impact of the LP pump on the refrigeration duty and on the COP would be inferior.

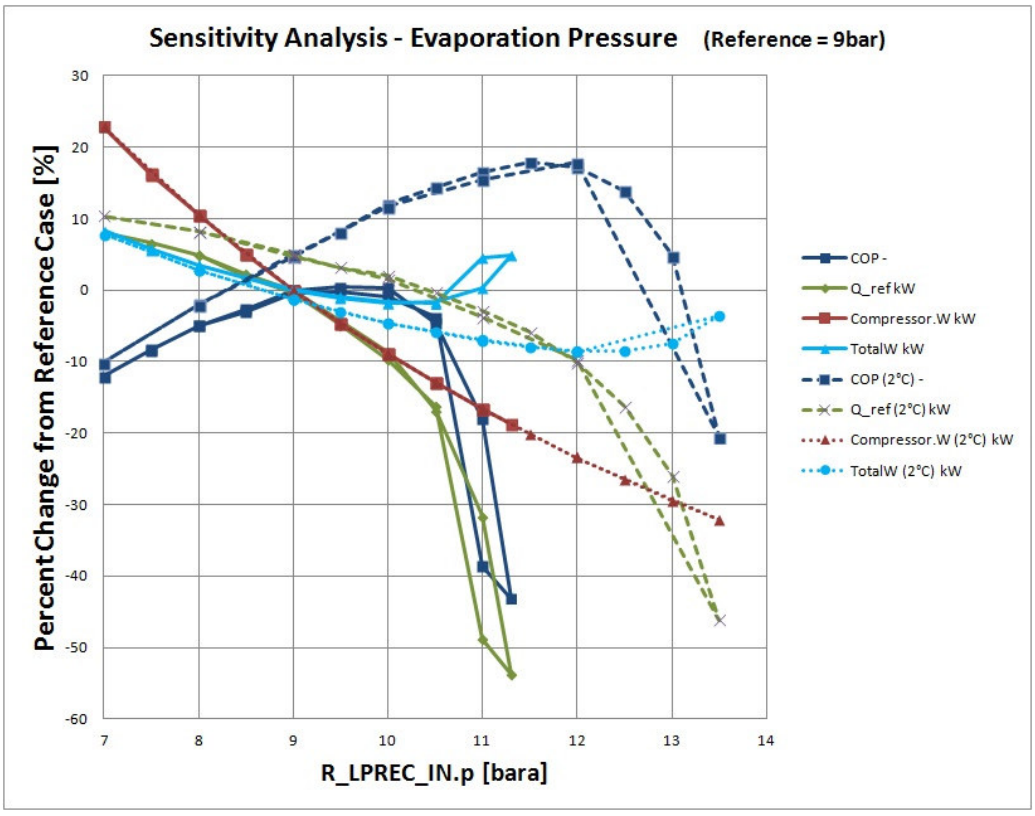


Figure 4.10: D-100%NCR: Sensitivity Analysys: Evaporation pressure

This analysis refers to a 5°CMITA specification for the evaporator (TRC), if the evaporator

MITA was lower the evaporation pressure could be slightly higher, for example if the evaporator MITA was set to 2℃(dotted line in Figure 4.10) the optimum evaporating pressure could be as high as 11-12 bara, for a COP about 18% higher than the reference case.

In addition to the above mentioned other important parameters are:

- REC low pressure side Temperature increase (Figure D.72);
  Even though it is not immediately visible from Figure 4.9 the role of the Recuperator (REC) heat exchanger is determinant to achieve a large refrigeration duty in the TRC heat exchanger and secondly to improve the COP. Because of this observation in the all the simulations carried out in this study the duty of the REC heat exchanger, or equivalently the temperature increase of its low pressure side stream, has been maximised until allowed by the MITA constraint.

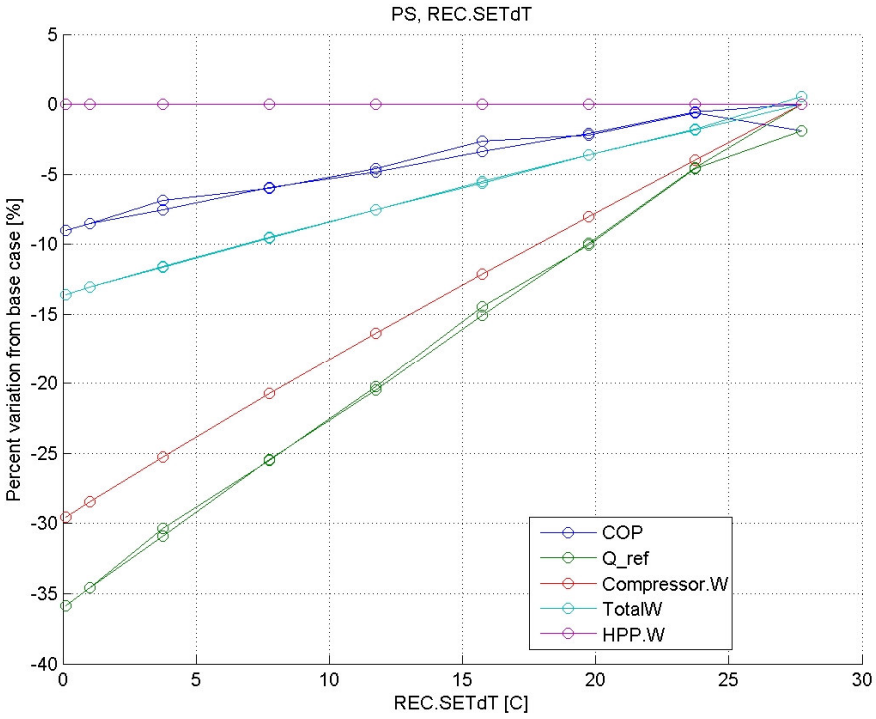


Figure 4.11: D-100%NCR: Sensitivity Analysys: REC Temperature increase on the LP side

- Refrigerant compressor suction temperature;
  With the current layout it is not possible to increase the compressor's suction temperature since the REC heat exchanger is pinched in the hot end, however there is an interest to evaluate the impact of a warmer compressor inlet on the process performance, due to

practical and economical considerations in the selection of the compressor. To assess this the model was modified inserting a heater between the REC and the compressor that increases the compressor suction temperature without affecting the upstream conditions, Figure 4.12 shows that the compressor energy consumption increases linearly with the suction temperature and is more than doubled if the suction is lifted to ambient temperature. If an air or seawater intercooler was included the compressor work would increase less in the right side of the graph where the first stage outlet temperature allows intercooling.

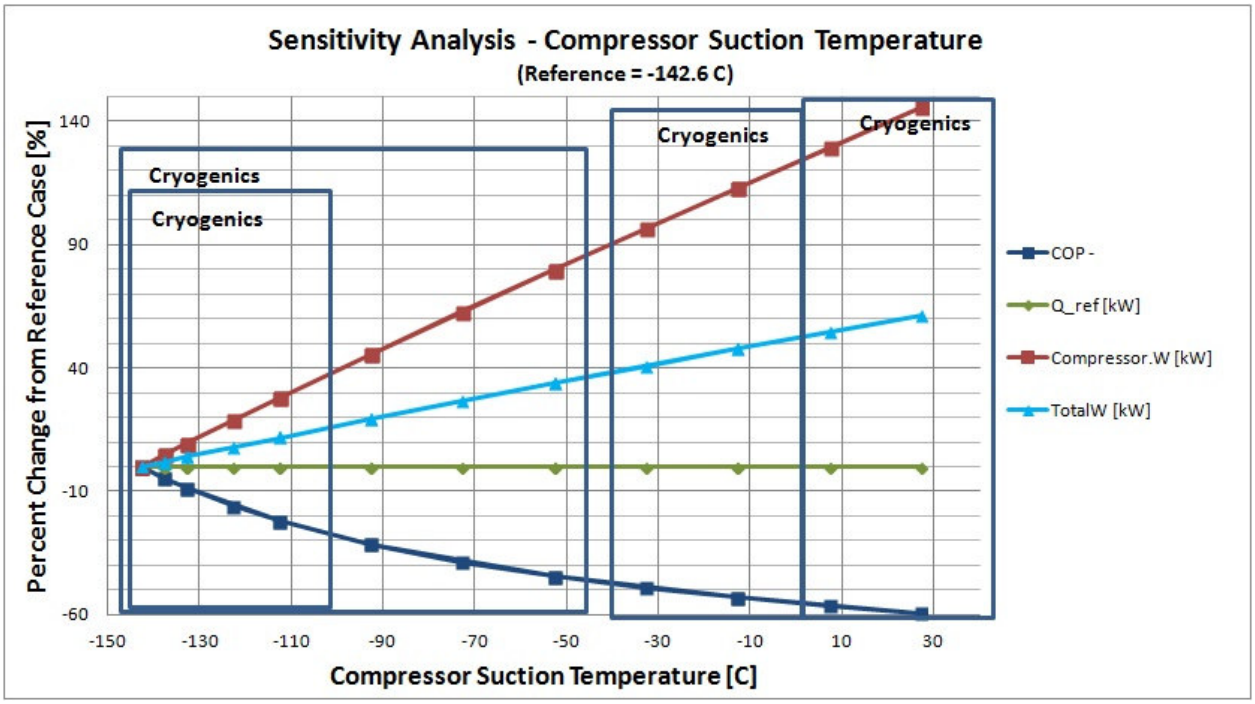


Figure 4.12: D-100%NCR: Sensitivity Analysys: Compressor suction temperature

- Use of expander instead of throttle valve;
  The benefit of using an expander upstream the throttle valve has been evaluated and the results are reported in Figures D.70 and D.71 in the appendix. In the sensitivity analisis the expansion was stopped near the Nitrogen critical pressure giving a increase in efficiency of 2-4%, depending on expander efficiency. Extrapolating the linear pattern it can be estimated that if the pressure was lowered until the evaporation pressure the efficiency would increase of about 4-8%. Since this gain in efficiency was considered modest the expander was switched off and it is not included in the results.

### 4.4.3 Part load scenario: D - 50% NCR

In the present chapter the operation of the system at 50% of main engine NCR, or equivalently at 50% of main engine fuel flowrate compared to the case 100% NCR, is analysed. Figure 4.13 shows the operation map generated by the two variable case study, similarly to Figure 4.5.

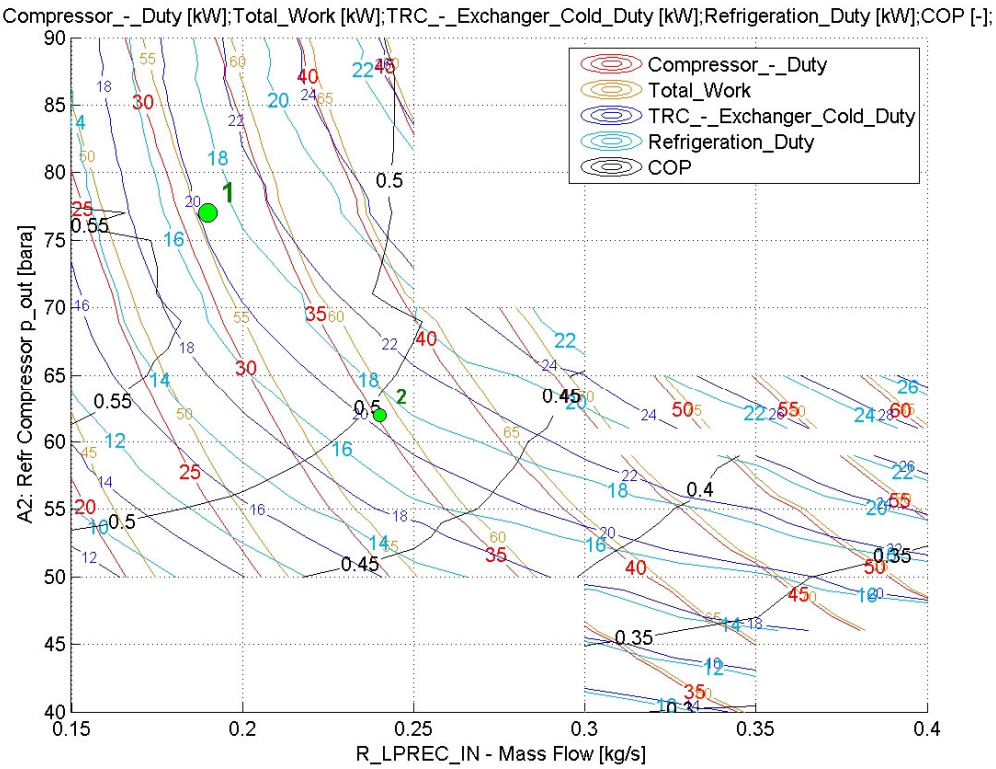


Figure 4.13: D-50%NCR: Operation map

The COP contour lines still show that for a given cooling duty (e.g. 18 kW) there exist an optimum pressure for heat discharge, in particular the pressure of 77 bar has been identified as a near optimum pressure for the selected cooling duty and the corresponding point 1 has been further analysed in Table 4.9 and in Figures 4.14 to 4.16. Details on point 2 are reported in the appendix D.2.

Table 4.9: D-50%NCR: Process Equipment mass and energy balance

| Equipment | Duty [kW] | m Ref [kg/s] | m Fuel [kg/s] | LP [bara] | HP [bara] |
|---|---|---|---|---|---|
| LP Pump | 2.79 | | 1.92 | 1.04 | 6.00 |
| HP Pump | 20.08 | | 0.20 | 6.00 | 300.90 |
| Ref Compr | 31.58 | 0.19 | | 8.70 | 77.00 |
| BOG Blower | 0.63 | | 0.02 | 1.04 | 1.50 |
| Total Work | 55.08 | | | | |
| HPFHX | 50.81 | 0.19 | 0.20 | 77.00 | 300.60 |
| LPFHX | 1.33 | 0.19 | 0.02 | 6.00 | 76.70 |
| REC | 9.53 | 0.19 | | 9.00 | 76.60 |
| TRC | 20.57 | 0.19 | 1.70 | 6.00 | 9.30 |
| Cooling Duty | 18.70 | | | | |
| COP | 0.59 | | | | |

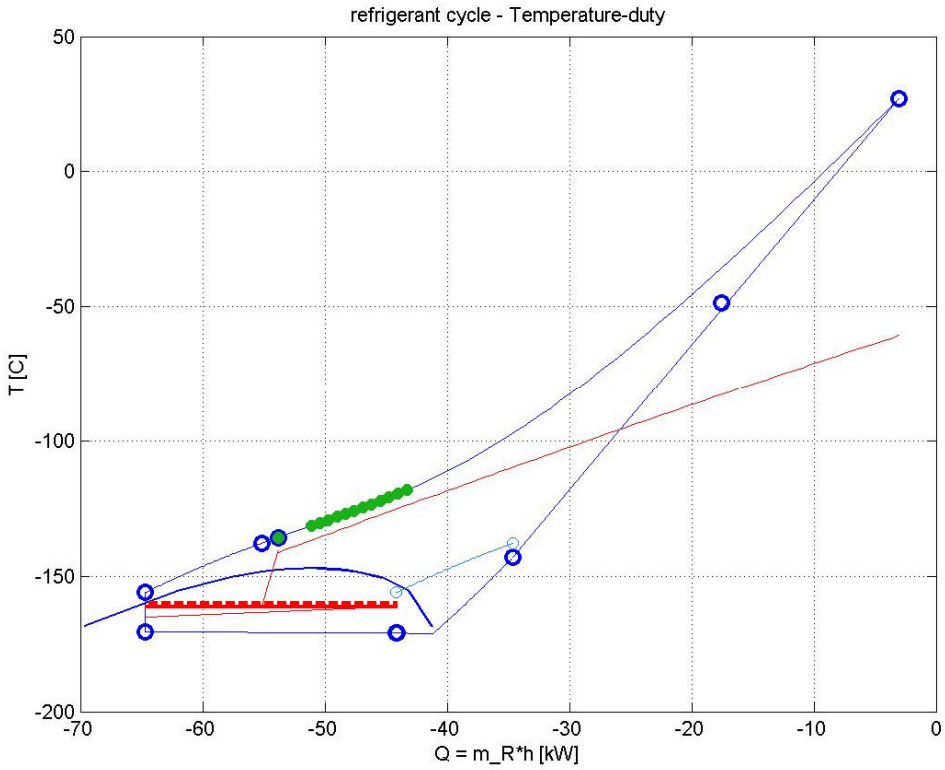


Figure 4.14: D-50%NCR: Refrigerant Temperature-Duty diagram

Compared to the normal operation case "D-100%NCR" the optimum pressure is now higher, the reason of this is that the HP fuel flowrate has decreased, correspondently its heat capacity in the HPFHX has decreased leading to a steeper heating path and pushing the cooling path of

the refrigerant to higher temperatures and pressure as shown in Figure 4.14.

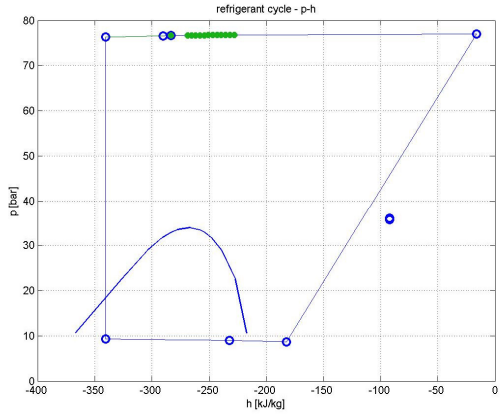


Figure 4.15: (D-50%NCR: Refrigerant cycle in the pressure - enthalpy diagram

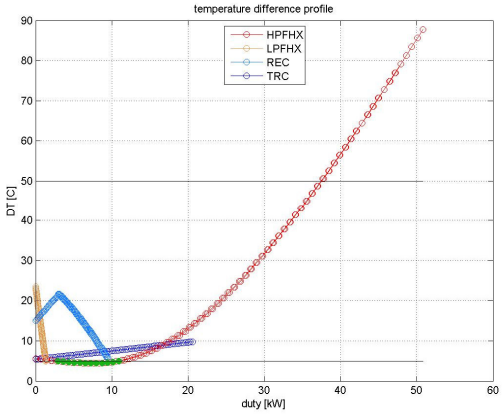


Figure 4.16: D-50%NCR: Temperature difference profile for process HX

### 4.4.4 Part load scenario: D - 20% NCR

Figure 4.17 represents the operation map for the part load scenario at 20% of the main engine NCR (or main engine gas flowrate). Differently from the higher load scenarios, in this map the shape of the cooling duty contour lines shows a minimum refrigerant high pressure value, below which it is not possible to achieve the desired cooling effect.

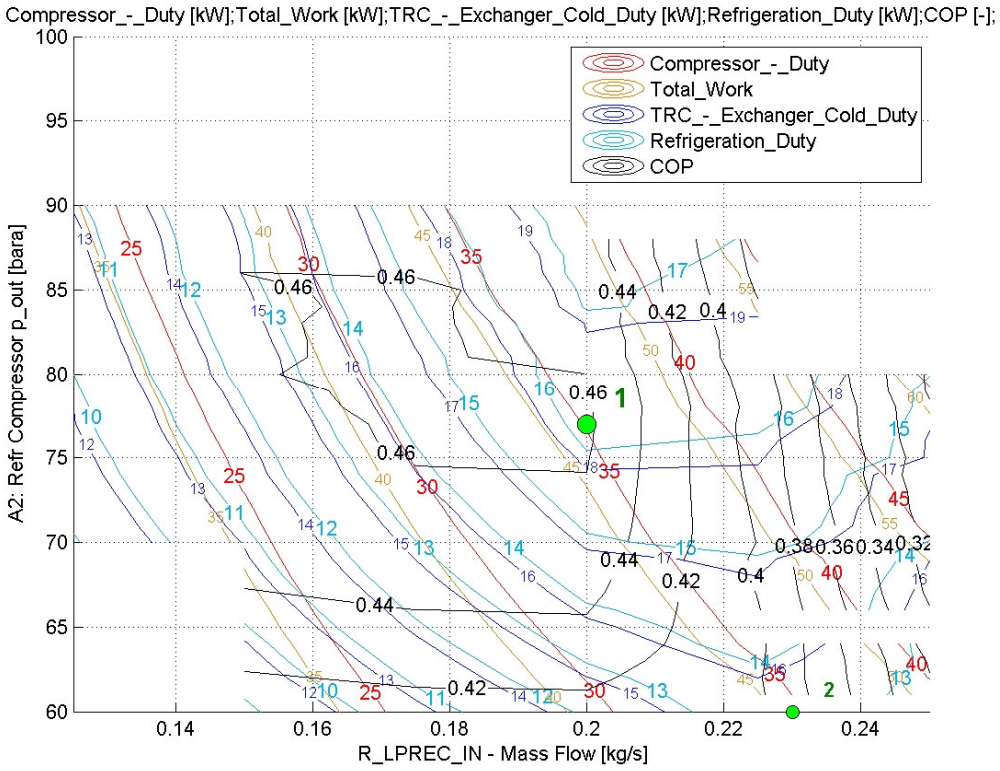


Figure 4.17: D-20%NCR: Operation map

In the limits of this map the target cooling duty of 18 kW is not reached because the calculations were stopped at 90 bar, therefore the cooling duty of 16 kW was chosen instead for the detail analysis in point 1 shown in the Table 4.10 and in Figures 4.18 to 4.20. Details on point 2 are reported in the appendix D.2.

Table 4.10: D-20%NCR: Process Equipment mass and energy balance

| Equipment | Duty [kW] | m Ref [kg/s] | m Fuel [kg/s] | LP [bara] | HP [bara] |
|---|---|---|---|---|---|
| LP Pump | 2.26 | | 1.56 | 1.04 | 6.00 |
| HP Pump | 8.05 | | 0.08 | 6.00 | 300.90 |
| Ref Compr | 35.40 | 0.20 | | 8.70 | 77.00 |
| BOG Blower | 0.63 | | 0.02 | 1.04 | 1.50 |
| Total Work | 46.34 | | | | |
| HPFHX | 44.62 | 0.20 | 0.08 | 77.00 | 300.60 |
| LPFHX | 9.30 | 0.20 | 0.02 | 6.00 | 76.70 |
| REC | 11.56 | 0.20 | | 9.00 | 76.60 |
| TRC | 18.48 | 0.20 | 1.46 | 6.00 | 9.30 |
| Cooling Duty | 16.06 | | | | |
| COP | 0.45 | | | | |

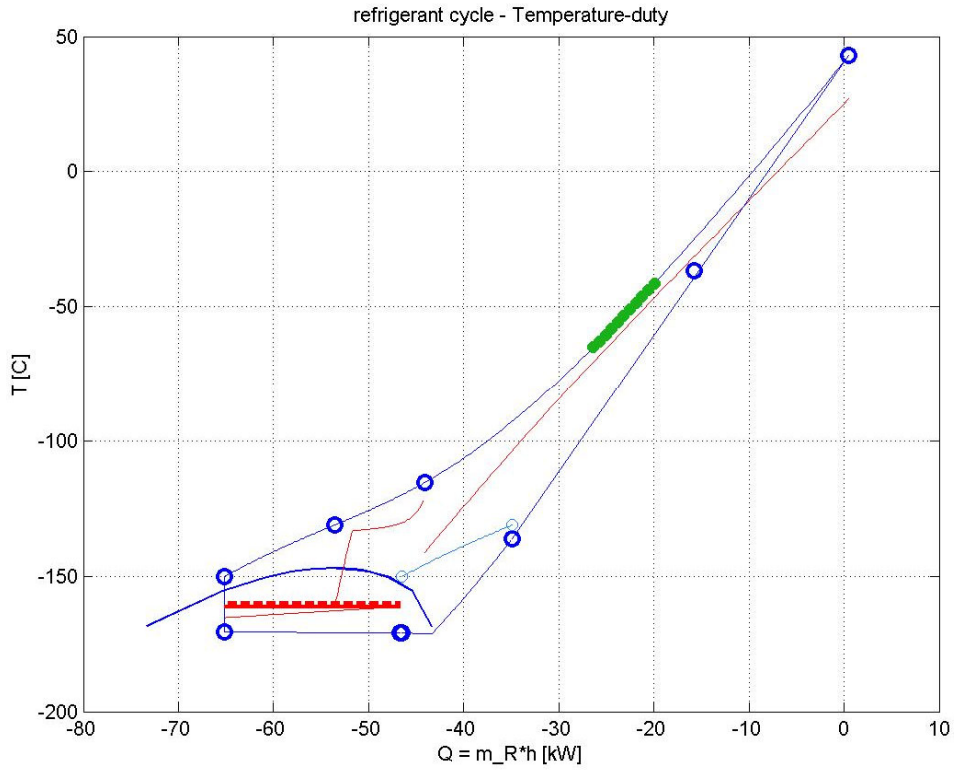


Figure 4.18: D-20%NCR: Refrigerant Temperature-Duty diagram

The plots show that the pinch point of the HPFHX has moved towards the center of the heat exchanger where the cooling curves are very sensitive on a variations in heat capacity of the two streams, this could be related to the rapid decay of performance with refrigerant flowrate, in

the right part of the operation map. It can also be observed that, unlike the previous scenarios, the LP LNG is evaporated in the LPFHX and not just heated in the liquid phase, and most importantly this heat exchanger's contribution to the cycle's energy balance is more substantial.

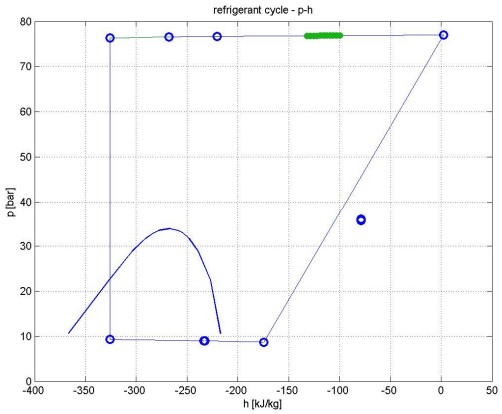


Figure 4.19: (D-20%NCR: Refrigerant cycle in the pressure - enthalpy diagram

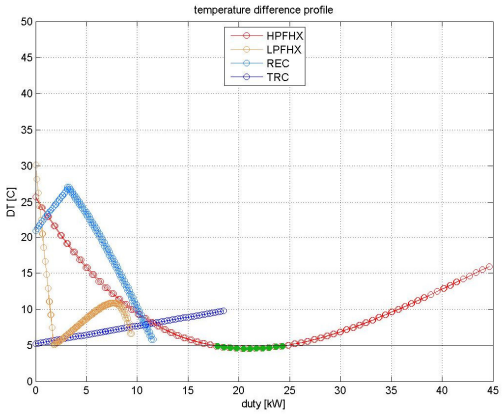


Figure 4.20: D-20%NCR: Temperature difference profile for process HX

### 4.4.5 Idle/Harbour scenario: D - 0% NCR - 100% AUX

This section describes the operation of the heat pump for the idle ship scenario where the main engine is shut down and the HP fuel flowrate corresponds to zero, this means that the HPFHX is not anymore contributing to the heat pump cycle which now uses only the LPFHX to discharge the heat. Figure 4.21 shows that the performance of the system is very poor in this scenario and it is not possible to achieve the target cooling duty of 18 kW. However keeping the refrigerant flowrate to very low values (roughly 1/3 of the normal and part load scenarios) it is still possible to produce a cooling effect of 4-6 kW, this is expected to be very much dependent on the load of the Auxiliary engines.

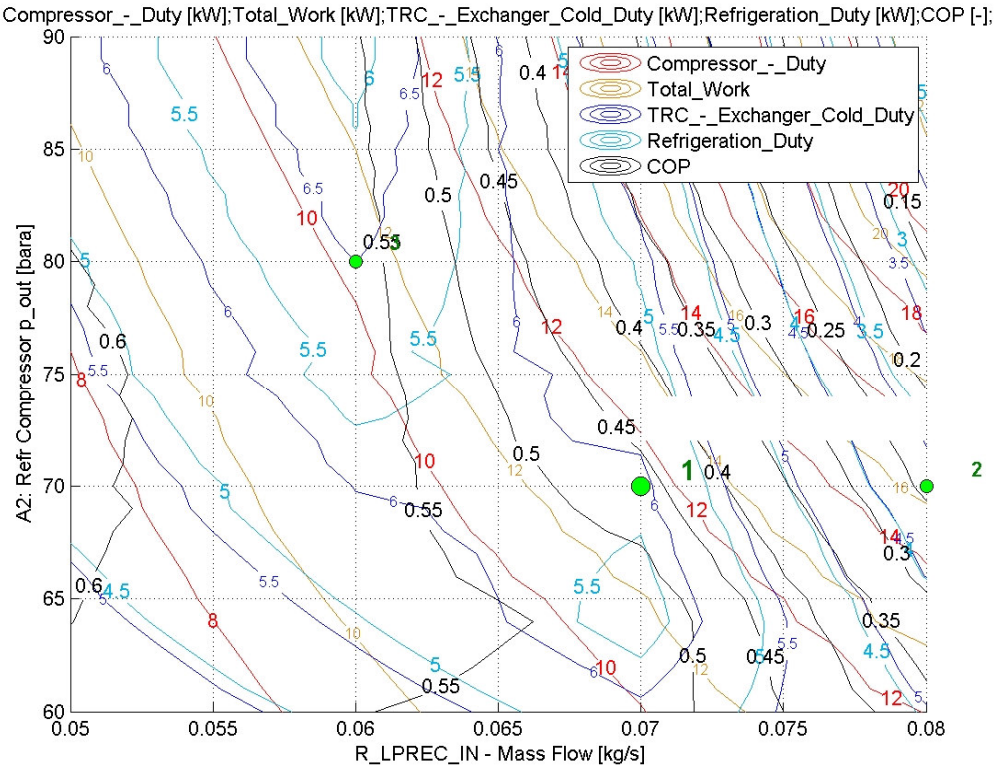


Figure 4.21: D-0%NCR-100%AUX: Operation map

An example of operation of this system is analyzed in the following Table 4.11 and in Figures 4.22 to 4.24. The red curve in Figure 4.22 shows that the LPFHX is now able to vaporize and superheat the LP LNG fuel up to ambient temperature.

Table 4.11: D-0%NCR-01: Process Equipment mass and energy balance

| Equipment | Duty [kW] | m Ref [kg/s] | m Fuel [kg/s] | LP [bara] | HP [bara] |
|---|---|---|---|---|---|
| LP Pump | 2.20 | | 1.52 | 1.04 | 6.00 |
| HP Pump | 0.00 | | 0.00 | 6.00 | 300.90 |
| Ref Compr | 11.61 | 0.07 | | 8.70 | 70.00 |
| BOG Blower | 0.63 | | 0.02 | 1.04 | 1.50 |
| Total Work | 14.44 | | | | |
| HPFHX | 0.00 | 0.07 | 0.00 | 70.00 | 300.60 |
| LPFHX | 17.15 | 0.07 | 0.02 | 6.00 | 69.70 |
| REC | 4.06 | 0.07 | | 9.00 | 69.60 |
| TRC | 6.06 | 0.07 | 1.50 | 6.00 | 9.30 |
| Cooling Duty | 4.50 | | | | |
| COP | 0.39 | | | | |

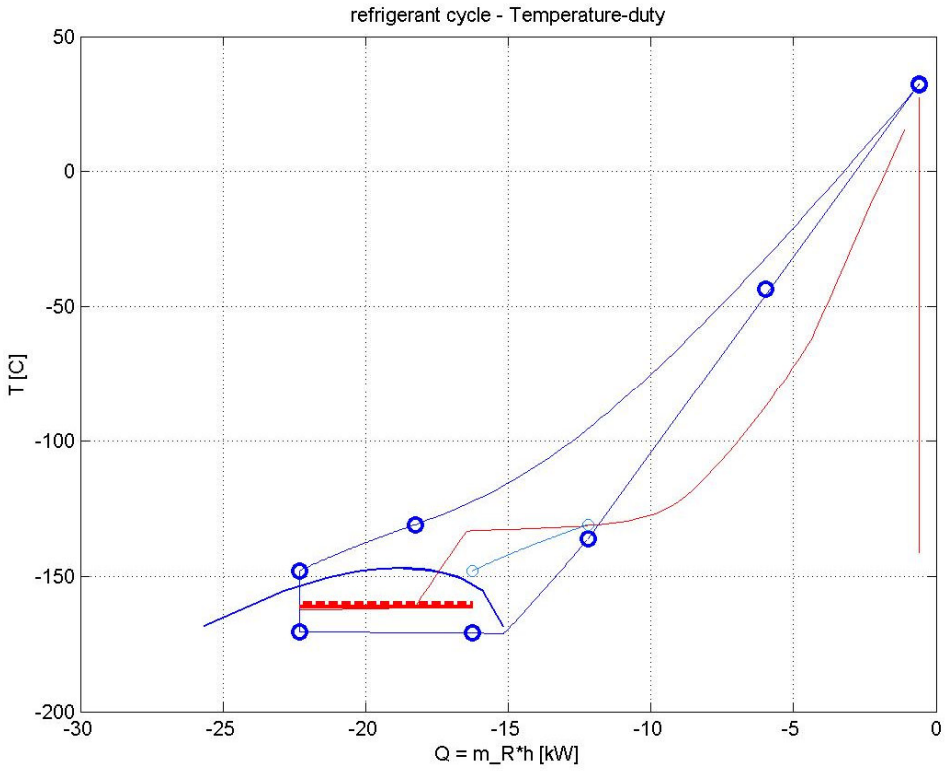


Figure 4.22: D-0%NCR-01: Refrigerant Temperature-Duty diagram

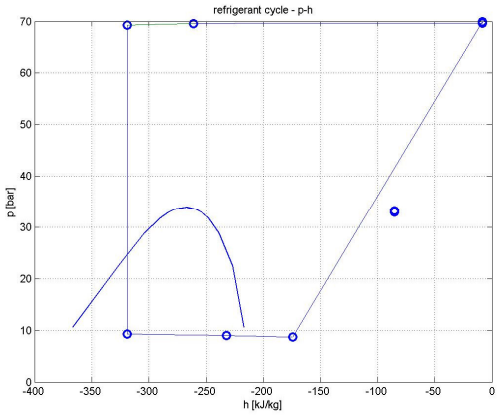


Figure 4.23: (D-0%NCR-01: Refrigerant cycle in the pressure - enthalpy diagram

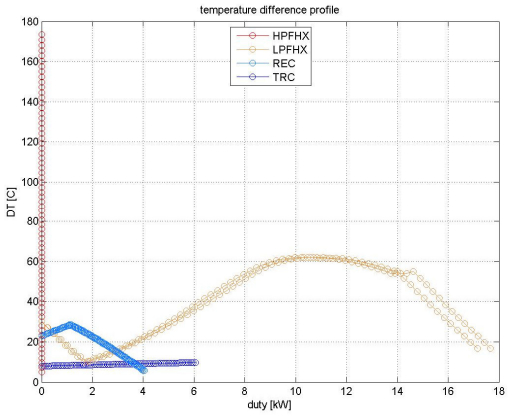


Figure 4.24: D-0%NCR-01: Temperature difference profile for process HX

## 4.5 Discussion of Simulation Results

The simulation results show that the process is able to cover the target refrigeration duty of 18 kW with a remarkably low energy consumption for the cases at 100% and 50% NCR. For the part load case at 20% NCR the heat pump can not generate the target duty in the pressure range explored in the case study, but can still extract 16 kW from the Tank Reflux system, which still exceeds the estimated heat leak of 12.5 kW. In the idle ship scenario "D-0%NCR-100%AUX" the heat pump has a very poor performance and can not generate more than 4-5 kW of effective cooling, which is insufficient to cover the estimated heat leak.

The performance of the heat pump process is compared to two commercially available reliquefaction processes for LNGC in Figure 4.25: the blue series represents the family of Nitrogen Brayton cycles from Table 2.1 (among those the Moss/Hamworthy cycle), the green series represents the Mini LNG process by Sintef.

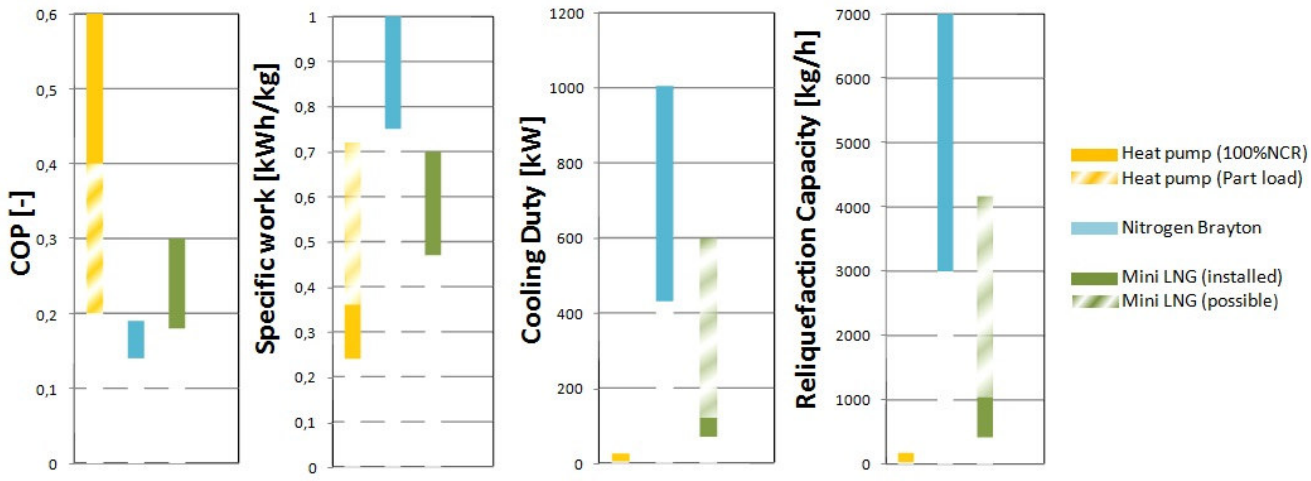


Figure 4.25: Comparison of the heat pump performance and capacity with commercially available liquefaction processes for LNGC [13, 31, 34], COP and specific work are related to each other through the evaporation enthalpy of the BOG, so are cooling duty and reliquefaction capacity

From the COP and specific work bars it appears that the process is about 3 times more efficient than the Nitrogen Brayton cycles and 2 times more efficient than the Mini LNG process, in its normal load scenario, for part load scenario the performance degrades to the level of the Mini LNG process, the brilliant performance of the system is attributable to the complete heat integration between the cycle and the FGSS and the low temperature compression.
On the other hand the cooling duty and reliquefaction capacity bars show that the application ranges of the three systems are extremely different: the Nitrogen Brayton cycles offer a very

high capacity that suits the requirements of large LNG Carriers, the novel Mini LNG saw its first installation on a small multigas carrier but the design can in principle be scaled up as shown by the dotted bar. The heat pump capacity however is only a fraction of that of the reliquefaction processes, mainly because the main engine fuel flowrates limits the load of the heat pump system as no heat is discharged to the environment. This is not necessarily a disadvantage since the heat pump is designed for LNG-fuelled ships for which the tank size and the heat leak increase proportionally with the fuel consumption, but it indicates that the heat pump process can not be used for LNG Carriers unless radical modifications are introduced.

To sum up the structural differences between the heat pump and the reliquefaction cycles, in particular the absence of heat discharge to the environment, constitute both the strength of the process represented by its high efficiency and the weaknesses such as poor performance at low loads and limited capacity.

## 4.6 Evaluation of alternative process layouts

### 4.6.1 BOG feed to Auxiliary engines

According to the heat leak calculations in chapter 3.2.3 the estimated heat leak in the tank would yield a LNG evaporation rate of 86,83 kg/h or 0.024 kg/s, this value is comparable with the normal Auxiliary engine fuel consumption of 0.02 kg/s. This means that, if a BOG compressor is installed, most of the normal BOG generated by the heat leak in the tank can be fed to the Auxiliary engines, thereby reducing the cooling requirement for the heat pump dramatically. Figure 4.26 compares the energy consumption of a compressor to feed the BOG to the Auxiliary engine at 6 bar with the heat pump work in the normal scenario per 1 kg of reliquefied BOG, it shows that it is more efficient to compress the BOG for the Auxiliary engine than to reliquefy the same amount.

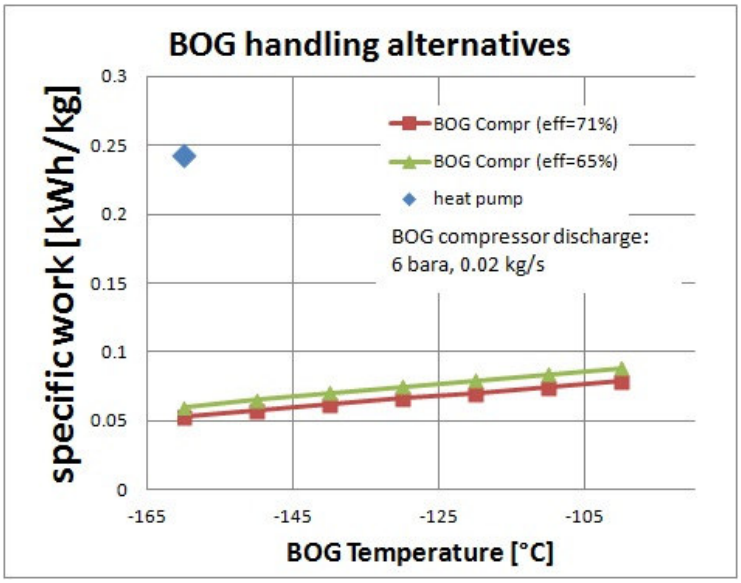


Figure 4.26: Comparison of energy consumption for BOG compression for Auxiliary engine and recondensation with the heat pump process

According to this analysis there is reason to believe that BOG compressor should be the preferred option to feed the Auxiliary engines in most situations where BOG is available in sufficient amount. This operation mode is described in Figure 4.27) where the LP liquid fuel supply line is shutdown and the LPFHX is bypassed. Since part of the BOG is handled by the Auxiliary engines the heat pump can operate for a reduced time (in case of On/Off operation), or at a reduced load if this allows the achievement of a better COP. Moreover the LP Pump can be set to work at a lower discharge pressure with a further increase of the overall efficiency of the heat pump process (Figure D.67).

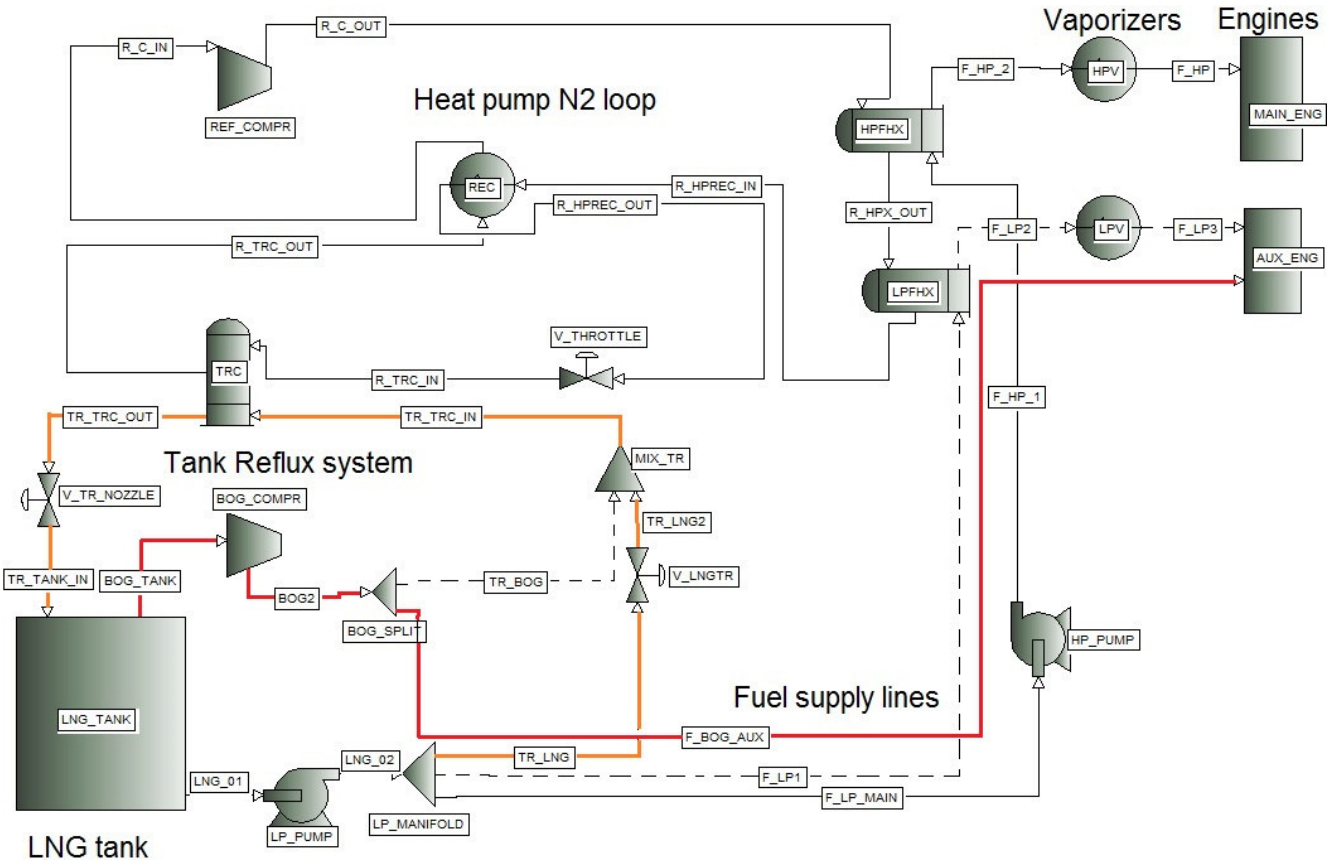


Figure 4.27: Preferred operation mode of the heat pump process, with compressed BOG feed to the Auxiliary engines

It should be taken into account that the exclusion of the LPFHX has a negative impact on the efficiency of the heat pump that varies according to the scenario. For the Normal operation (D-100%NCR) it is calculated that the COP can drop by only 5% if the LPFHX does not contribute to the heat pump cycle (Figure D.69), therefore the use of the BOG compressor is recommended in this scenario. If the ship is Idle (D-0%NCR-100%AUX) the heat pump can not operate without the LPFHX, therefore the choice to compress the BOG in this scenario will imply that the heat pump is shut down. This could be the best choice since the refrigeration duty of 5 kW that the heat pump can provide in the "Idle" operation of the ship can reliquefy about 0.009 kg/s of BOG which accounts for less than half of the Auxiliary fuel consumption.

Even if the the previous arguments show that the LPFHX could be unused most of the times there are still a some scenarios where the LPFHX could prove useful, for example:

- If the ship is idle and the Auxiliary fuel consumption exceeds the BOG generation rate, but the heat pump needs to run at reduced load to maintain the temperature in the Nitrogen circuit;

- If the ship is idle or manouvering, and the heat pump is used to cool down the bunker line and the tank prior to bunkering.

### 4.6.2 Intercooled heat pump cycle

Within this chapter the effect of an intercooler (IC) in the refrigerant compressor is assessed, since the compression takes place almost entirely below ambient temperature the only possible intercooling can be done with a cryogenic medium, here HP fuel was selected as a intercooling fluid in a parallel arrangement with the HPFHX as described by Figure 4.28.

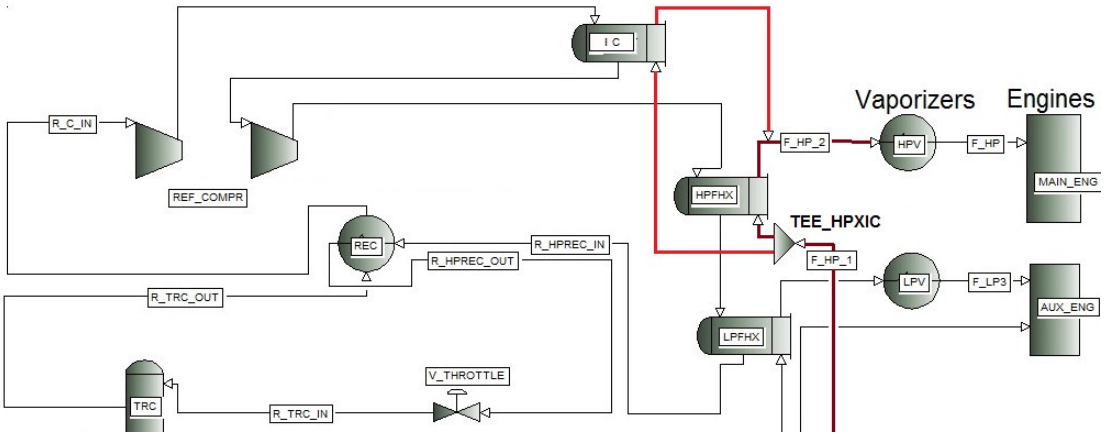


Figure 4.28: Process layout with refrigerant compressor Intercooling by HP fuel

The simulation results in this chapter refer to a case with higher fuel flowrates than the case D-100% NCR, precisely 73% more for the main engine (the inconsistency with the cases presented so far is due to the fact that the intercooler analysis was performed before the reference case selection and was not considered worth repeating afterwards).
To study the performance of the cycle with intercooler the intermediate pressure and the amount of HP fuel to the intercooler were varied in a case study in Figure 4.29. The horizontal axis contains the fraction of the HP fuel flowrate that is diverted to the intercooler (red stream in Figure 4.28), when the Tee flow ratio is zero all the HP fuel is directed to the HPFHX and there is no intercooling. The vertical axis represents the ratio between the first stage pressure rise and the total pressure rise of the compressor, as in equation 4.3.

$$\Delta p_{fraction} = \frac{\Delta p_{Stage1}}{\Delta p_{Tot}} = \frac{p_{IC} - p_{in}}{p_{out} - p_{in}} \tag{4.3}$$

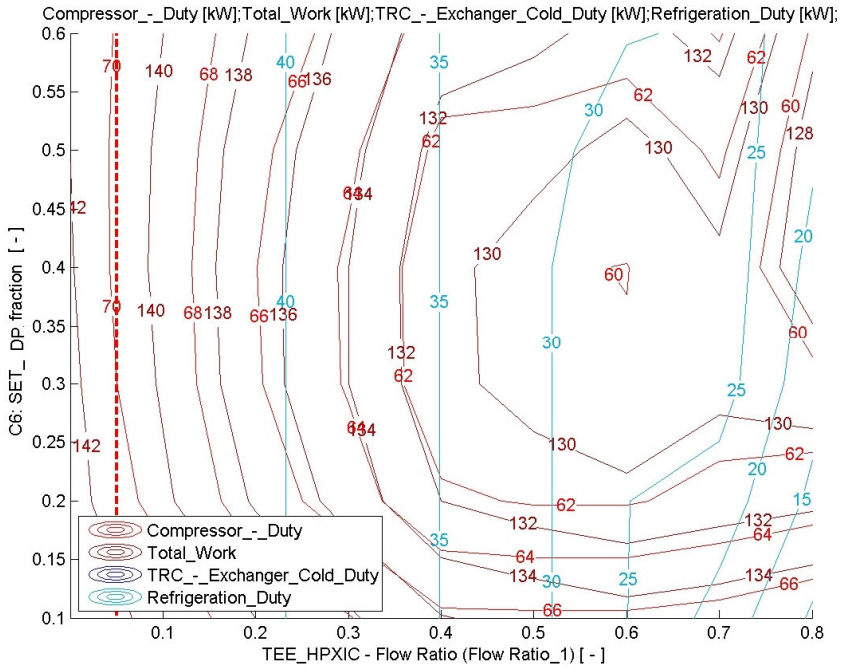


Figure 4.29: Operation map of the refrigerant compressor intercooler IC

The figure shows that there is an optimum intercooling pressure corresponding to a first stage pressure rise of about 40% of the total, at the same time the cooling duty lines show that diverting the HP fuel towards the IC and subtracting it to the HPFHX reduces the refrigeration capacity of the heat pump. An example of operation of this system with a $\Delta$p fraction of 0.4 and a flow ratio of 0.2 is analyzed in the following Table 4.12 and in Figures 4.30 to 4.32.

Table 4.12: Case "173%NCR" with IC: Process Equipment mass and energy balance

| machine | Duty [kW] | m Ref [kg/s] | m Fuel [kg/s] | LP [bara] | HP [bara] |
|---|---|---|---|---|---|
| LP Pump | 8.80 | | 5.92 | 1.04 | 6.00 |
| HP Pump | 61.84 | | 0.70 | 6.00 | 300.90 |
| Ref Compr | 65.38 | 0.80 | | 8.70 | 40.00 |
| BOG Blower | 0.62 | | 0.02 | 1.04 | 1.50 |
| Total Work | 136.64 | | | | |
| HPFHX | 83.77 | 0.80 | 0.56 | 40.00 | 300.60 |
| LPFHX | 1.86 | 0.80 | 0.03 | 6.00 | 39.70 |
| REC | 30.46 | 0.80 | | 9.00 | 39.60 |
| IC | 19.33 | 0.80 | 0.14 | 21.22 | 300.90 |
| TRC | 39.61 | 0.80 | 5.19 | 0.80 | 5.19 |
| Cooling Duty | 31.16 | | | | |
| COP | 0.48 | | | | |

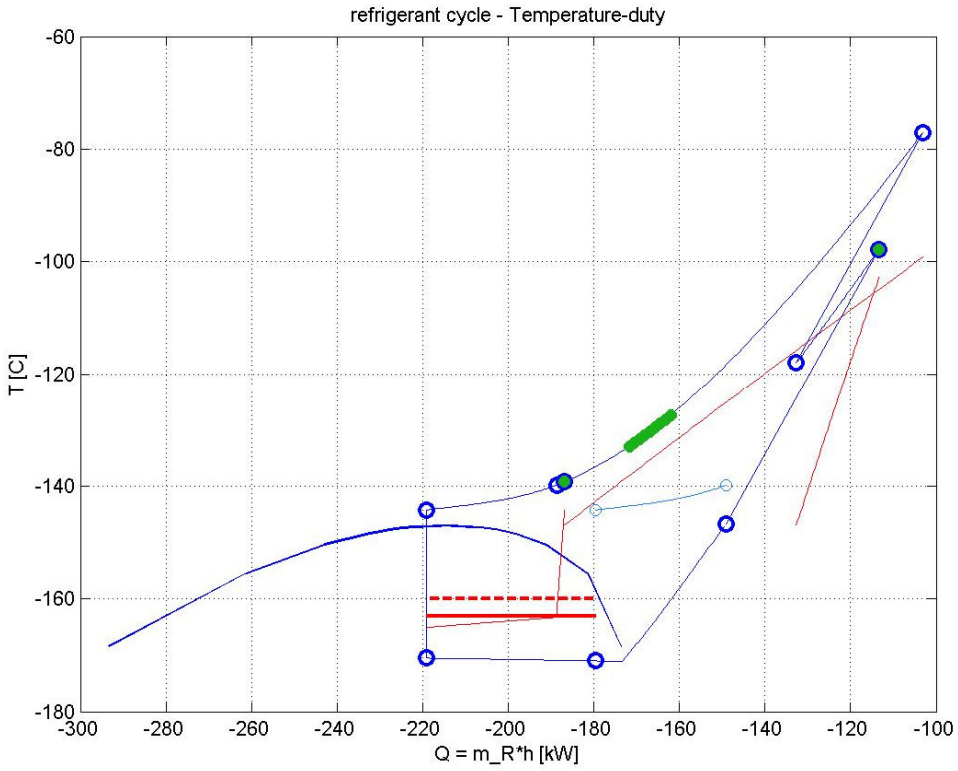


Figure 4.30: Case "173%NCR" with IC: Refrigerant Temperature-Duty diagram

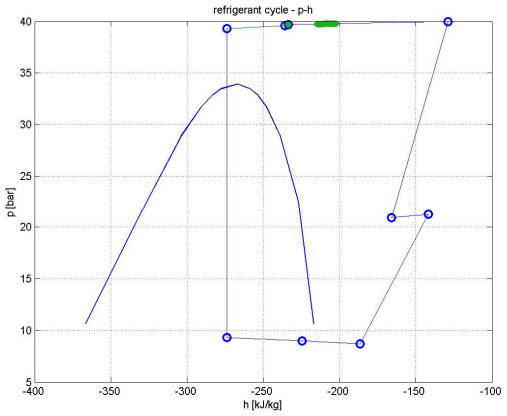


Figure 4.31: Case "173%NCR" with IC: Refrigerant pressure - enthalpy diagram

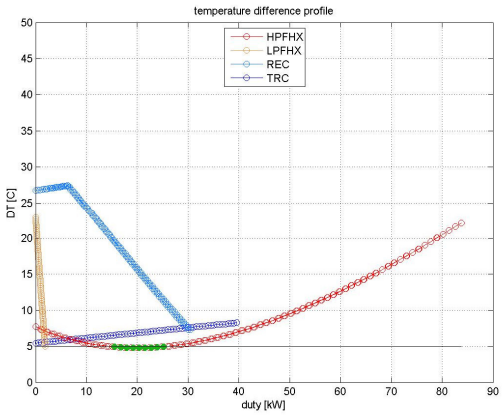


Figure 4.32: Case "173%NCR" with IC: Temperature difference profile for process HX

The discrepancy between the cooling duty and the TRC duty in Table 4.12 is due to the very high flowrate of LNG recirculated in the Tank Reflux system. From the HPFHX and IC cooling curves in Figure 4.30 it can be observed that the HP LNG fuel is now only heated to about

-100℃ , implying that the rest of the exergy from that temperature to ambient is not used by the heat pump as a heat sink, seen from another perspective since the HPFHX pinch is internal to the heat exchanger and corresponds to the point where the heat capacity of the two streams are equal, a reduction in flowrate and heat capacity of the HP fuel will move the pinch towards the hot side and correspondently increase the outlet temperature of the refrigerant and the gas fraction at the throttle valve outlet, ultimately decreasing the available cooling duty. Overall it appears that the utilization of the HP fuel for intercooling is not a recommendable option as it penalizes the refrigeration capacity of the process. For these reasons and to limit the number of optimization variables the intercooling option was abandoned and has not been investigated any further in the course of this thesis.

For further development of the process different options for intercooling could be explored, since it was observed that the HP fuel is not a suitable fluid a valid alternative to this could be the LP refrigerant itself, as described by the layout in Figure 4.33 where heat is exchanged between the inlet and the outlet of the first stage of the compressor.

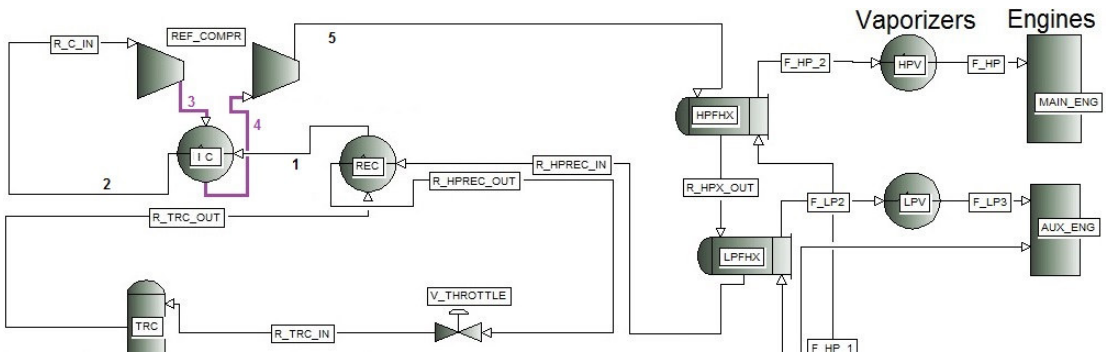


Figure 4.33: Process layout with refrigerant compressor Intercooling by LP refrigerant

This option was not simulated in the course of the thesis, but it deserves further considerations due to the following features:

- the use of LP refrigerant at the REC outlet as a intercooling fluid would not affect or penalize the cold side of the heat pump;
- the inlet temperature of the first compressor stage would be increased by some extent, thereby relaxing the materials specifications for the cryogenic compressor (in principle the whole compression path could be lifted to ambient temperatures allowing the implementation of a standard type of compressor).

However regarding the energy consumption of the compressor the following two effects are expected:

- the higher temperature at the first stage inlet would necessarily increase the stage compression work;
- despite the mitigating effect of the intercooler, the compressor work of the second stage would increase due to the diverging shape of the isentropic lines, as shown by the position of point 4 in Figure 4.34.

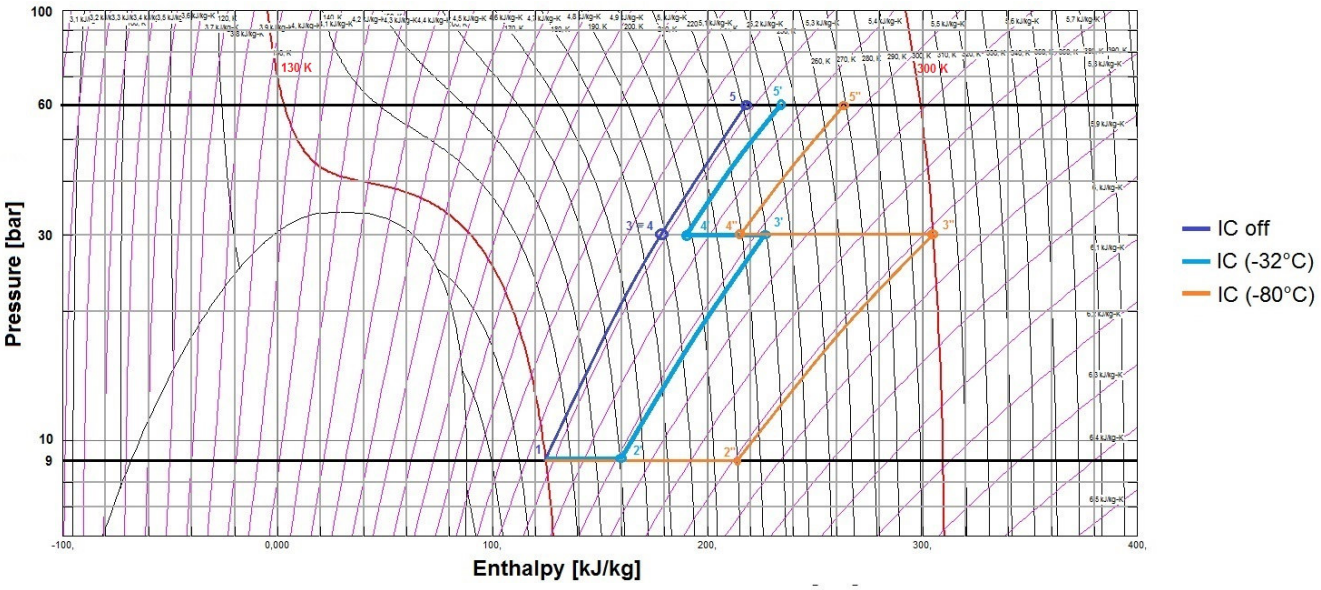


Figure 4.34: Comparison between isentropic compression paths with and without intercooling, in the Nitrogen pressure enthalpy chart generated with RefProp

In conclusion this layout of the intercooled cycle would increase the compressor work and penalize the COP but it could lead to a reduction in equipment cost with respect to the compressor selection, therefore the existence of a trade off could be expected in which case the use of the intercooler would be based on a more detailed cost analysis.

### 4.6.3 BOG recirculation in the Tank Reflux system

All the simulation results presented so far refer to a process configuration where LNG liquid is subcooled in the Tank Reflux system and recirculated in the tank, it is however possible to recirculate BOG in the Tank Reflux system by means of a BOG compressor (dotted stream in the main process PFD in Figure 3.2). The expected advantage of reliquefying the BOG instead of subcooling the LNG is that the higher temperature on the hot side of the TRC heat exchanger allows to rise the evaporation pressure and improve the heat pump performance.

This option has been assessed with simulations in a early stage of the model development. It was found that if the BOG compressor operates at 6 bar outlet pressure (i.e. the Auxiliary engine specification) the relatively high energy consumption of the compressor will introduce a too large energy input to the Tank Reflux system that will consume the refrigeration duty. However, if the BOG compressor is operated in a way that it does the smallest amount of work on the BOG, with a pressure ratio just high enough to compensate the pressure drop in the system, this operation mode might be competitive with the basic subcooling mode.

The following Table 4.13 and Figure 4.35 show an example of a simulation where BOG is recirculated in the Tank Reflux system. Like in the previous chapter the case inputs do not match with the normal operation scenario "D-100%NCR" since the simulation was executed before the final inputs were defined.

Table 4.13: Case "173%NCR" with BOG recirculation: Process Equipment mass and energy balance

| Equipment | Duty [kW] | m Ref [kg/s] | m Fuel [kg/s] | LP [bara] | HP [bara] |
|---|---|---|---|---|---|
| LP Pump | 1.09 | | 0.73 | 1.04 | 6.00 |
| HP Pump | 61.84 | | 0.70 | 6.00 | 300.90 |
| Ref Compr | 56.24 | 0.70 | | 9.70 | 45.00 |
| BOG Blower | 3.22 | | 0.10 | 1.04 | 1.50 |
| Total Work | 122.39 | | | | |
| HPFHX | 94.83 | 0.70 | 0.70 | 45.00 | 300.60 |
| LPFHX | 1.86 | 0.70 | 0.03 | 6.00 | 44.70 |
| REC | 45.64 | 0.70 | | 10.00 | 44.60 |
| IC | 0.00 | 0.70 | 0.00 | 23.82 | 300.90 |
| TRC | 40.45 | 0.70 | 0.10 | 0.10 | 0.70 |
| Cooling Duty | 37.19 | | | | |
| COP | 0.66 | | | | |

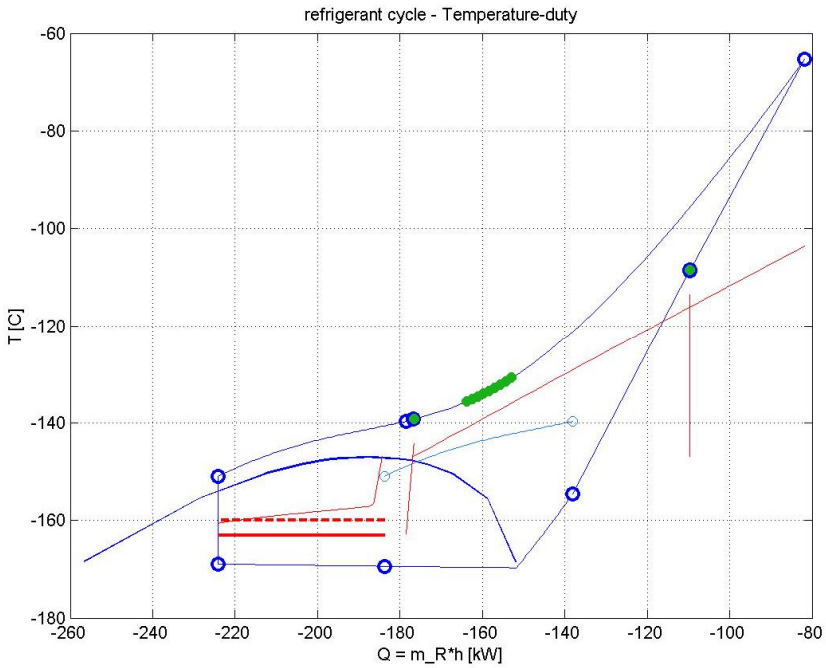


Figure 4.35: Case "173%NCR" with BOG recirculation: Refrigerant Temperature-Duty diagram

It is not correct to compare the performance of this process with the case D-100%NCR because several inputs are different, however the results show that the heat pump can run in the BOG recirculation mode without an abnormal gap between the TRC duty and the refrigeration duty, and allowing some increase in the evaporation pressure. This option should be further investigated with accurate simulations, studying the impact of a number of variables such as:

- BOG temperature in the tank;
- BOG Compressor outlet pressure;
- BOG Compressor efficiency.

# Chapter 5

# Equipment selection

## 5.1 LNG pumps

Cryogenic pumps for LNG applications are available as standard products in the market, for different applications in the various steps of the LNG chain, LNG pumps for marine applications include submersible pumps for marine tanks and HP pumps for fuel supply to HP engines.

### 5.1.1 LNG High Pressure pump

When it comes to the selection of the HP pump, centrifugal pumps are not considered an option given the high pressure required by the ME-GI engines. Reciprocating HP cryogenic piston pumps are available on the market, designed for applications in fuelling stations for Compressed Natural Gas (CNG) vehicles, or specifically for Fuel Gas Supply System with ME-GI engines (eg. by Cryostar, Vanzetti...). As highlighted by the sensitivity analysis in the figure D.64 of the appendix, the efficiency of the LNG HP pump is extremely determinant for the overall performance of the heat pump due to the pinch in the HPFHX (an increase in pump efficiency of 1% yields to a gain in the system's COP of about 2%). More in general the overall temperature rise across the pump related to the pump efficiency or to heat leak through the pump body, should be minimized in order to have a HP fluid as cold as possible in the HPFHX. These characteristics, that would not be of particular importance in the equipment selection of a standard FGSS, deserve full consideration for the process described in this thesis and should be taken into account in the pump selection process.

### 5.1.2 LNG Low Pressure pump

For the selection of the low pressure pump, a wide number of products are available on the market. For FGSS in marine application LP submersible and non-submersible pumps are available.
Non-submersible pumps could be used if the position of the pump guarantees the NPSH required. For type-C tanks it is possible to position the pump at a low elevation next to the tank. For other types of tanks the position of the tank in the hull structure will favour the implementation of a submersible pump.
Technology for submersible pumps is well developed and models of submersible pump with submerged electric motor are available for a wide range of head and flowrate and for different applications [57, p.22]. Among other applications, submersible pumps are being manufactured specifically for extraction of LNG from the fuel tank and delivery to HP Pump and Auxiliary engines, EBARA produces submersible centrifugal LNG fuel pumps for non-LNGC ships' Fuel Gas Supply System with ME-GI engines [58, p.22].
Cryogenic pumps can have a minimum flowrate specification to ensure that the heat leak in the pump body and in the piping is not sufficient to induce cavitation in the impeller [40], for this reason and for simplicity the present design prescribes that the LP pump is used to feed both the Fuel Supply system and the Tank Reflux system, so that the flow is maintained also when the fuel supply is reduced. As a more efficient alternative to this design a dedicated pump could have been assigned to the LNG recirculation in the TRC.
On LNG Carriers dedicated LNG spray pumps are installed to distribute LNG to the spray ring [59, p.184] to control the tank atmosphere temperature, and occasionally to send LNG to forcing vapoizers. Typically spray pumps for LNGC are 2 stage centrifugal pumps with a capacity of 40 to 50 m3/h [7, p.152], the efficiency for these machines is in the range 50 to 60% [7, p.144].

## 5.2 Refrigerant compressor

### 5.2.1 Requirements

One important feature that differentiaties this heat pump process from other reliquefaction cycles is that the heat exits the heat pump cycle at low sub-ambient temperatures and is discharged to a process stream instead of the environment.
In the studies developed so far, the refrigerant compressor is placed after the recuperator REC and handles cold Nitrogen gas with suction temperature in the cryogenic range. The minimum suction temperature that the compressor should be able to withstand approaches the Nitro-

gen dew point termperature of about -170℃ at its the evaporation pressure. Most construction materials and metals are not applicable in this conditions because of the degradation of mechanical properties at low temperatures, for example most unalloyed carbon steels become brittle at temperatures higher than -50℃ [60]. The use of lubricant fluids is also restricted as they would freeze at low temperature.
For these reasons, the cold suction constrains dramatically the selection of the compressor, making it one of the most delicate step in the design of the system.

Figure 5.1 illustrates the operation conditions and specifications for the refrigerant compressor as simulated by the design model for the different main engine load scenarios, in a compressor operation map with mass flowrate in the horizontal axis and pressure ratio on the vertical axis. The results for each of the cases presented in the Chapter 4.4 are plotted together with the Refrigeration duty contour lines from the performance maps for each scenario. The bottom part of the graph in the figure shows the actual volume flowrate at suction condition which is a more adequate property for selecting a compressor.

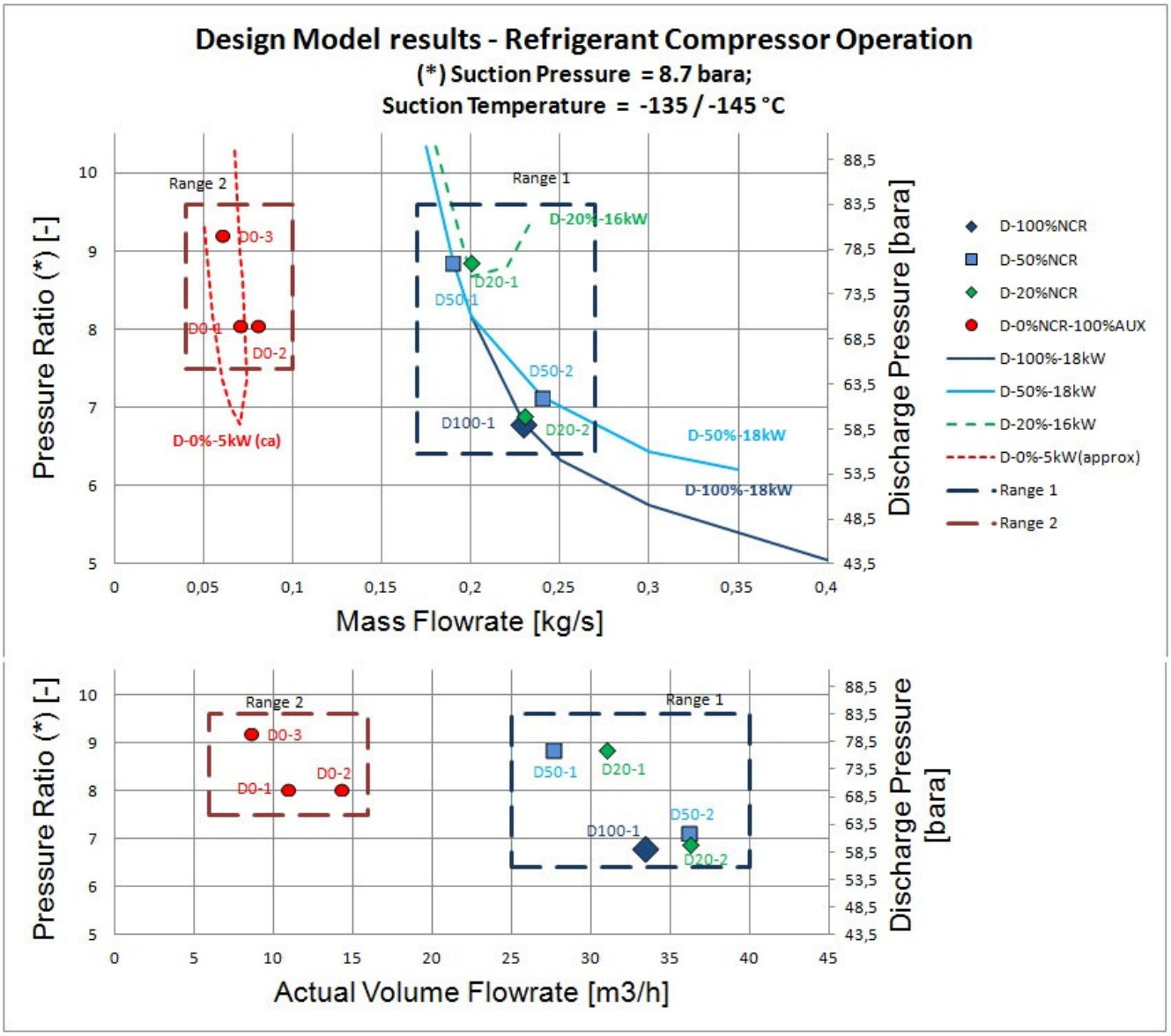


Figure 5.1: Operation range of Refrigerant Compressor

According to these results, one possible set of specifications for the compressor could be:

- Compression ratio of 7 to 9 (7 is enough for the normal operation scenario, "D-100%NCR" labeled "D100-1");
- Flowrate of 30-35 $m^3/h$ at suction conditions for normal and part load operation;
- Maximum allowable pressure higher than 80-90 bar;
- Considerable turndown capability for the idle scenario "D-0%NCR-100%AUX".

A compressor with these characteristics would be able to operate the system in all of the scenarios analyzed, generating a refrigeration duty equal to the target value of 18 kW for the 100%NCR and 50%NCR scenarios. For the 20%NCR scenario a maximum cooling duty of 16 kW is achievable unless the pressure ratio is higher; for the idle scenario "D-0%NCR-100%AUX" a refrigeration duty of 4-6 kW can be reached with this configuration.

### 5.2.2 Compressor alternatives

The following types of machine have been considered in this study as possible options for the refrigerant compressor:

- Reciprocating;
- Screw;
- Centrifugal.

In addition the above mentioned, also other types of compressors among those listed in Figure 5.2 could be taken into consideration.

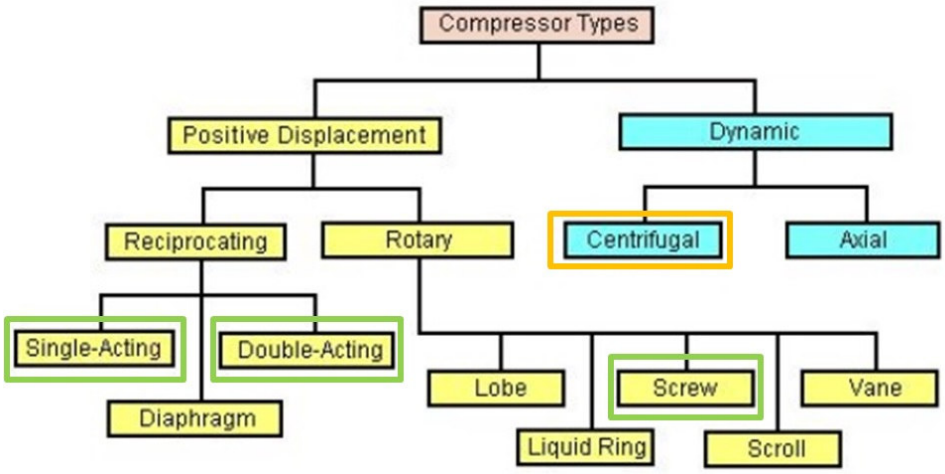


Figure 5.2: Types of compressors sorted by family [61]

Table 5.1 compares three types of compressors for standard applications (non cryogenic suction) with respect to operational range. It appears that both reciprocating and screw machines exist in a oil-free configuration, but they cover a smaller range than the standard lubricated machines.

Table 5.1: Comparison table of three types of compressors [62]

| | Compressor Type | Reciprocating | | Screw | | Centrifugal |
|---|---|---|---|---|---|---|
| | | Lube | Non-lube | Oil Flooded | Oil Free | |
| Pressure | Maximum Discharge Pressure | 4500psiG (300barG) | 1500psiG (100barG) | 1500psiG (100barG) | 600psiG (40barG) | 3,000psiG (200barG) |
| | Maximum Pressure Ratio by Single Stage | 3 : 1 | 3 : 1 | > 50 : 1 | 4 : 1 ~7 : 1 | 1.5 : 1 ~ 3 : 1 |
| Flow rate | Maximum Actual Inlet Volume | 8800 ACFM (15000 m3/h) | 8800 ACFM (15000 m3/h) | 15000 ACFM (25000 m3/h) | 41000 ACFM (70000 m3/h) | 240000 ACFM+ (400000 m3/h+) |
| | Turndown accomplished by: | Suction valve unloaders (step and stepless) Clearance pockets Bypass | Suction valve unloaders (step and stepless) Clearance pockets Bypass | Slide valve (15-100%) step less Bypass | (None) Bypass | Inlet guide vane Speed control (70-100%) Bypass |
| | Polymer gas | Difficult | Difficult | Difficult | Possible | Difficult |
| | Dirty Gas | Possible | Difficult | Possible | Possible | Difficult |
| | MW Change | Possible | Possible | Possible | Possible | Difficult |

(*1) Two stage tandem arrangement maybe adopted in actual high pressure ratio application due to better efficiency.

Figure 5.3 maps the available options for BOG compression for LNG terminals, the operational range of the heat pump is shown with a green square in the very low flowrate region. The map shows that only reciprocating and rotary BOG compressors (of which screw) are produced for applications with low flowrates, this could discourage the use of turbomachines, secondly it seems that the reciprocating type can more easily support high compression ratios (or high discharge pressures) which makes it more suitable for the heat pump application.

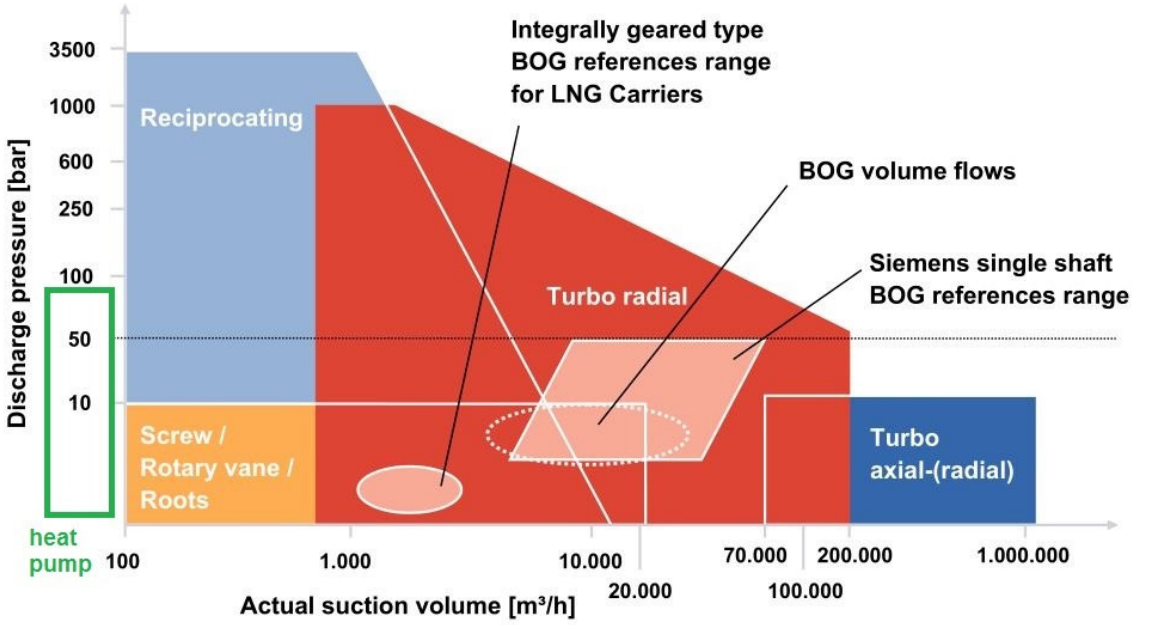


Figure 5.3: Applicable range of different types of compressors for BOG handling in LNG terminals [63], the green rectangle indicates the heat pump operation range outside the horizontal axis

### Reciprocating compressors

Oil-free Labyrinth compressors are built for LNG BOG applications with cryogenic suction temperature down to -160℃, mainly for LNG terminals and storage facilities or LNG carriers applications.
Burckhardt Compression produces BOG compressors with a oil-free contact-free labyrinth sealing system, applied between the piston and cylinder walls and between the piston rod and the piston rod gland separating the oil free and lubricated areas [64]. Other maufacturers (of which SIAD, Kobelco, Dresser-Rand, Howden, IHI) offer more standard solutions with oil-free sealings with contact between the sliding parts (eg. piston rings, or sliders in PTFE or alloys [65]) and the cylinder body.
The reciprocating compressor appears particularly suitable for the heat pump because of the following features:

- relatively low flowrate or swept volume (Figure 5.3);
- high compression ratio, with multiple stages (Figure 5.3);
- large turndown capability (reduction of flowrate) for off-design operation (eg. with Variable Frequency Drive, suction valve unloaders [66] or bypass systems);

- possible reduction in compression ratio for off-design operation [65];

In other words besides being available in the required operating range, reciprocating machines offer good performance at part load operation (lower swept volume or lower pressure ratio than for design) [65]. When the pressure ratio deviates from the design value some reduction in efficiency is expected, this needs to be assessed and should be included in a complete Off-Design model of the heat pump process. A qualitative idea of how the efficiency can vary with the discharge pressure and with the number of stages can be provided by Figure 5.4. A optimum stage compression ratio exists and the efficiency drops when the compression ratio deviates from this value, when more stages are added in series the optimum compression ratio is increased and the efficiency profile flattens out.

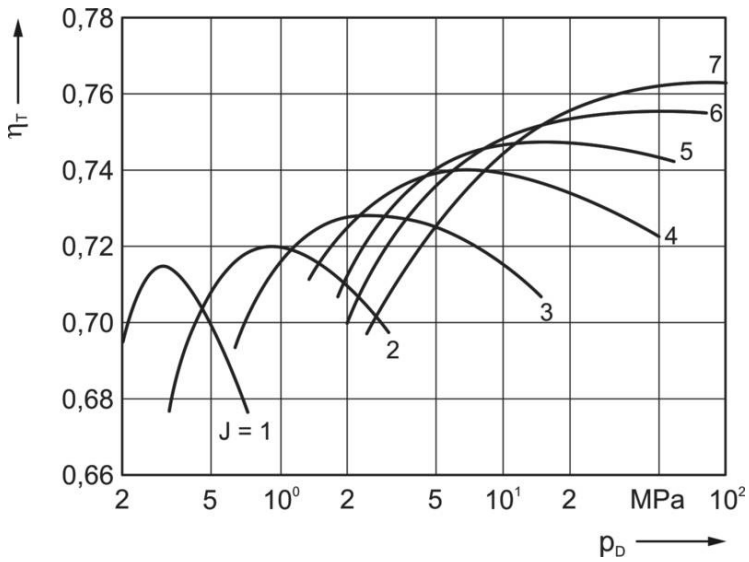


Figure 5.4: Reciprocating compressor isothermal efficiency as a function of discharge pressure, for varying number of compression stages [67]

For a cold-suction oil-free compressor the efficiency is expected to be lower than for standard lubricated compressors, due to the complications in the design and the clearance volumetric losses, especially for labyrinth compressors [66]. The efficiency of a Burckhardt Labyrinth compressor has been estimated from the specifications for one particular compressor package in Table 5.2, using a isentropic compression model.

Table 5.2: Specifications for LNG BOG Oil-free Labyrinth compressor package from Burckhardt, at 0.99 bara and -142℃ suction, gas composition 11 mole% $N_2$, 89 mole% $CH_4$ at 100% and 50% capacity [68]

**Specifications for Burckhardt 2K158-2D_1.**

| Discharge pressure bara | Inlet volume flow m3/h | Mass flow 100% kg/h | Shaft power at 100% kW | Mass flow 50% kg/h |
|---|---|---|---|---|
| 22.22 | 771 | 1238 | 179 | 619 |
| 19.19 | 798 | 1282 | 170 | 641 |
| 18 1) | 810 | 1301 | 159 | 650 |
| 10.29 | 893 | 1434 | 132 | 717 |

1) Estimated.

Figure 5.5 shows that this compressor package operatres with a polytropic efficiency of about 69%, it is assumed that a similar value of the poltropic efficiency can be expected if a Burckardt Oil-free Labyrinth BOG compressor is used for the heat pump described in the present thesis.

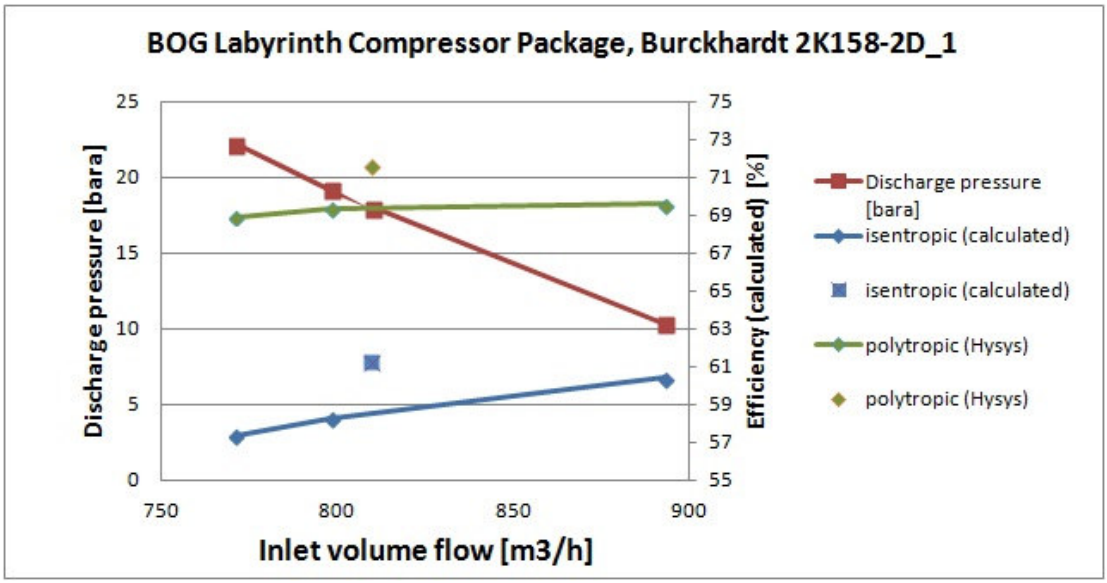


Figure 5.5: Efficiency of a BOG Oil-free Labyrinth compressor package [68]

Since the normal value inputed in the design model is 75% (Table 4.6), a compressor efficiency of 69% yields to a moderate degradation of the system performance, as can be seen in Figure D.62 the compressor work would be about 12% higher for the normal operation scenario.

It has so far been argued that the heat pump refrigerant compressor can be selected from within the LNG BOG compressor market that represents the largest market for cold-suction

compressors, this is desirable for economic reasons since the implementation of an existing compressor type or package or even better a "off-the-shelf" product would require an investment cost that accounts for only a fraction of a taylored solution.
However there are some features that differentiate the heat pump refrigerant compressor from the BOG compressors, in particular the suction pressure (8.7 bara) and the maximum allowable pressure. In fact most BOG compressors are designed for atmospheric suction pressure since they receive BOG from large atmospheric tanks, this means that the suction casing is designed for atmospheric pressure and lower density than specified here. At the same time, if a BOG compressor with a given pressure ratio is fed a gas at higher pressure, the outlet pressure will be many times higher than for atmospheric suction, and this might conflict with the pressure rating of the compressor structure. As an example one can consider a compressor with atmospheric suction and compressor ratio assumed constant and equal to 9: if gas at 8.7 bara is fed to the same machine it will be compressed to about 80 bara with a similar work. The implication is that if the compressor body is designed for a discharge pressure of 9 bara, it would most likely not be qualified to work at 80 bara without structural modifications.

#### Screw compressors

Screw compressors are also available with an oil-free design, where a clearance between the the two screws guarantees that there is no contact between the moving parts [62]. Even though it seems that screw compressors can replace reciprocating compressors in a number of applications [62], no information has been found regarding use of screw compressors with cold suction temperatures.

#### Centrifugal compressors

Centrifugal compressors are used for LNG BOG handling in LNG terminals and LNG carriers, they have also been developed for low temperature cryogenics Helium applications [69], [70, p.174].
Since in any kind of centrifugal compressor the clearance between the impeller and the casing is not lubricated the use of these machines for cold-suction applications poses less challenges that other types of compressors do. In the Low Duty BOG compressor design for LNG carriers the lubricated shaft bearings are located in the warm gearbox separated from the cold impeller channels, pressurized seal gas (eg. Nitrogen) is injected in the labyrinth sealings between the bearings and the compressor weel to avoid any oil slip into the impeller and gas penetration in the gearbox [7].
There are a number of reasons why the centrifugal compressors are considered not suitable for

the heat pump application:

- they are designed for large volume flowrate and low compression ratio;
- they have poor turndown capability, usually work around 80-100% of capacity [69, p.215][66];
- they require stable suction temperature and density to keep within the surge limits [66]

## 5.3 BOG compressor

Even if the purpose of the heat pump process is to handle LNG liquid with cryogenic pumps and eliminate the need to handle the LNG BOG, it could still be convenient to install a BOG compressor for different kind of operations such as

- BOG feed to Auxiliary engines during normal operation (if considered convenient) or while the heat pump is in stand by;
- BOG feed to Gas Combustion Units;
- BOG recirculation and recondensation in the Tank Reflux system (not considered efficient)

If a LNG BOG compressor is chosen similar considerations as the previous chapter can be made, and a reciprocating compressor could be the best option.

## 5.4 Heat exchangers

The system described in this thesis is constituted by four heat exchangers belonging to the heat pump (HPFHX, LPFHX, REC, TRC) and two belonging to the Fuel Gas Supply System (High Pressure Vaporisers "HPV" and Low Pressure Vaporiser "LPV"), the use of an intercooler (IC) has been discussed but needs to be quantitatively assessed in a futher study.

The two vaporisers (HPV and LPV) are only part of the FGSS and need to be sized independently from the heat pump as they might run when the heat pump is off, moreover they are standard process equipment that is produced for ME-GI systems for which specifications alread exist, for these reasons the requirements for the vaporisers have not been covered in the present thesis.

Regarding the four heat pump heat exchangers the requirements regarding flowrate and pressure rating can be extracted from the "Process equipment mass and energy balance" Tables

for each of the design model scenarios. From the simulations presented in this thesis, some suggestions can be made regarding the types of heat exchangers to be used, this would set the basis for further detailed calculations and provide accurate inputs to a future off design model. The heat exchangers types taken into considerations in this chapter are Shell&Tube heat exchangers (S&T) and Plate (Plate&Frame) heat exchangers. The former are considered a default choice since they are available in many different configurations and built for a wide range of operating parameters, S&T heat exchangers can also support high pressure on the shell and especially the tube side and high differential pressure between the two sides [71]. Plate heat exchangers are more compact and cheap than S&T but can be used in a more limited range of applications [72], in particular they are not designed for high pressure and do not support high differential pressure between the two sides that would bend the plates. Copper brazed plate heat exchangers are used in the Mini LNG reliquefaction process by Sintef at cryogenic temperatures and with differential pressures up to 17 bar between the hot and cold side, this application proves that these components can work also with multicomponent mixtures undergoing phase change.
Plate-Fin heat exchangers are even more compact than Plate&Frame but have not been taken into consideration because they are more complex and delicate and require slow thermal transients due to the poor mechanical resistance to thermal stress. Considered the type of fluids and the pressures in the heat pump process a possible set of choices for the heat exchangers could be:

- HPFHX: Shell&Tube
  due to the relatively HP on the HP LNG side and the differential pressure;
- LPFHX: Shell&Tube
  due to the relatively HP on the refrigerant side and the differential pressure; it should be noted that if the refrigerant is on the tube side the evaporating LNG mixture could observe liquid enrichment on the shell side with degradation of heat transfer effectiveness, if this is considered a problem LNG should be evaporated in the tube side;
- REC: Shell&Tube
  similarly as LPFHX, in this case the HP refrigerant should flow in the tube side so that the shell is not exposed to HP.
- TRC: Plate
  since it is allowed by the moderate pressure on both sides.

The main parameter for the heat exchanger sizing that can be extracted from the simulations is the U*A product between the heat transfer coefficient (U [kJ/(kg*K)]) and the heat exchange

area (A [$m^3$]). In Figure 5.6 the ranges of U*A value for each heat exchangers are displayed for the four different scenarios, the data are extracted from the Case Study plots in Appendix D.3.

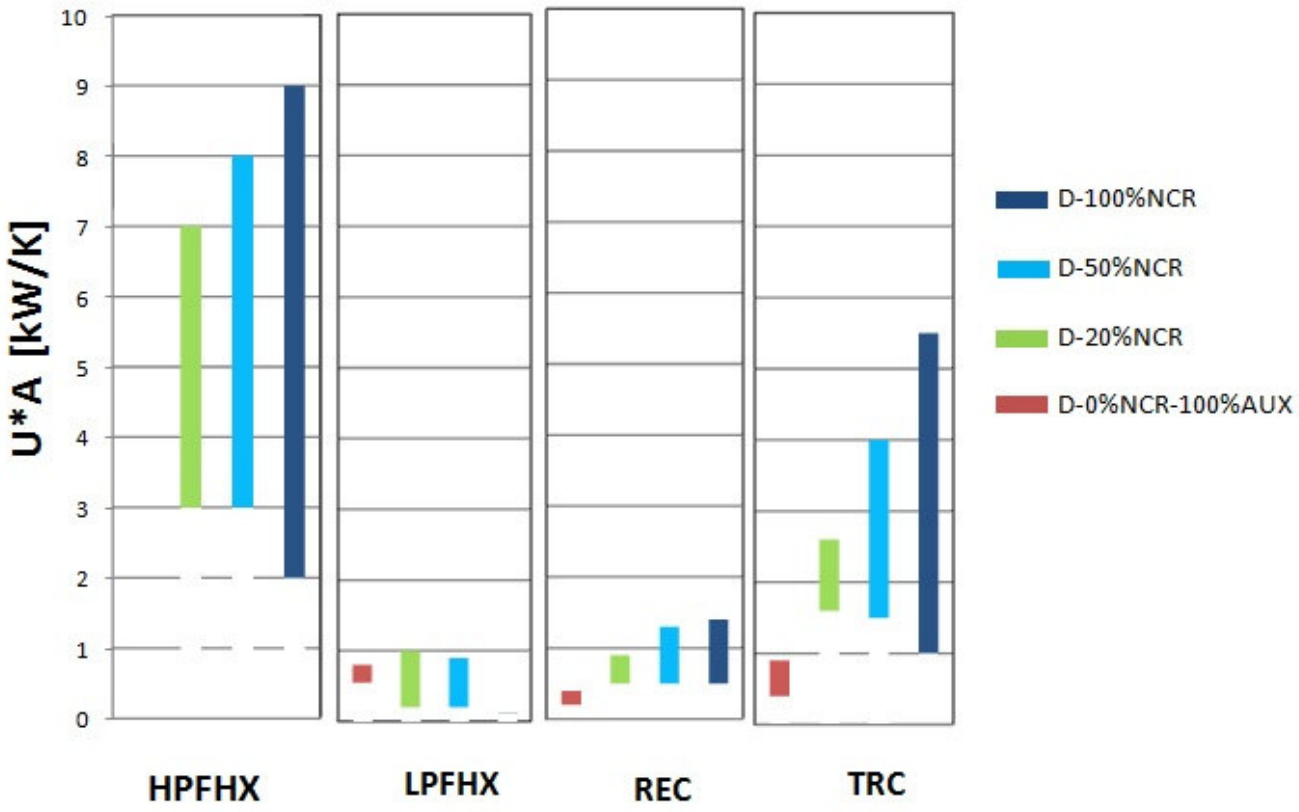


Figure 5.6: Process Heat Exchangers U*A value ranges, from the Design Model Case Studies (Appendix D.3)

Naturally the required U*A value decreases when the engine load is reduced together with the fuel and refrigerant flowrates. One important exception is the Low Pressure Fuel Heat Exchanger (LPFHX) that evaporates the LNG directed to the Auxiliary Engine, this heat exchanger which gives a almost neglectable contribution to the cycle energy balance for the normal operation scenario (D-100%NCR) delivers a larger duty for the part load and "idle" scenarios, therefore requiring a larger size and U*A value. A proper off-design model will have to receive as input a fixed heat exchanger U*A value instead of the MITA specification of the Design model, in this case Figure 5.6 can be used to assign a U*A value to each heat exchanger.

# Chapter 6

# Conclusion

A heat pump process has been designed for extracting heat from the LNG fuel tank on LNG fuelled ships. The main characteristic features of the system that differentiate it from standard reliquefaction cycles for LNGCs are the cold compressor suction, the absence of heat discharge to the environment and the complete heat integration with the FGSS.
One selected layout of the heat pump system has been simulated with the same HYSYS model in four different scenarios corresponding to four engine loads, namely the normal load scenario "D-100%NCR", two part load scenarios "D-50%NCR" and "D-20%NCR" and one idle ship scenario "D-0%NCR-100%AUX".
The simulations results indicate that the heat pump process can be 2-3 time more efficient than commercial reliquefaction processes for LNG Carriers. Its capacity is many times lower but sufficient for the estimated cooling requirement of the LNG fuel tank. The main disadvantages of the simulated process are the poor performance during idling operation of the ship, and the expectedly high investment cost for the refrigerant compressor with cryogenic suction.
Some modifications to the basic layout of the process have been proposed in order to alleviate the above problems. In particular feeding the compressed BOG to the Auxiliary engines could be a more efficient option in all scenarios and especially in the idle ship scenario. Secondly, the installation of a compressor intercooler with internal heat exchange with the compressor inlet could release the low temperature requirements for the compressor at the price of a higher energy consumption of the machine. Finally, the BOG recirculation and recondensation in the Tank Reflux system could be competitive with the basic liquid subcooling option.

The equipment selection reveals that most of the heat pump system can be built with standard process equipment (e.g. cryogenic pumps, Shell&Tube or Plate heat exchangers and Joule Thompson throttle valve) with the important exception of the refrigerant compressor. The recommended type of machine for the refrigerant compressor is a reciprocating oil-free com-

pressor designed for low temperature suction (e.g. BOG compressor) with suitable pressure rating for the operating conditions of the heat pump. This unit is expected to represent a major component of the investment cost.

In the course of further work the discussed modifications of the process should be investigated with simulations. In parallel an approximate cost assessment of the refrigerant compressor should be carried out, with a particular focus on the influence of the suction temperature on the cost of the machine. After all the options have been assessed and one is identified as optimal, a real Off-Design model should be created from the design model, modifying the equipment specifications and revising the adjust structure.

# Appendix A

# Acronyms

**AUX** Auxiliary Engine

**bara** bar absolute

**BOG** Boil Off Gas

**COP** Coefficient Of Performance

**FGSS** Fuel Gas Supply System

**HFO** Heavy Fuel Oil

**HP** High Pressure

**HPFHX** High Pressure Fuel Heat Exchanger

**HPP** High Pressure Pump

**IC** InterCooler

**LNG** Liquefied Natural Gas

**LP** Low Pressure

**LPFHX** Low Pressure Fuel Heat Exchanger

**LPP** Low Pressure Pump

**MCR** Maximum Continuous Rating

**MDO** Marine Diesel Oil

**MITA** Minimum Internal Temperature Difference

**NCR** Normal Continuous Rating = continuous service rating (S)

**NMCR** Nominal Maximum Continuous Rating (L1)

**PFD** Process Flow Diagram

**REC** RECuperator

**SFOC** Specific Fuel Oil Consumption

**SMCR** Selected Maximum Continuous Rating (M)

**TRC** Tank Reflux Cooler

# Appendix B

# ME-GI engines

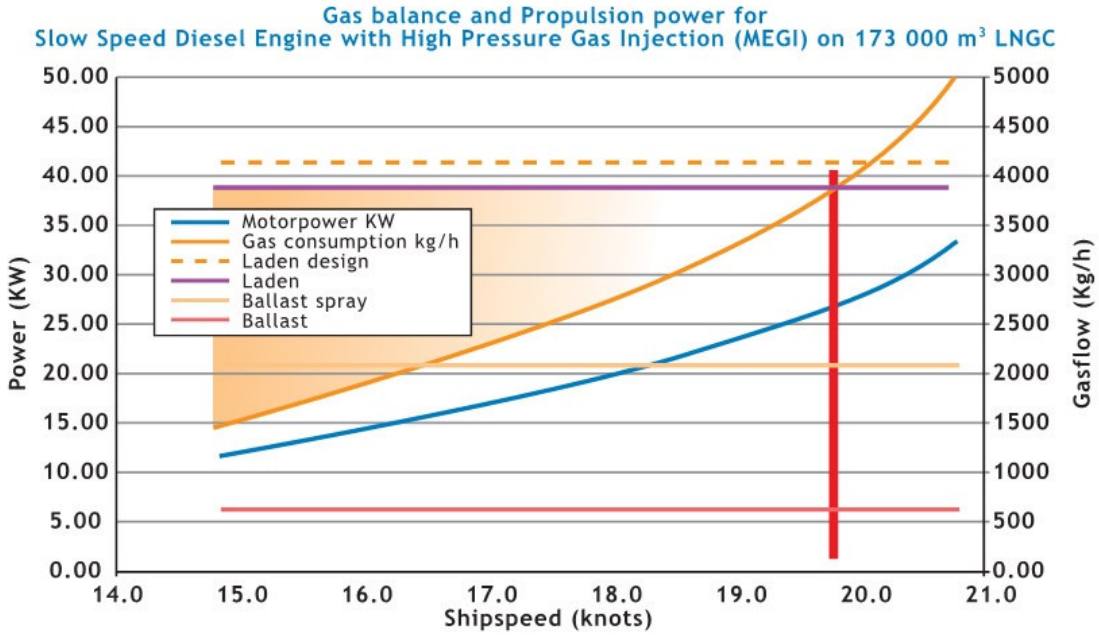


Figure B.1: LNG Carrier estimated BOG evaporation and consumption rate as a funcion of ship speed [45, p.5]

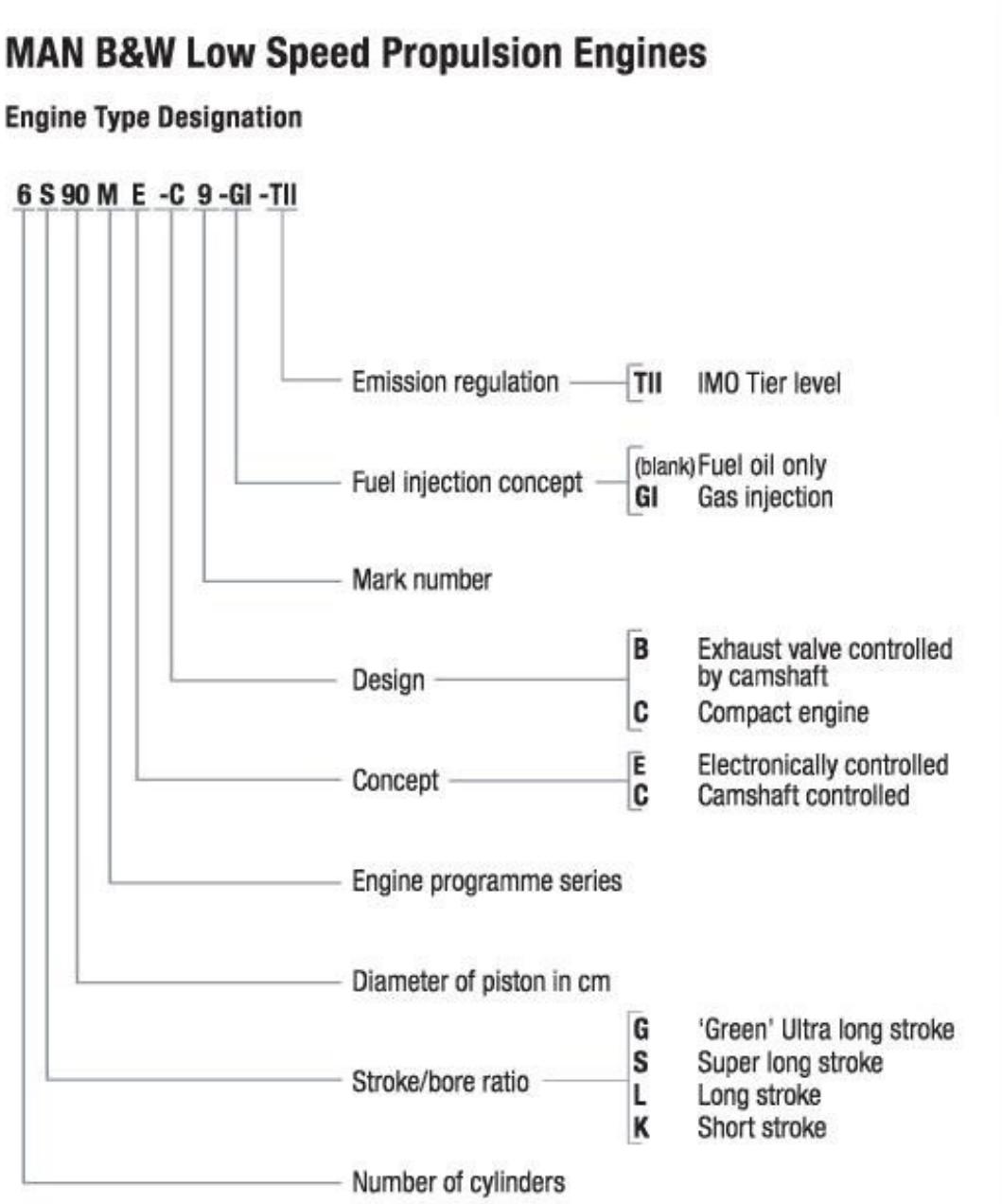


Figure B.2: Nomenclature for MAN engines [43, p.18]

## MAN B&W S60ME-C8-GI

| Cyl. | $L_1$ kW |
|---|---|
| 5 | 11,900 |
| 6 | 14,280 |
| 7 | 16,660 |
| 8 | 19,040 |

**Stroke:** 2,400 mm

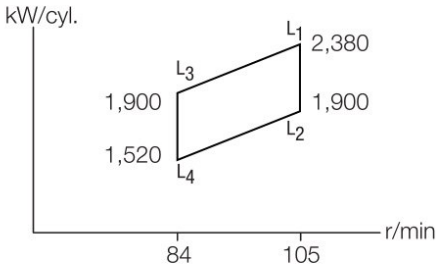


**SFOC gas engines [g/kWh]** — **$L_1/L_3$ MEP:** 20.0 bar – **$L_2/L_4$ MEP:** 16.0 bar

| | | 50% | 75% | 100% |
|---|---|---|---|---|
| Gas and pilot fuel (42,700 kJ/kg) | $L_1$ | 164.5 | 162.0 | 168.0 |
| | $L_2$ | 160.5 | 156.0 | 162.0 |
| | $L_3$ | 164.5 | 162.5 | 168.0 |
| | $L_4$ | 160.5 | 156.5 | 162.0 |
| Liquid fuel only (42,700 kJ/kg) | $L_1/L_3$ | 167.5 | 165.0 | 169.0 |
| | $L_2/L_4$ | 163.5 | 159.0 | 163.0 |

*Specific gas consumption consists of 3% pilot liquid fuel and gas fuel.*
*Gas fuel LCV (50,000 kJ/kg) is converted to diesel fuel LCV (42,700 kJ/kg) for comparison with diesel engine*

**Distributed fuel data [g/kWh]**

| | | 50% | 75% | 100% |
|---|---|---|---|---|
| Gas fuel (50,000 kJ/kg) | $L_1$ | 133.7 | 133.1 | 139.2 |
| | $L_2$ | 128.5 | 126.7 | 133.0 |
| | $L_3$ | 133.7 | 133.6 | 139.2 |
| | $L_4$ | 128.5 | 127.1 | 133.0 |
| Pilot fuel (42,700 kJ/kg) | $L_1/L_3$ | 8.0 | 6.1 | 5.0 |
| | $L_2/L_4$ | 10.0 | 7.6 | 6.3 |

**Specifications**

| Dimensions: | | A | B | C | $H_1$ | $H_2$ | $H_3$ |
|---|---|---|---|---|---|---|---|
| | mm | 1,020 | 3,770 | 1,300 | 10,825 | 10,000 | 9,775 |

| Cylinders: | | 5 | 6 | 7 | 8 | | |
|---|---|---|---|---|---|---|---|
| $L_{min}$ | mm | 6,439 | 7,459 | 8,479 | 9,499 | | |
| Dry mass | t | 308 | 350 | 393 | 452 | | |

Figure B.3: ME-GI Engine datasheet for the design case selection [43, p.53]

# Appendix C

# Ships Operational Profiles

## C.1 Main engine

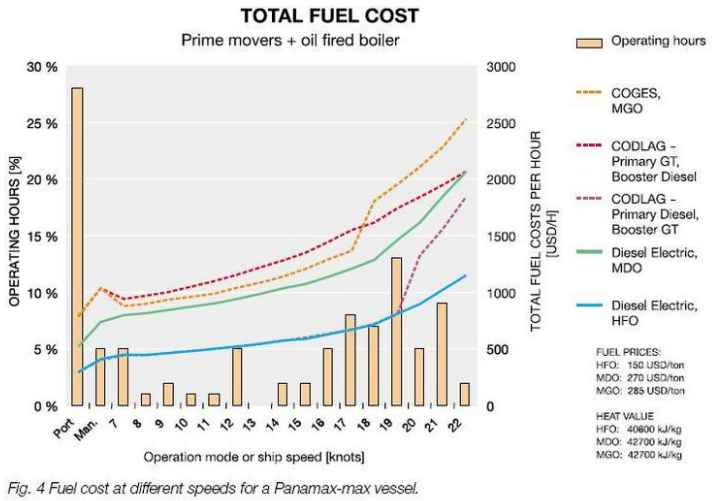

*Fig. 4 Fuel cost at different speeds for a Panamax-max vessel.*

Figure C.1: (Operation profile of a Panamax-max vessel, [61]

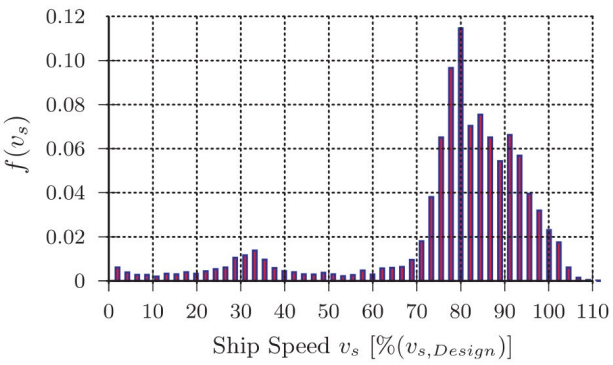

Figure C.2: Operation profile of a North Sea ferry, [73]

Table C.1: Measurement of power consumption of a chemical tanker vessel during the analysed navigation conditions [3]

| **Operation Scenario** | **Speed** [kn] | **Mechanical Power** [KW] | **Electrical Power** [KW] | **Thermal Power** [KW] | **% time** [%] |
|---|---|---|---|---|---|
| Navigation-full load | 15 | 7363 | 752 | 6949 | 41,4 |
| Navigation-full load | 12 | 4400 | 752 | 6844 | 2,8 |
| Navigation-full load | 9 | 2200 | 752 | 6759 | 1,0 |
| Navigation-ballast trip | 15 | 6000 | 752 | 694 | 41,4 |
| Navigation-ballast trip | 12 | 3500 | 752 | 603 | 2,8 |
| Navigation-ballast trip | 9 | 1930 | 752 | 541 | 1,0 |
| Manoeuvring full load | | 2018 | 1782 | 4645 | 0,3 |
| Manoeuvring ballast | | 1930 | 1782 | 386 | 0,1 |
| Waiting full load | | 0 | 489 | 6654 | 1,5 |
| Waiting ballast | | 0 | 489 | 447 | 2,7 |
| Harbour cargo handling | | 0 | 2123 | 4838 | 4,7 |
| *(Harbour)* | | *0* | *470* | *331* | *0,4* |

Table C.2: Operation profile of the vessel with respect to main and auxiliary engines load, calculated from table C.1

| Aux Engine | | | | | | |
|---|---|---|---|---|---|---|
| 5 | 80-105% | 5 | 0,4 | | | |
| | 40-80% | | | | | |
| 95 | **20-40%** | 5 | 2 | 6 | 41 | 41 |
| | 0-20% | | | | | |
| | 0% | | | | | |
| | % Installed Power | 0% | 0-30% | 30-60% | **60-80%** | **80-100%** |
| % Time | | 9 | 2 | 6 | 41 | 41 |

Main Engine

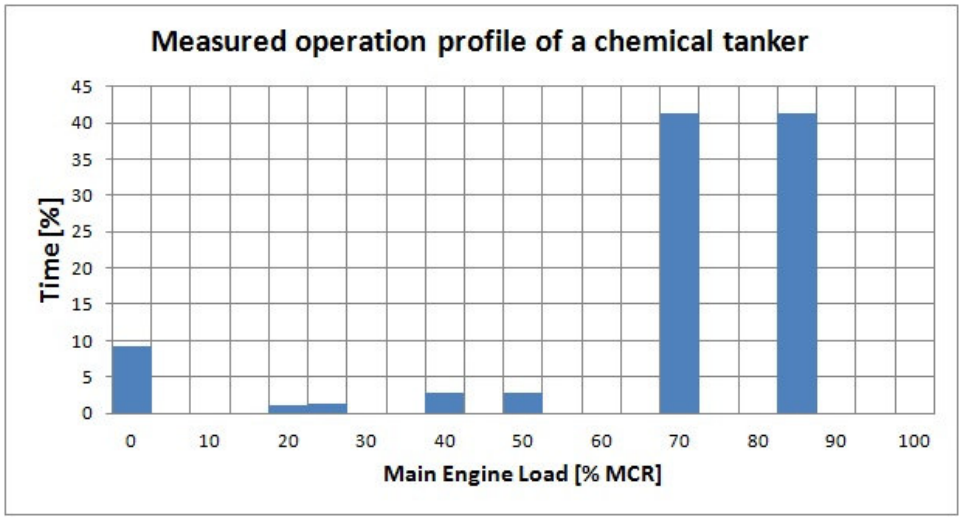


Figure C.3: Main engine operation profile of the vessel, from Table C.1

## C.2 Auxiliary engines

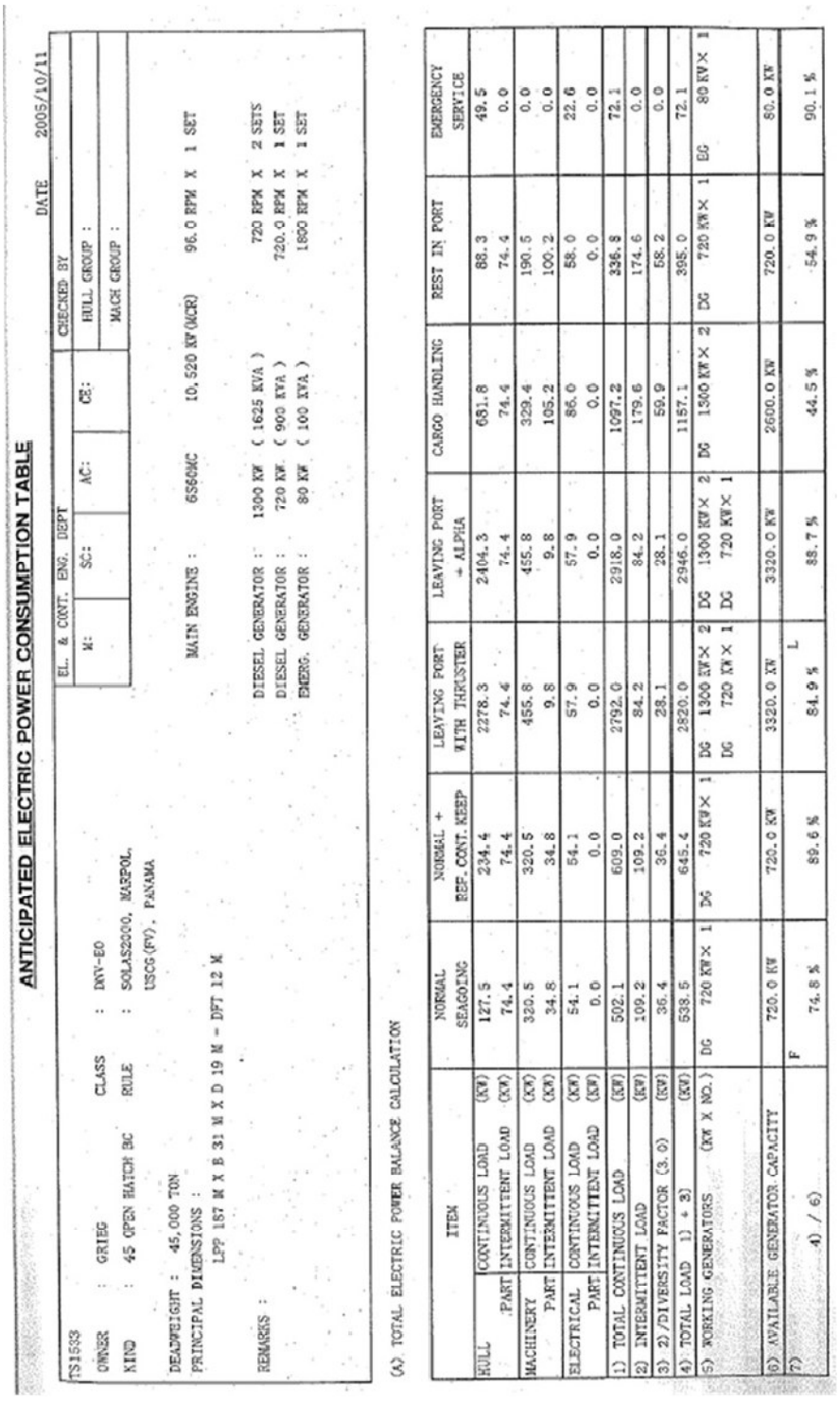

**ANTICIPATED ELECTRIC POWER CONSUMPTION TABLE**

DATE 2005/10/11

TS1533

EL. & CONT. ENG. DEPT — CHECKED BY

M: | SC: | AC: | CE: | HULL GROUP :

MACH GROUP :

OWNER : GRIEG CLASS : DNV-E0

KIND : 45 OPEN HATCH BC RULE : SOLAS2000, MARPOL, USCG(FV), PANAMA

DEADWEIGHT : 45,000 TON

PRINCIPAL DIMENSIONS :

LPP 187 M X B 31 M X D 19 M - DFT 12 M

MAIN ENGINES : 6S60MC 10,520 KW (MCR) 96.0 RPM X 1 SET

REMARKS :

DIESEL GENERATOR : 1300 KW ( 1625 KVA ) 720 RPM X 2 SETS

DIESEL GENERATOR : 720 KW ( 900 KVA ) 720.0 RPM X 1 SET

EMERG. GENERATOR : 80 KW ( 100 KVA ) 1800 RPM X 1 SET

(A) TOTAL ELECTRIC POWER BALANCE CALCULATION

| ITEM | | | NORMAL SEAGOING | NORMAL + REF.CONT.KEEP | LEAVING PORT WITH THRUSTER | LEAVING PORT + ALPHA | CARGO HANDLING | REST IN PORT | EMERGENCY SERVICE |
|---|---|---|---|---|---|---|---|---|---|
| HULL | CONTINUOUS LOAD | (KW) | 127.5 | 234.4 | 2278.3 | 2404.3 | 681.8 | 88.3 | 49.5 |
| PART | INTERMITTENT LOAD | (KW) | 74.4 | 74.4 | 74.4 | 74.4 | 74.4 | 74.4 | 0.0 |
| MACHINERY | CONTINUOUS LOAD | (KW) | 320.5 | 320.5 | 455.8 | 455.8 | 329.4 | 190.5 | 0.0 |
| PART | INTERMITTENT LOAD | (KW) | 34.8 | 34.8 | 9.8 | 9.8 | 105.2 | 100.2 | 0.0 |
| ELECTRICAL | CONTINUOUS LOAD | (KW) | 54.1 | 54.1 | 57.9 | 57.9 | 86.0 | 58.0 | 22.6 |
| PART | INTERMITTENT LOAD | (KW) | 0.0 | 0.0 | 0.0 | 0.0 | 0.0 | 0.0 | 0.0 |
| 1) TOTAL CONTINUOUS LOAD | | (KW) | 502.1 | 609.0 | 2792.0 | 2918.0 | 1097.2 | 336.8 | 72.1 |
| 2) INTERMITTENT LOAD | | (KW) | 109.2 | 109.2 | 84.2 | 84.2 | 179.6 | 174.6 | 0.0 |
| 3) 2)/DIVERSITY FACTOR (3.0) | | (KW) | 36.4 | 36.4 | 28.1 | 28.1 | 59.9 | 58.2 | 0.0 |
| 4) TOTAL LOAD 1) + 3) | | (KW) | 538.5 | 645.4 | 2820.0 | 2946.0 | 1157.1 | 395.0 | 72.1 |
| 5) WORKING GENERATORS | (KW X NO.) | | DG 720 KW× 1 | DG 720 KW× 1 | DG 1300 KW× 2<br>DG 720 KW× 1 | DG 1300 KW× 2<br>DG 720 KW× 1 | DG 1300 KW× 2 | DG 720 KW× 1 | DG 80 KW× 1 |
| 6) AVAILABLE GENERATOR CAPACITY | | | 720.0 KW | 720.0 KW | 3320.0 KW | 3320.0 KW | 2600.0 KW | 720.0 KW | 80.0 KW |
| 7) | | F | | | L | | | | |
| 4) / 6) | | | 74.8 % | 89.6 % | 84.9 % | 88.7 % | 44.5 % | 54.9 % | 90.1 % |

Figure C.4: Anticipated electric power consumption table for a vessel of a similar size than the design case [6]

Table C.3: Auxiliary engine load in relation to the value at normal operation and as a fraction of the installed capacity, extracted from Table C.4

| Ship Regime | Total Load [kW] | Fraction of Normal Power | Fraction of Installed Power |
|---|---|---|---|
| **Normal Seagoing** | **538.5** | 100% | 16% |
| **Normal + Rep. Cont. Keep** | 645.4 | 120% | 19% |
| **Leaving Port with Thruster** | 2820.1 | 524% | 83% |
| **Leaving Port + Alpha** | 2946.1 | 547% | 87% |
| **Cargo Handling** | 1157.1 | 215% | 34% |
| **Rest In port** | 395.0 | 73% | 12% |
| **Emergency Service** | 72.1 | 13% | 2% |

# Appendix D

# Simulation results

## D.1 Tank energy balance and cooling duty calculations

When simulation results are presented the refrigeration duty is calculated on the basis of an energy balance on the LNG fuel tank.

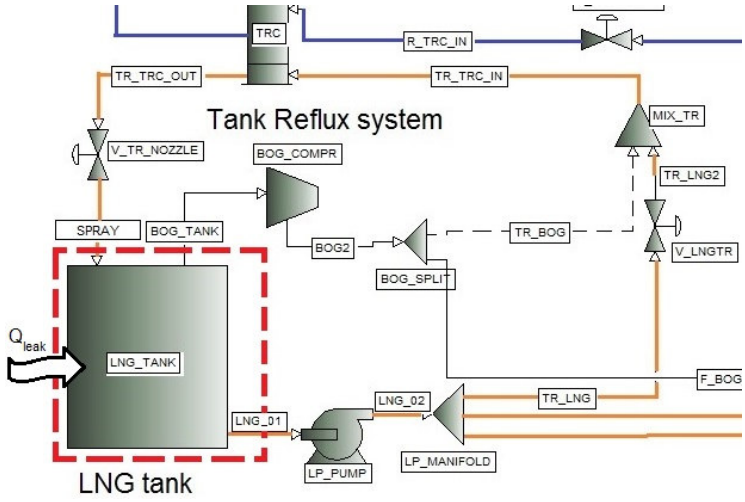


Figure D.1: Energy balance control volume

Energy balance of the LNG fuel tank, including BOG extraction

$$\frac{dE}{dt} = \dot{Q}_{leak} - m_{LPP} \cdot h_{LNG} + m_{TR} \cdot h_{Spray} - m_{BOG} \cdot h_{BOG} \tag{D.1}$$

Energy balance of the LNG fuel tank, excluding BOG extraction

$$\frac{dE}{dt} = \dot{Q}_{leak} - m_{LPP} \cdot h_{LNG} + m_{TR} \cdot h_{Spray} \tag{D.2}$$

Energy balance of the LNG fuel tank, LP pump term is split

$$\frac{dE}{dt} = \dot{Q}_{leak} - m_{fuel} \cdot h_{LNG} - m_{TR} \cdot (h_{LNG} - h_{Spray}) \tag{D.3}$$

Refrigeration duty is calculated from the enthalpy increase of the Tank Reflux stream, the contribution of the fuel to the energy balance is neglected

$$\dot{Q}_{Ref} = m_{TR} \cdot (h_{LNG} - h_{Spray}) \tag{D.4}$$

Refrigeration duty needs to cover the heat leak with a engineering safety factor

$$\dot{Q}_{ref} := \dot{Q}_{leak} \cdot (1 + 0.5) \tag{D.5}$$

## D.2 Extra cases

**Case: D - 50% NCR - point 2**

Table D.1: D-50%NCR(2): Process Equipment mass and energy balance

| Equipment | Duty [kW] | m Ref [kg/s] | m Fuel [kg/s] | LP [bara] | HP [bara] |
|---|---|---|---|---|---|
| LP Pump | 2.93 | | 2.02 | 1.04 | 6.00 |
| HP Pump | 20.08 | | 0.20 | 6.00 | 300.90 |
| Ref Compr | 35.45 | 0.24 | | 8.70 | 62.00 |
| BOG Blower | 0.63 | | 0.02 | 1.04 | 1.50 |
| Total Work | 59.09 | | | | |
| HPFHX | 54.49 | 0.24 | 0.20 | 62.00 | 300.60 |
| LPFHX | 1.55 | 0.24 | 0.02 | 6.00 | 61.70 |
| REC | 13.11 | 0.24 | | 9.00 | 61.60 |
| TRC | 20.60 | 0.24 | 1.80 | 0.24 | 1.80 |
| Cooling Duty | 18.00 | | | | |
| COP | 0.51 | | | | |

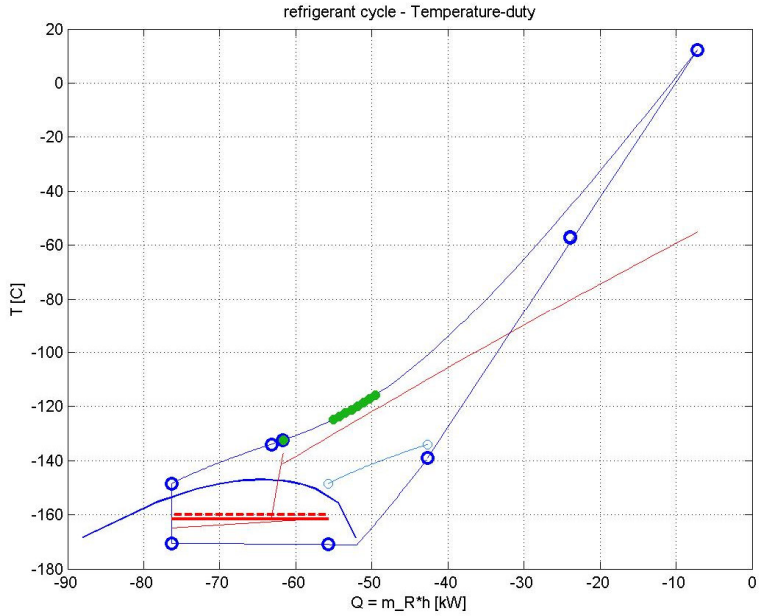


Figure D.2: D-50%NCR(2): Refrigerant Temperature-Duty diagram

**Case: D - 20% NCR - point 2**

Table D.2: D-20%NCR(2): Process Equipment mass and energy balance

| Equipment | Duty [kW] | m Ref [kg/s] | m Fuel [kg/s] | LP [bara] | HP [bara] |
|---|---|---|---|---|---|
| LP Pump | 2.03 | | 1.40 | 1.04 | 6.00 |
| HP Pump | 8.05 | | 0.08 | 6.00 | 300.90 |
| Ref Compr | 34.60 | 0.23 | | 8.70 | 60.00 |
| BOG Blower | 0.63 | | 0.02 | 1.04 | 1.50 |
| Total Work | 45.31 | | | | |
| HPFHX | 40.61 | 0.23 | 0.08 | 60.00 | 300.60 |
| LPFHX | 9.57 | 0.23 | 0.02 | 6.00 | 59.70 |
| REC | 13.78 | 0.23 | | 9.00 | 59.60 |
| TRC | 15.79 | 0.23 | 1.30 | 0.23 | 1.30 |
| Cooling Duty | 14.30 | | | | |
| COP | 0.41 | | | | |

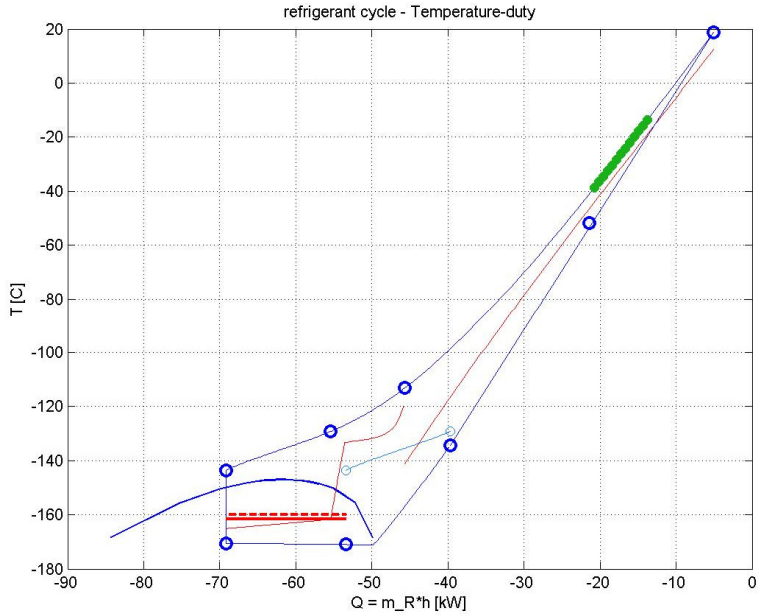


Figure D.3: D-20%NCR(2): Refrigerant Temperature-Duty diagram

**Cases: D - 0% NCR - 100% AUX - points 2 and 3**

Table D.3: D-0%NCR(2): Process Equipment mass and energy balance

| Equipment | Duty [kW] | m Ref [kg/s] | m Fuel [kg/s] | LP [bara] | HP [bara] |
|---|---|---|---|---|---|
| LP Pump | 0.49 | | 0.34 | 1.04 | 6.00 |
| HP Pump | 0.00 | | 0.00 | 6.00 | 300.90 |
| Ref Compr | 15.17 | 0.08 | | 8.70 | 70.00 |
| BOG Blower | 0.63 | | 0.02 | 1.04 | 1.50 |
| Total Work | 16.29 | | | | |
| HPFHX | 0.00 | 0.08 | 0.00 | 70.00 | 300.60 |
| LPFHX | 18.75 | 0.08 | 0.02 | 6.00 | 69.70 |
| REC | 6.10 | 0.08 | | 9.00 | 69.60 |
| TRC | 4.16 | 0.08 | 0.32 | 0.08 | 0.32 |
| Cooling Duty | 3.84 | | | | |
| COP | 0.25 | | | | |

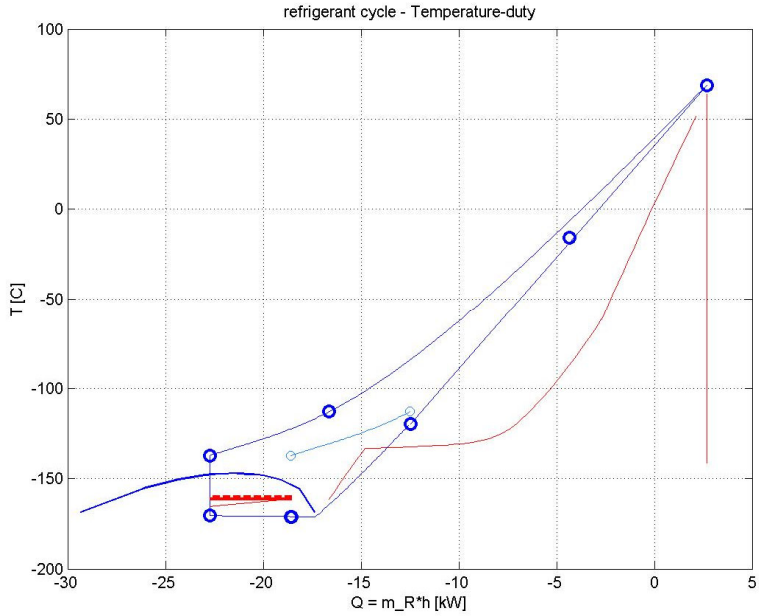


Figure D.4: D-0%NCR(2): Refrigerant Temperature-Duty diagram

Table D.4: D-0%NCR(3): Process Equipment mass and energy balance

| Equipment | Duty [kW] | m Ref [kg/s] | m Fuel [kg/s] | LP [bara] | HP [bara] |
|---|---|---|---|---|---|
| LP Pump | 0.72 | | 0.50 | 1.04 | 6.00 |
| HP Pump | 0.00 | | 0.00 | 6.00 | 300.90 |
| Ref Compr | 10.07 | 0.06 | | 8.70 | 80.00 |
| BOG Blower | 0.63 | | 0.02 | 1.04 | 1.50 |
| Total Work | 11.42 | | | | |
| HPFHX | 0.00 | 0.06 | 0.00 | 80.00 | 300.60 |
| LPFHX | 16.02 | 0.06 | 0.02 | 6.00 | 79.70 |
| REC | 2.89 | 0.06 | | 9.00 | 79.60 |
| TRC | 6.44 | 0.06 | 0.48 | 0.06 | 0.48 |
| Cooling Duty | 5.76 | | | | |
| COP | 0.57 | | | | |

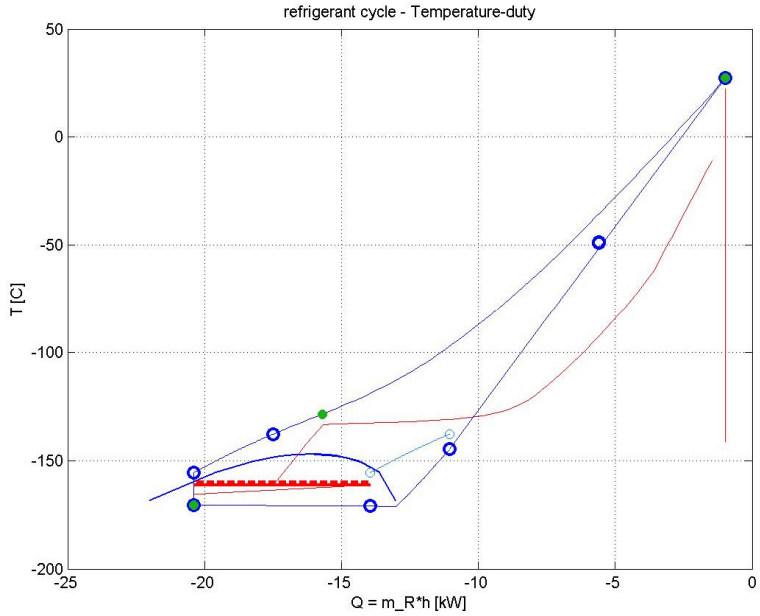


Figure D.5: D-0%NCR(3) Refrigerant Temperature-Duty diagram

# D.3 Case studies

## D.3.1 Case D-100 % NCR

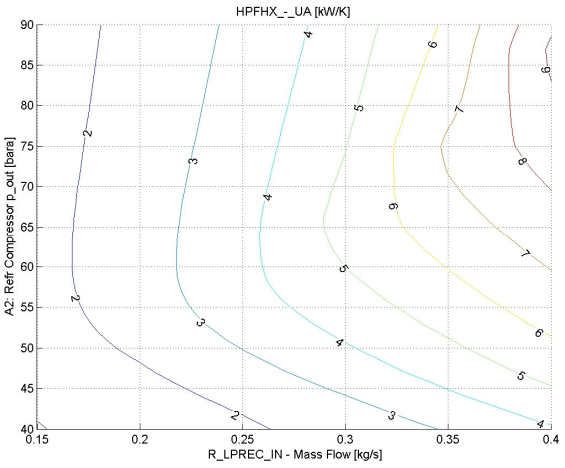


Figure D.6: HPFHX: UA

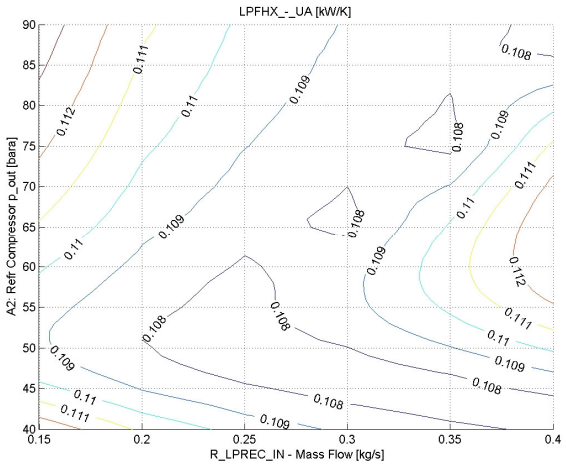


Figure D.7: LPFHX: UA

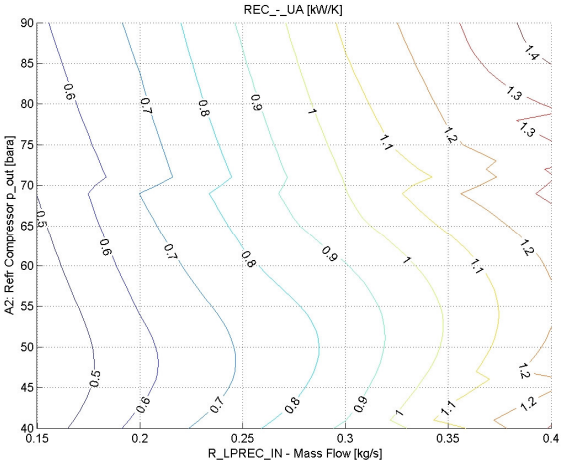


Figure D.8: REC: UA

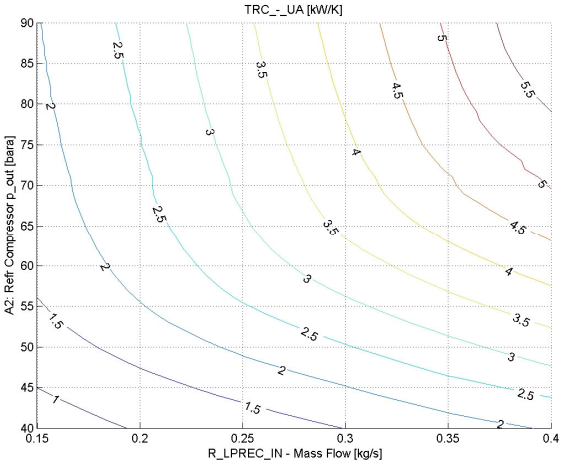


Figure D.9: TRC: UA

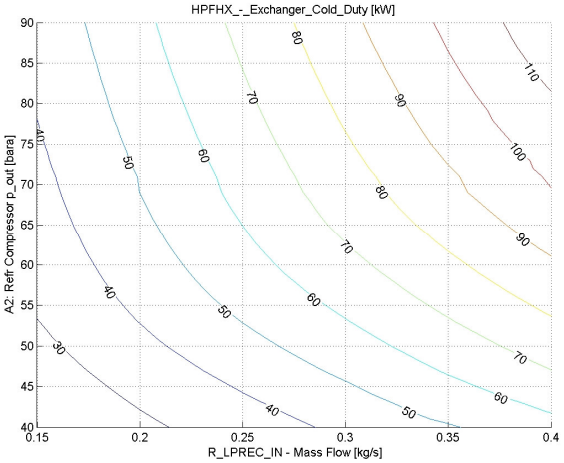


Figure D.10: HPFHX: Duty

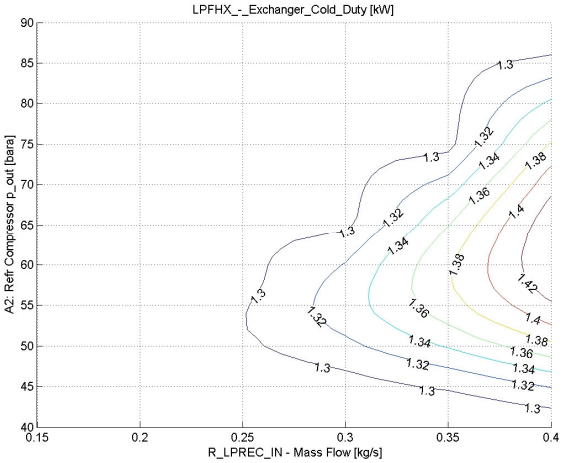


Figure D.11: LPFHX: Duty

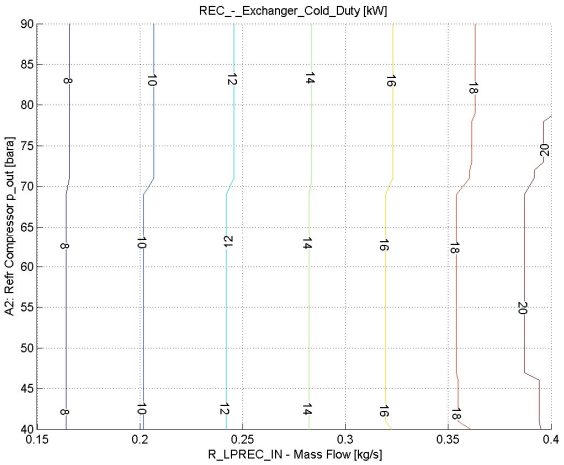


Figure D.12: REC: Duty

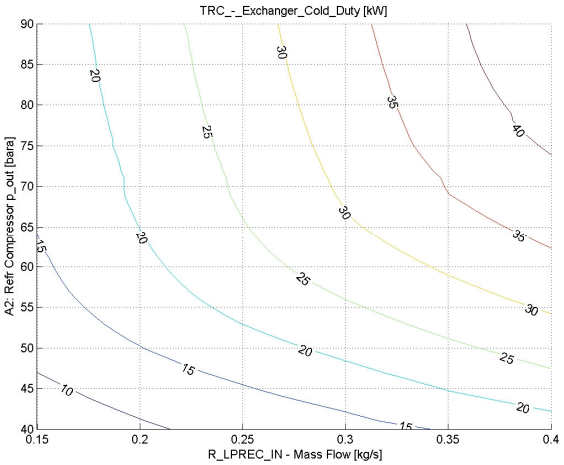


Figure D.13: TRC: Duty

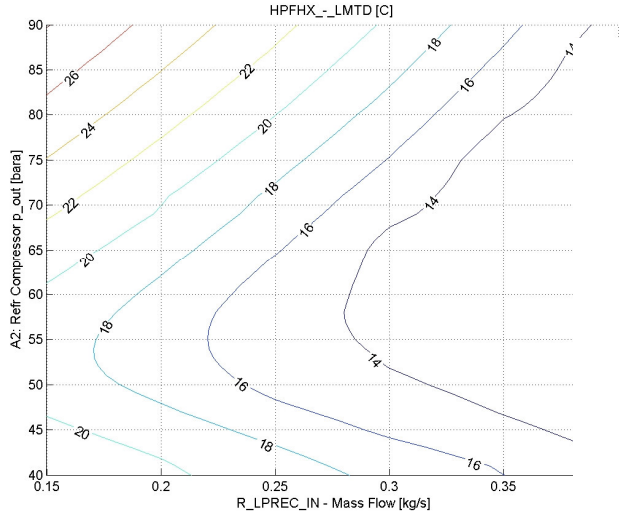


Figure D.14: HPFHX: LMTD

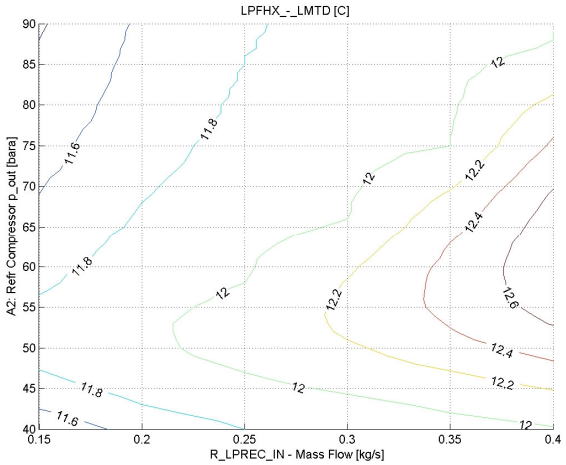


Figure D.15: LPFHX: LMTD

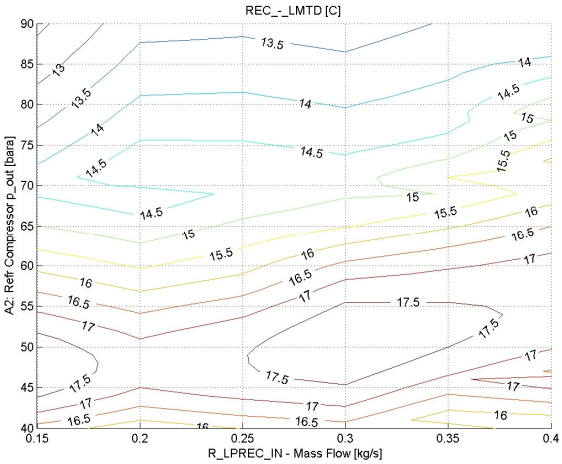


Figure D.16: REC: LMTD

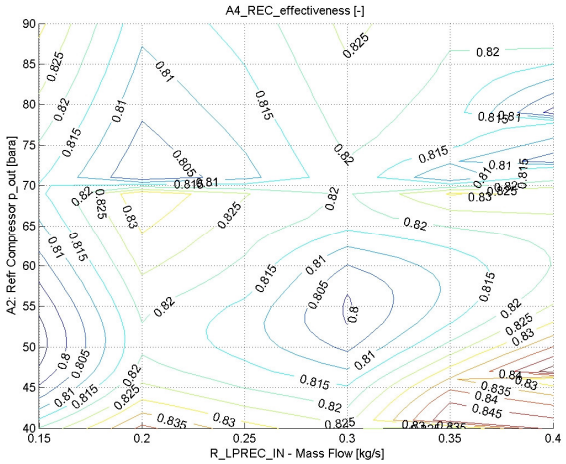


Figure D.17: REC: Effectiveness

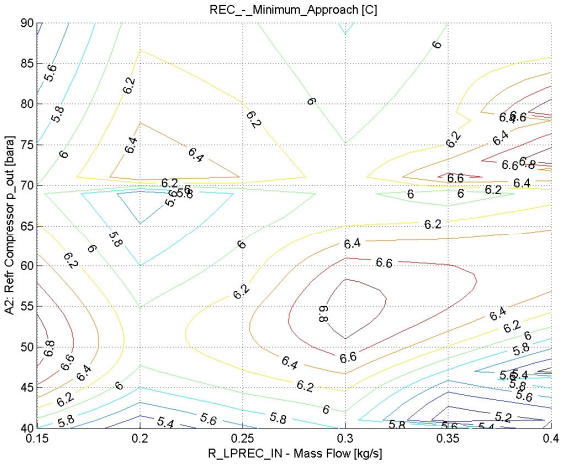


Figure D.18: REC: MITA

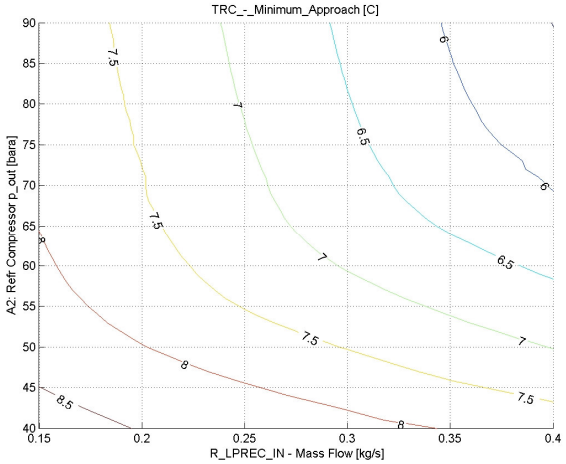


Figure D.19: TRC: MITA

### D.3.2 Case D-50 % NCR

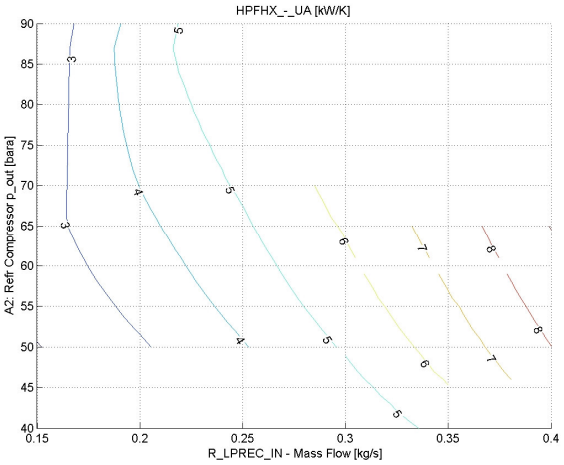


Figure D.20: HPFHX: UA

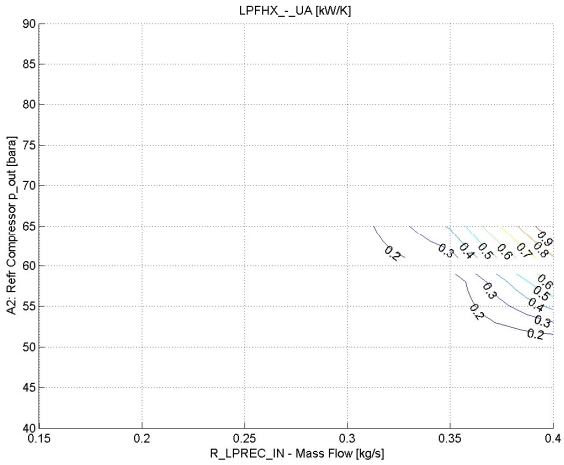


Figure D.21: LPFHX: UA

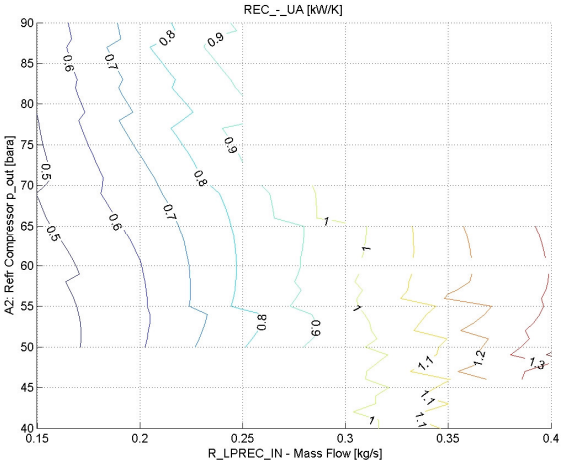


Figure D.22: REC: UA

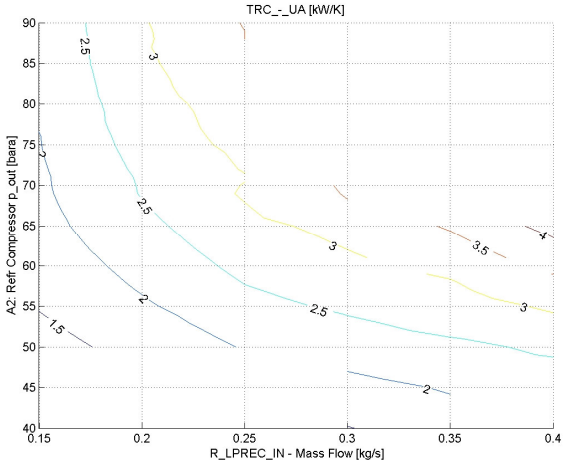


Figure D.23: TRC: UA

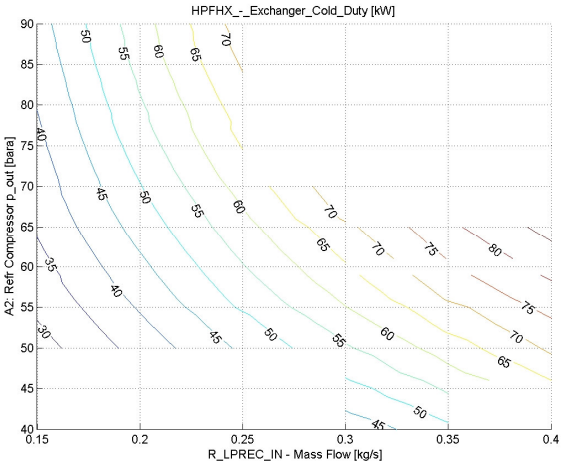


Figure D.24: HPFHX: Duty

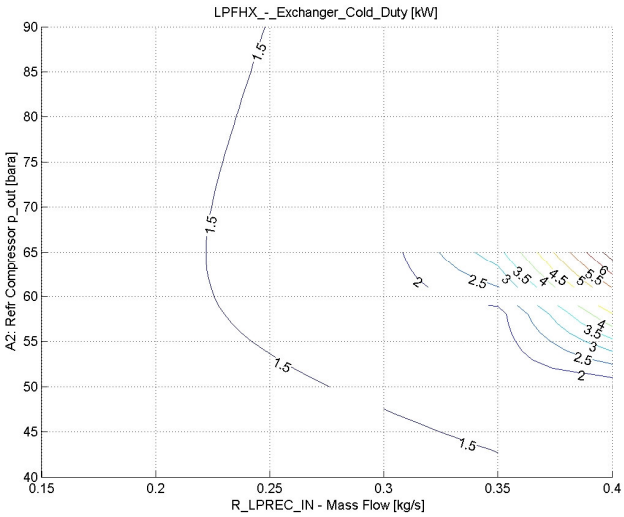


Figure D.25: LPFHX: Duty

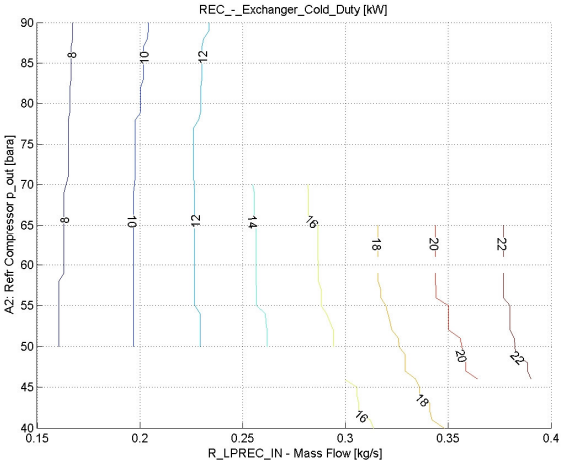


Figure D.26: REC: Duty

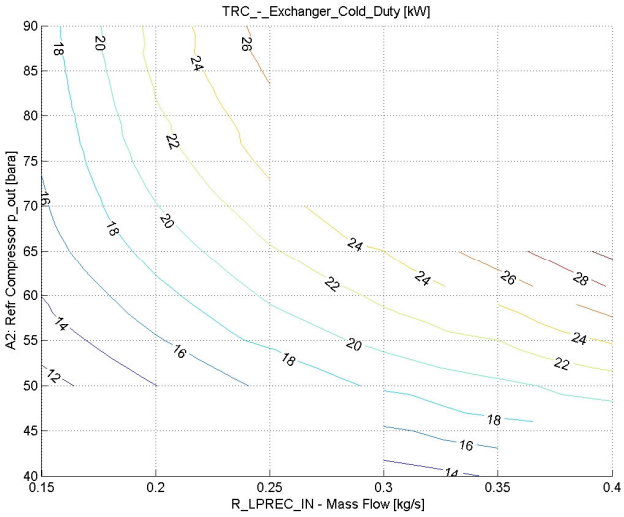


Figure D.27: TRC: Duty

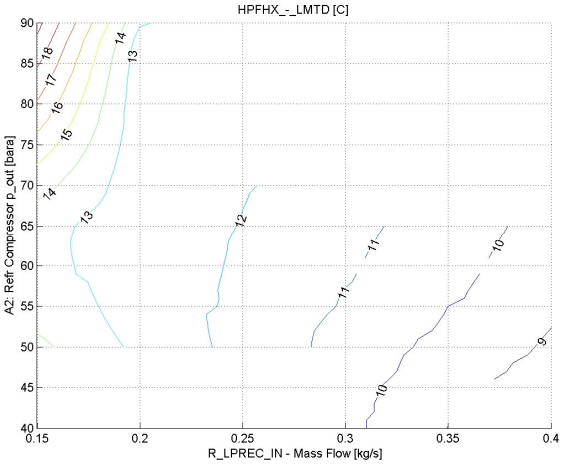


Figure D.28: HPFHX: LMTD

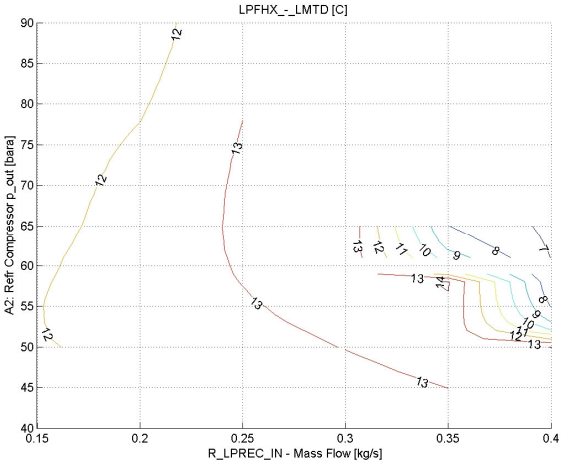


Figure D.29: LPFHX: LMTD

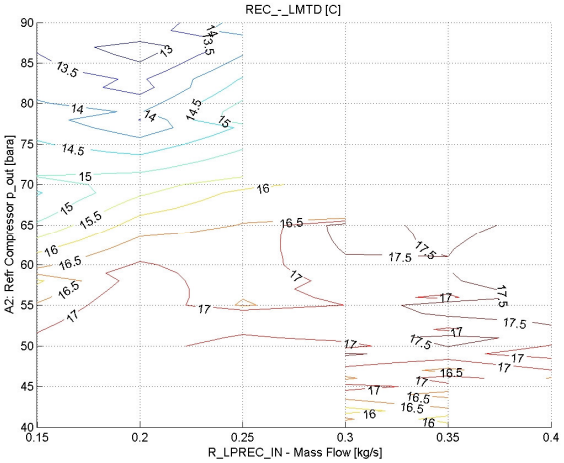


Figure D.30: REC: LMTD

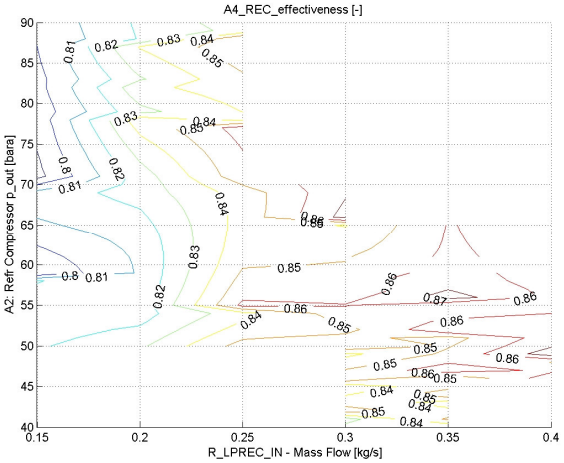


Figure D.31: REC: Effectiveness

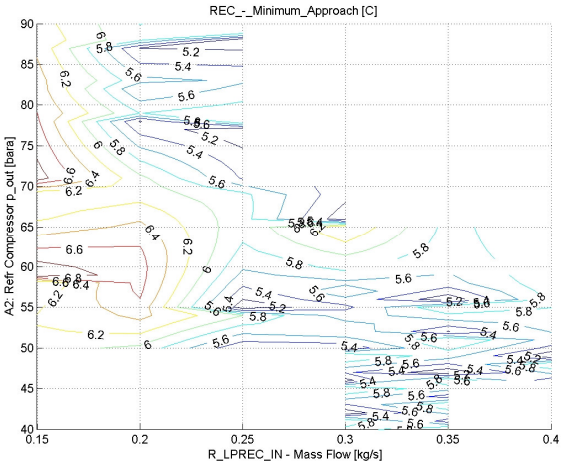


Figure D.32: REC: MITA

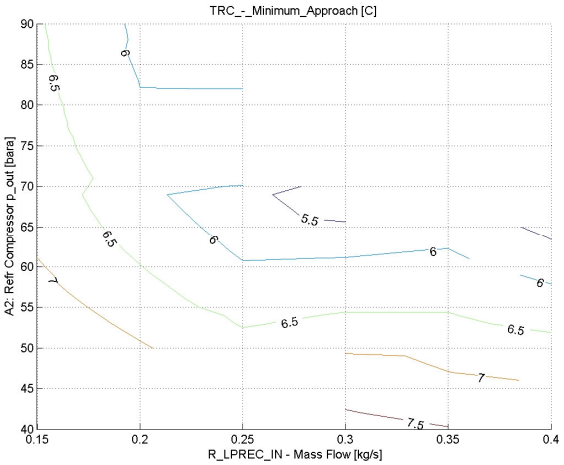


Figure D.33: TRC: MITA

### D.3.3 Case D-20 % NCR

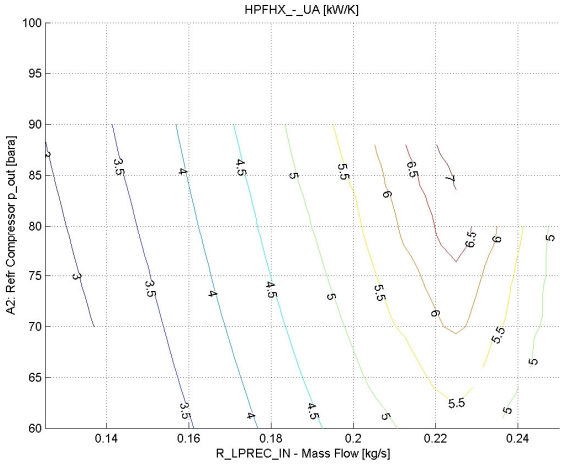


Figure D.34: HPFHX: UA

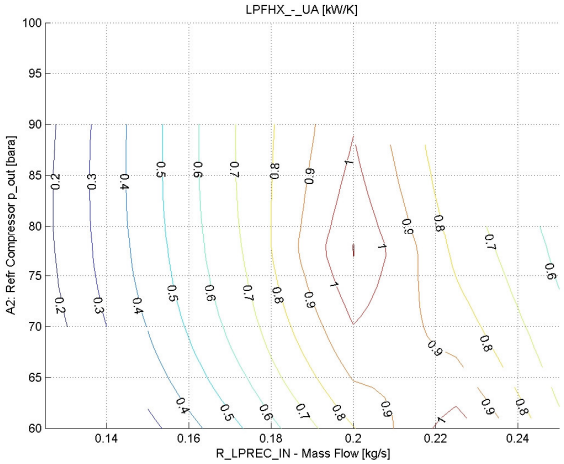


Figure D.35: LPFHX: UA

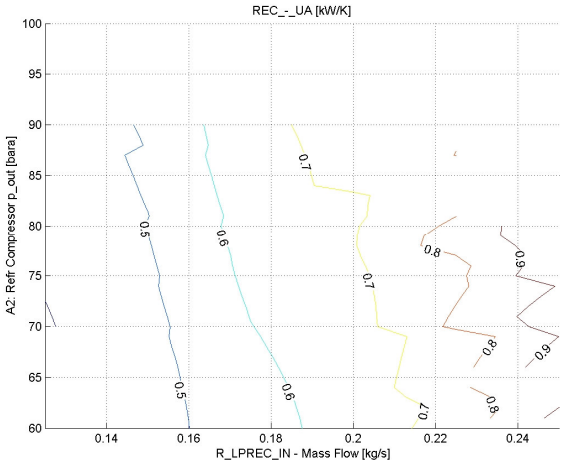


Figure D.36: REC: UA

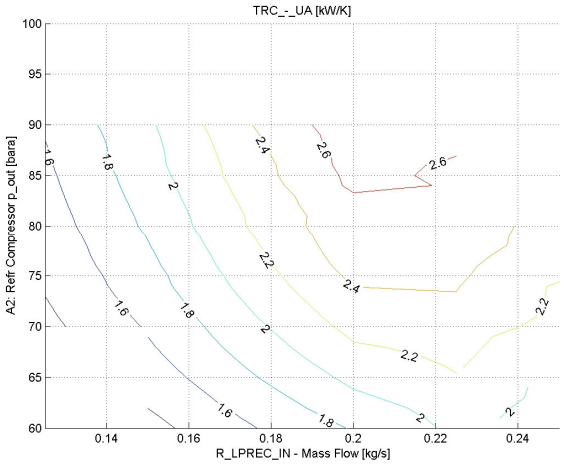


Figure D.37: TRC: UA

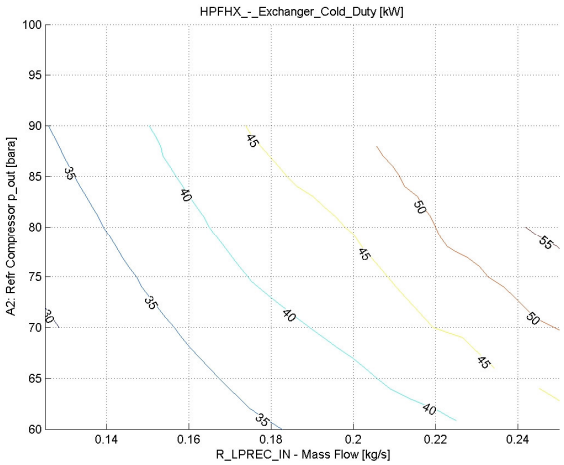


Figure D.38: HPFHX: Duty

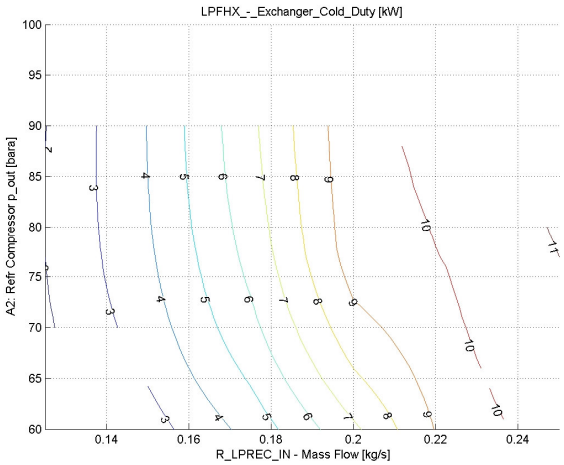


Figure D.39: LPFHX: Duty

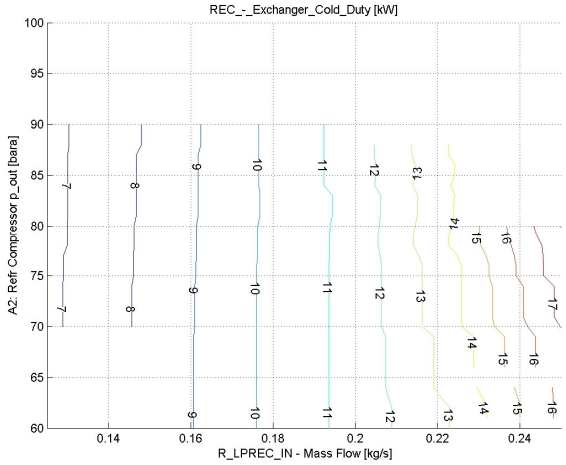


Figure D.40: REC: Duty

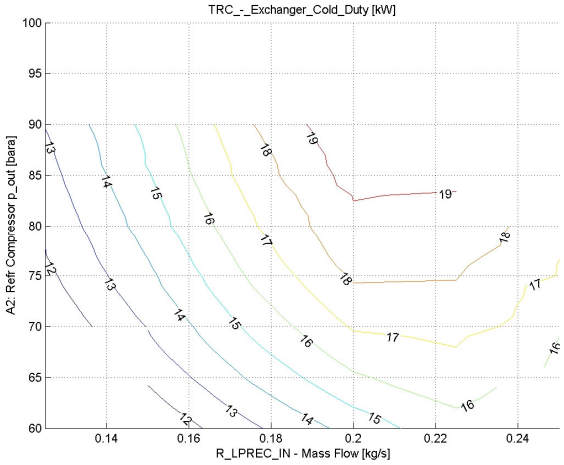


Figure D.41: TRC: Duty

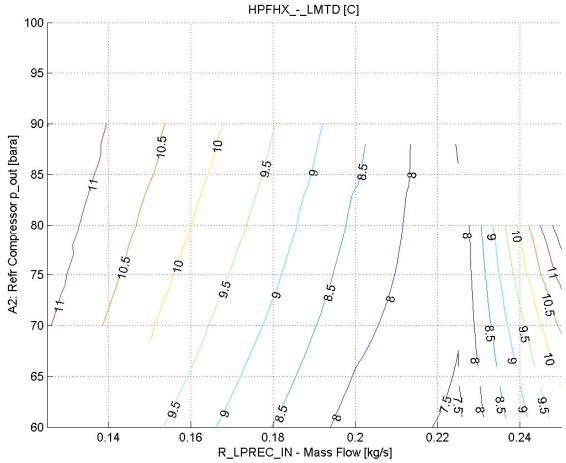


Figure D.42: HPFHX: LMTD

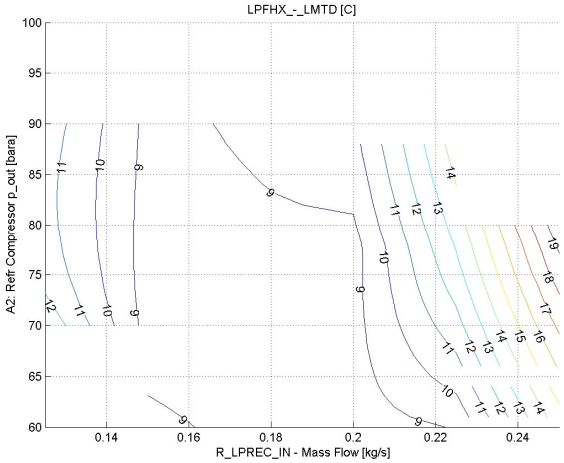


Figure D.43: LPFHX: LMTD

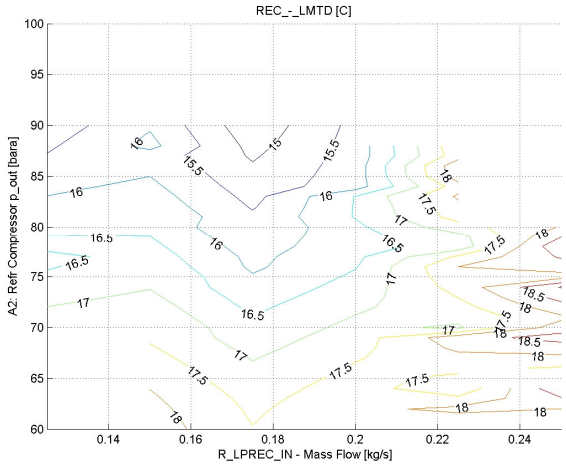


Figure D.44: REC: LMTD

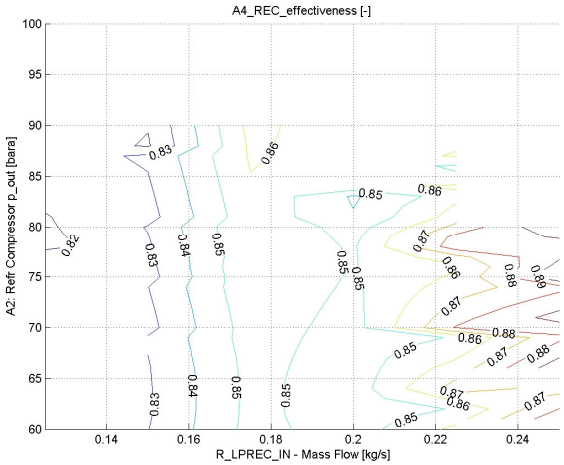


Figure D.45: REC: Effectiveness

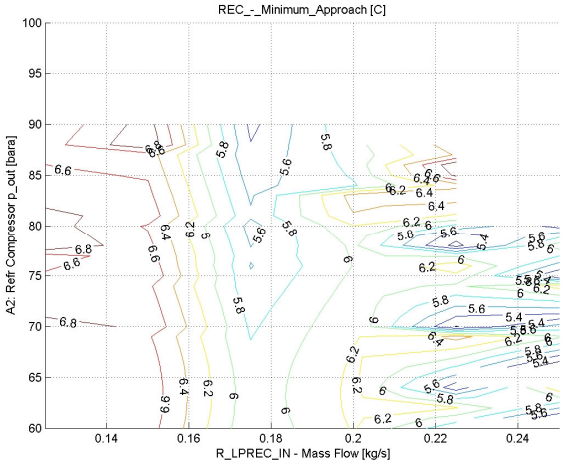


Figure D.46: REC: MITA

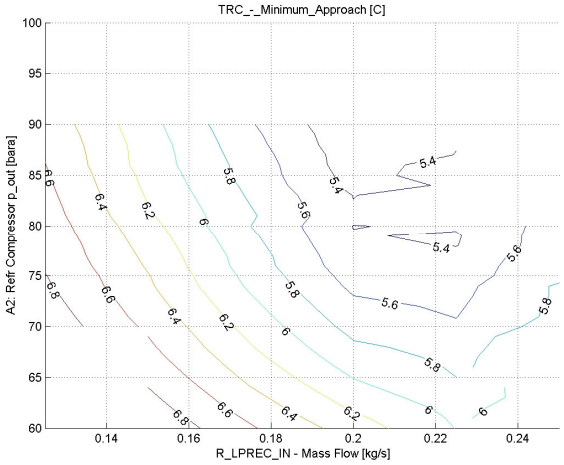


Figure D.47: TRC: MITA

### D.3.4 Case D-0 % NCR - 100% Auxiliary Normal Load

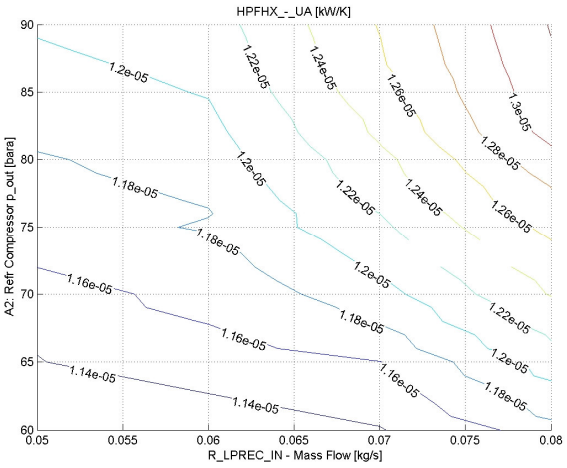


Figure D.48: HPFHX: UA

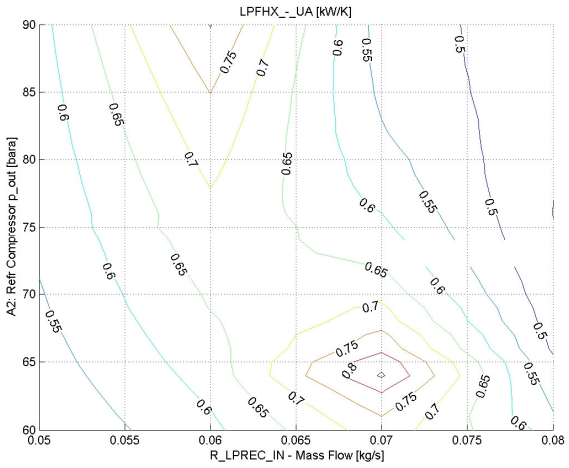


Figure D.49: LPFHX: UA

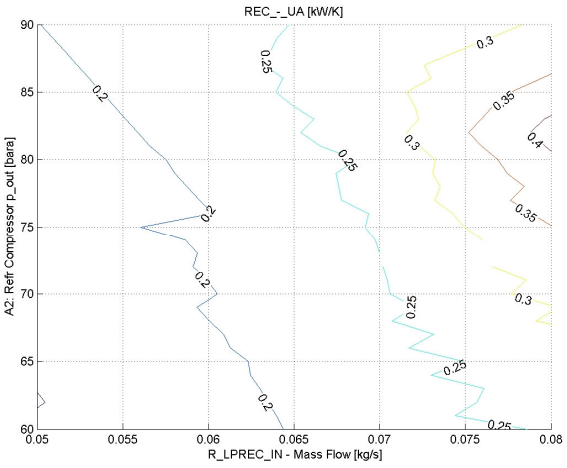


Figure D.50: REC: UA

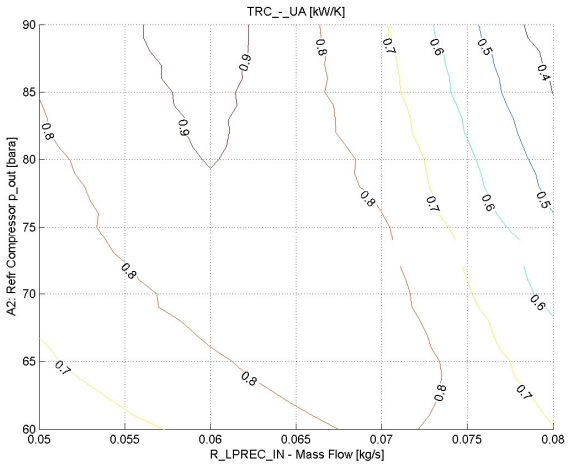


Figure D.51: TRC: UA

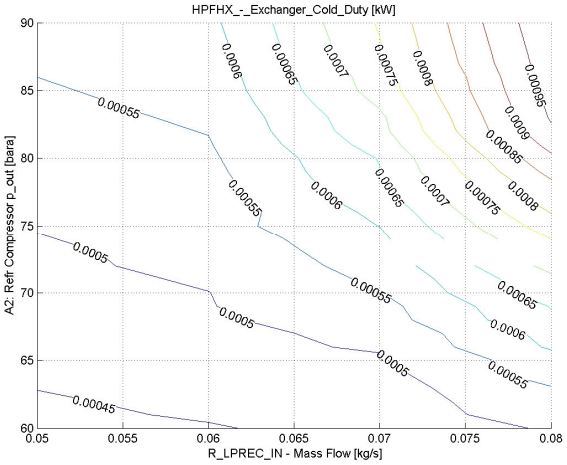


Figure D.52: HPFHX: Duty

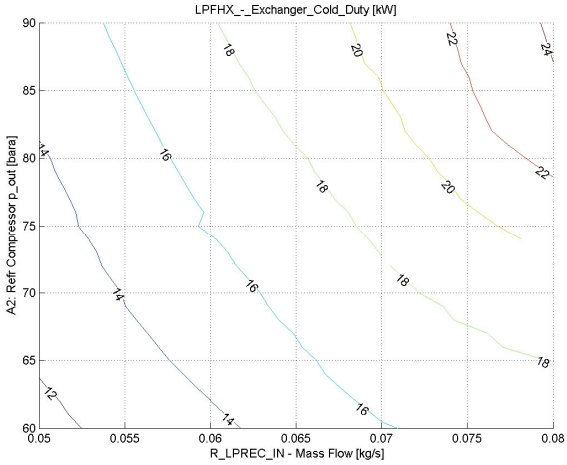


Figure D.53: LPFHX: Duty

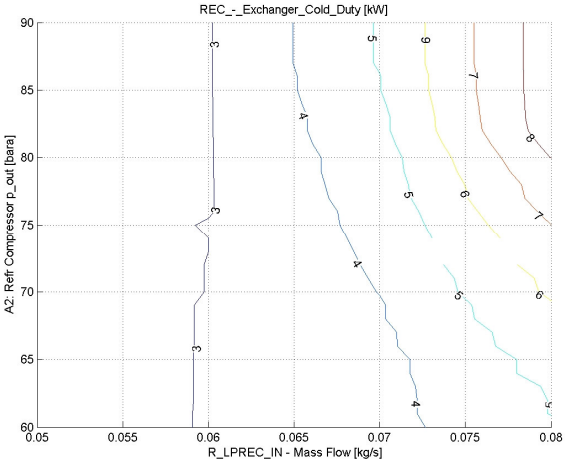


Figure D.54: REC: Duty

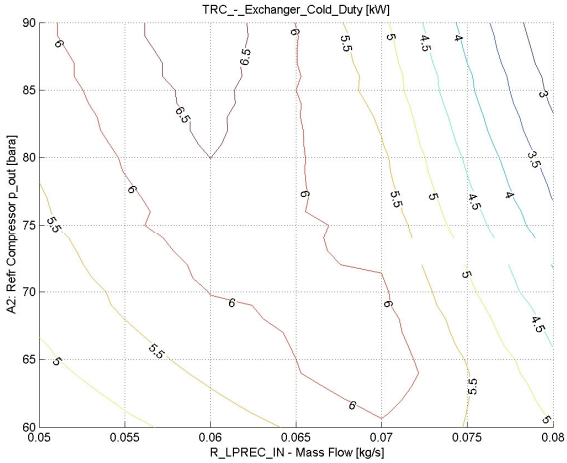


Figure D.55: TRC: Duty

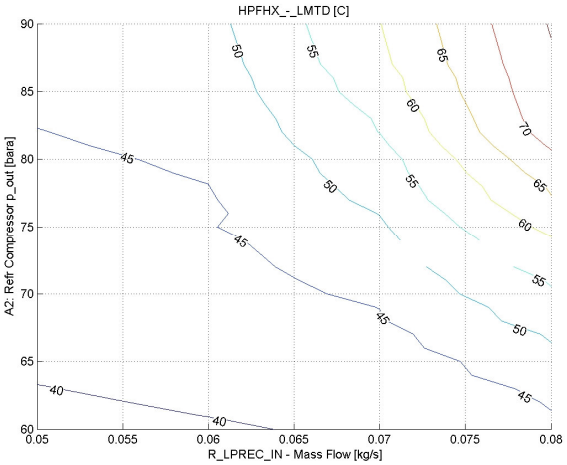


Figure D.56: HPFHX: LMTD

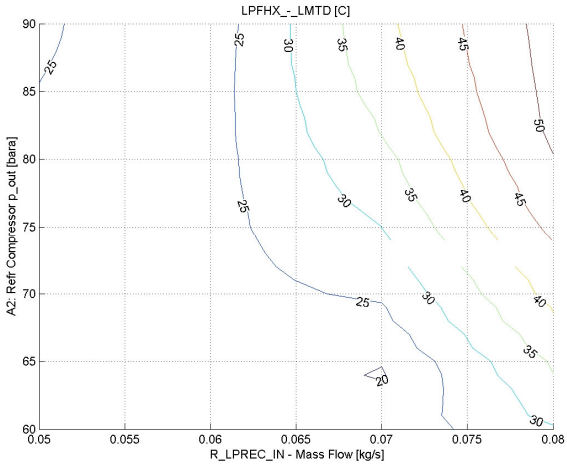


Figure D.57: LPFHX: LMTD

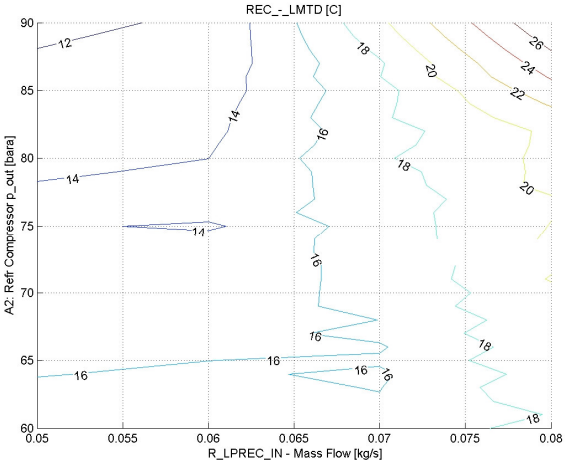


Figure D.58: REC: LMTD

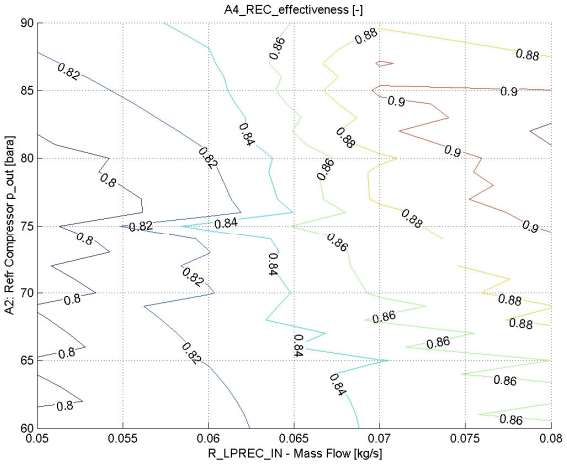


Figure D.59: REC: Effectiveness

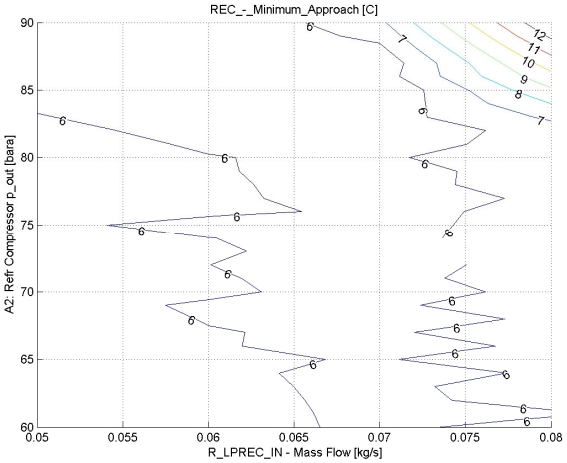


Figure D.60: REC: MITA

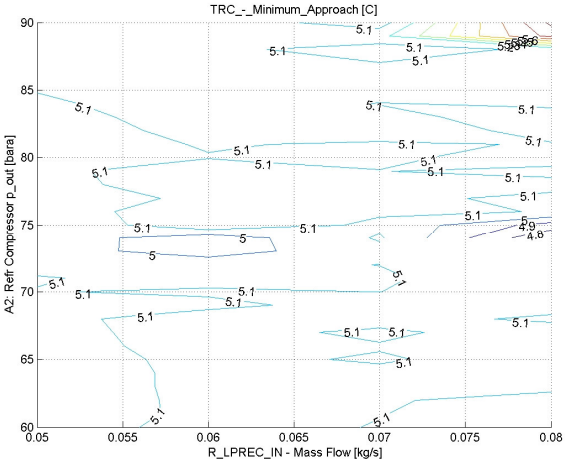


Figure D.61: TRC: MITA

# D.4 Sensitivity Analyses

## D.4.1 Case D-100 % NCR

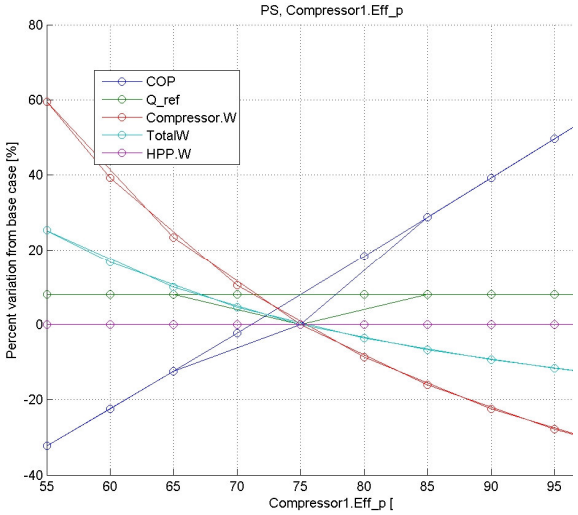


Figure D.62: Refrigerant Compressor polytropic efficiency

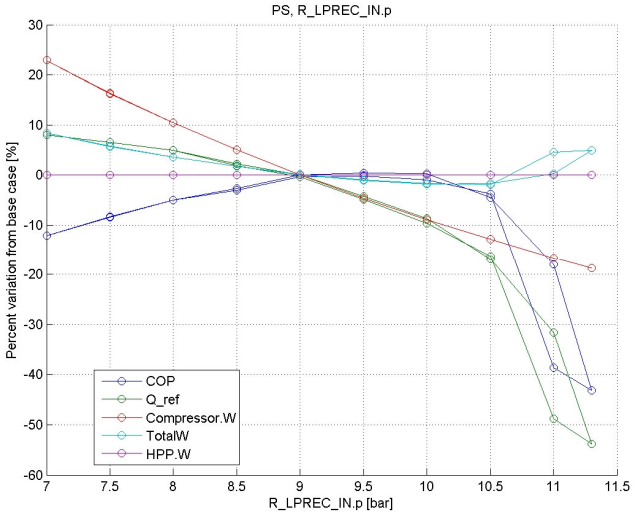


Figure D.63: Evaporation pressure (R-LPREC-IN)

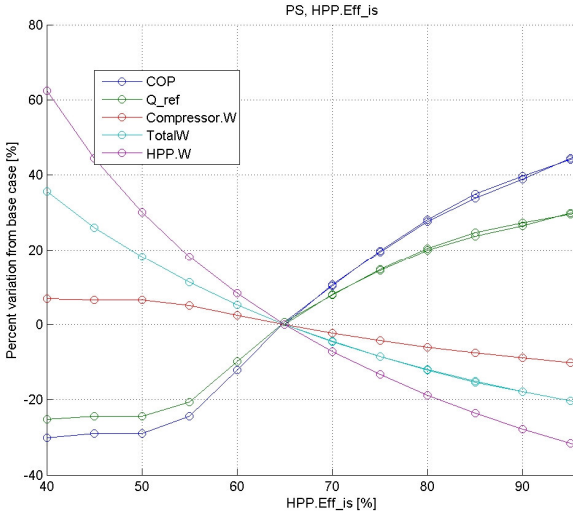


Figure D.64: HP Pump efficiency

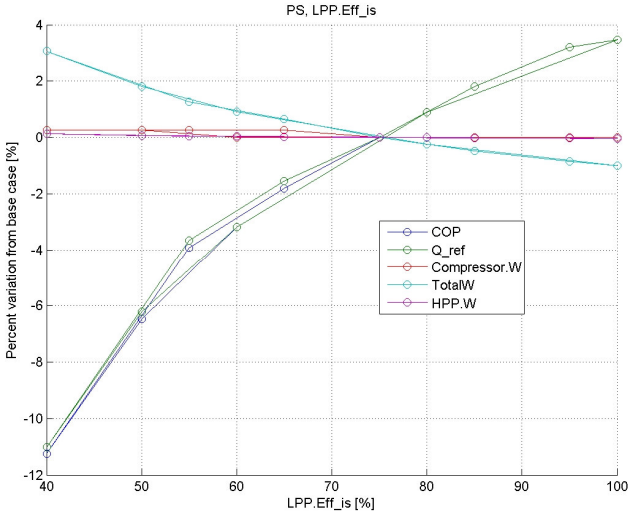


Figure D.65: LP Pump efficiency

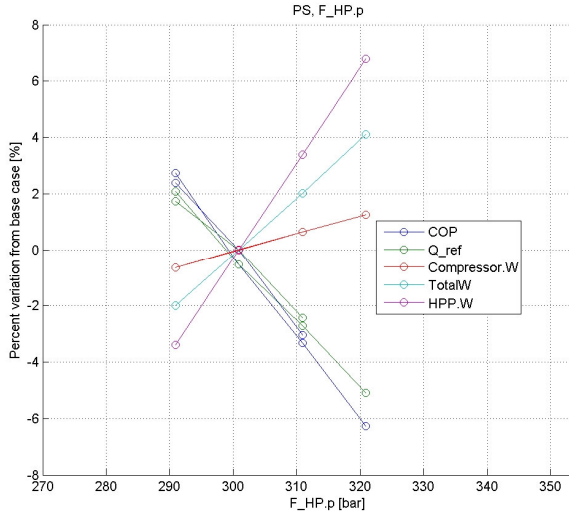


Figure D.66: HP Fuel pressure

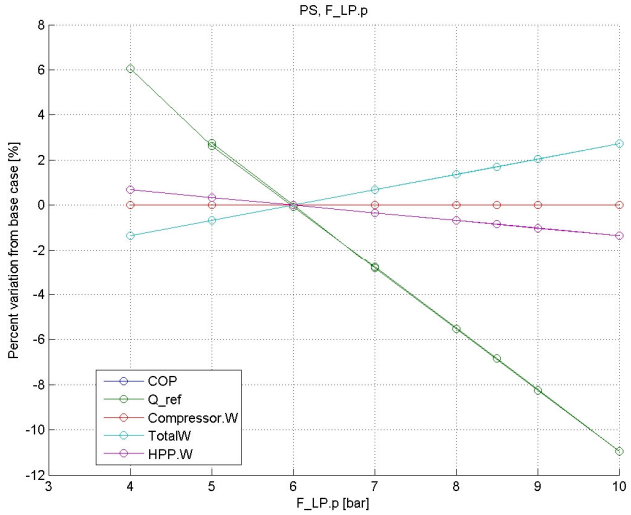


Figure D.67: LP Fuel pressure

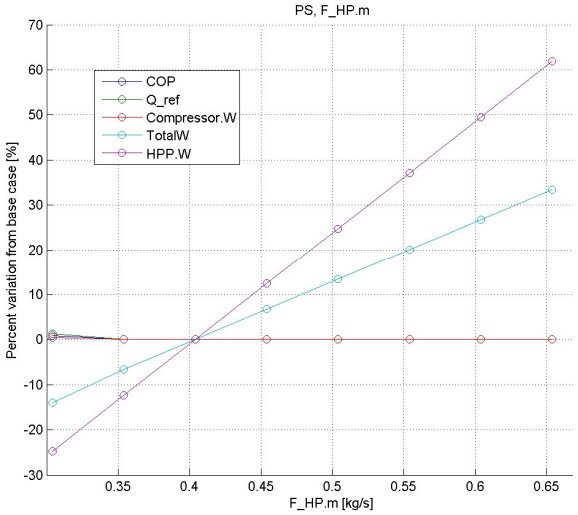


Figure D.68: HP Fuel flowrate

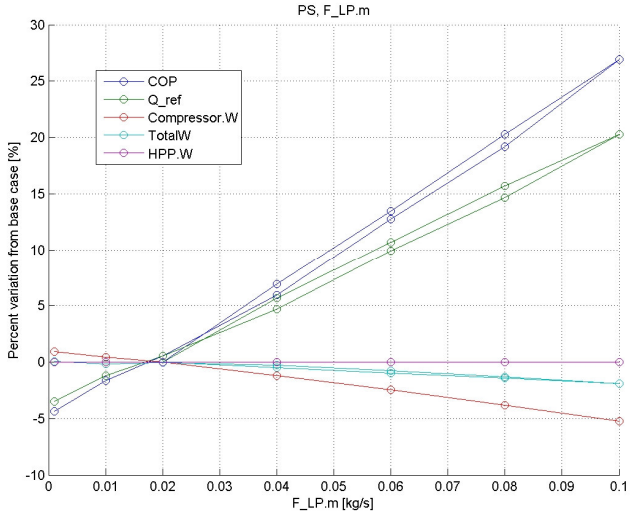


Figure D.69: LP Fuel flowrate

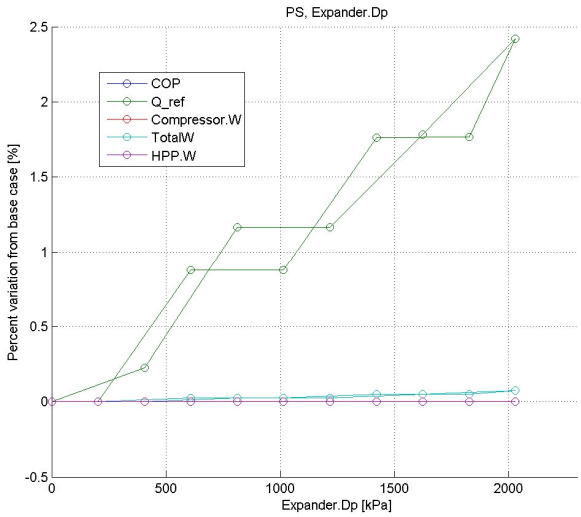


Figure D.70: Expander pressure difference (efficiency=60%)

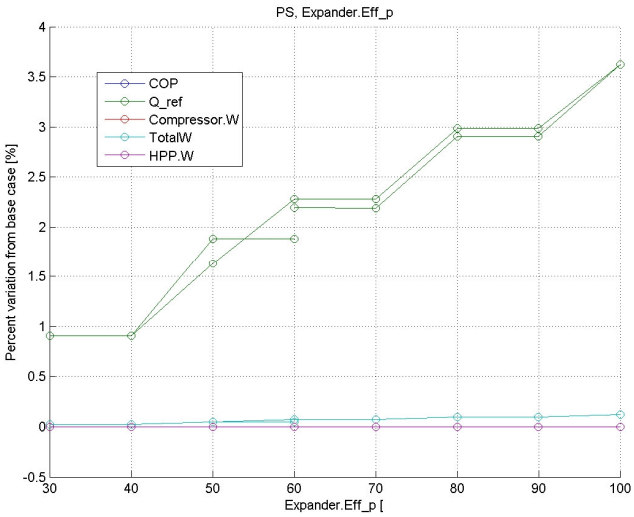


Figure D.71: Expander efficiency (Expander pressure drop=2030kPa)

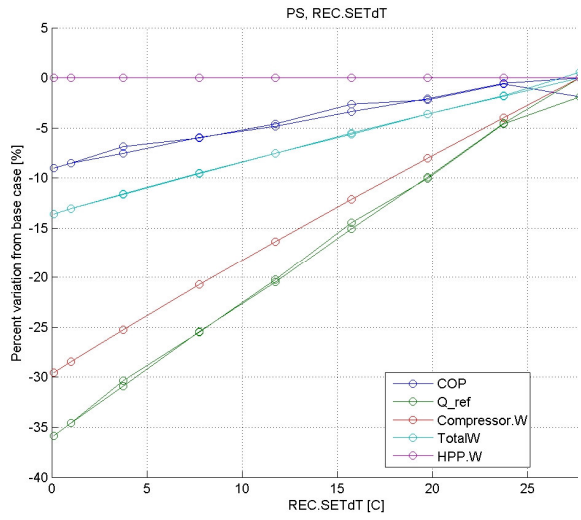


Figure D.72: REC Temperature increase on the LP side

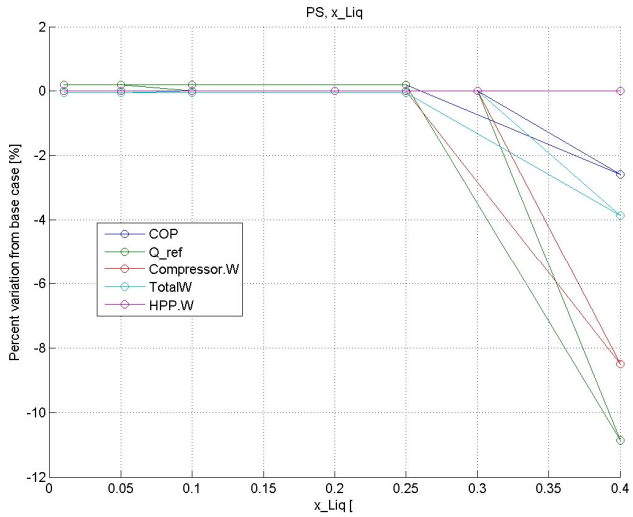


Figure D.73: TRC outlet liquid fraction

# Bibliography


[1] Pierre Sames. Costs and benefits of lng as a ship fuel for container vessels. Technical report, Germanischer Lloyd, 2011.

[2] Meike Baumgart. Lng-fueled vessels in the norwegian short-sea market. Master's thesis, Norges Handeleshoyskole, 2010.

[3] Fabio Burel, Rodolfo Taccani, and Nicola Zulian. Improving sustainability of maritime transport through utilization of liquefied natural gas (lng) for propulsion. *Energy*, 57:412–420, August 2013.

[4] Jerzy Herdzik. Lng as a marine fuel, possibilities and problems. *Journal of KONES Powertrain and Transport*, 18(2), 2011.

[5] MAN. Man diesel and turbo website, 0.

[6] Dag Stenersen. Master thesis supervision. personal communication, 2014.

[7] Witherby. *LNG Shipping Knowledge*. Witherby Seamanship International Ltd, 2011.

[8] Vilmar Aesoy, Per Magne Einang, Dag Stenersen, Erik Hennie, and Ingebrigt Valberg. Lng-fuelled engines and fuel systems for medium-speed engines in maritime applications. *JSAE*, 2011.

[9] TGE. Efficient, low cost lng bog handling by integration of cascade liquefaction and laby-gi fuel gas compressor for me-gi propulsion system. In *Gastech*, May 2009. Abu Dhabi.

[10] R P Sinha and Wan Mohd Norsani Wan Nik. Investigation of propulsion system for large lng ships. In *1st International Conference on Mechanical Engineering Research 2011*, 2011.

[11] Denis Griffiths. *Marine low speed diesel engines*. Institute of Marine Engineers, Science and Technology, 2006.

[12] Wartsila. Wartsila 2-stroke low pressure dual-fuel engines. Wartsila Ship Power Business White Paper, 2013.

[13] J. Romero Gomez, M. Romero Gomez, R. Ferreiro Garcia, and A. De Miguel Catoira. On board lng reliquefaction technology: a comparative study. *Polish Maritime Research*, 21:77–88, 2014.

[14] Addy Majewski. Dieselnet technology guide, 2006.

[15] Richard Gilmore, Stavros Hatzigrigoris, Steve Mavrakis, Andreas Spertos, and Antonis Vordonis. Lng carrier alternative propulsion systems. Technical report, SNAME GREEK SECTION, February 2005.

[16] JungHan Lee, Jin Yeol Yu, John Linwood, and Martin Fux. New generation lngc with 2 stroke gas engine and innovative re-liquefaction system. In *Gastech Conference and Exibition*. DSME, Burckhardt Compression, October 2012.

[17] Per Magne Einang. The norwegian lng ferry. In *Natural Gas Vehicle*, 2000.

[18] George Teriakidis. Lng as fuel - recent development. Technical report, DNVGL, february 2014.

[19] Mogens Schroder Bech. North european lng infrastructure project - baseline report. Technical report, Danish Maritime Authority, october 2011.

[20] Lars Petter Blikom. The only thing that matters is cost of fuel, November 2011.

[21] Nitin Sharma. Lng fuelled container vessel. Slideshare, 2014.

[22] Jeong Hwan Kim and Joong Hyo Choi. Structural development of lng fueled large container ship. In *ASME 2013 32nd International Conference on Ocean, Offshore and Arctic Engineering*, June 2013.

[23] Vilmar Aesoy and Dag Stenersen. Low emission lng fuelled ships for evnvironmental friendly operations in artic areas. In *Proceedings of the ASME 2013 32nd International Conference on Ocean, Offshore and Arctic Engineering*, OMAE2013-11644, June 2013.

[24] Samsung. Gas fuelled ship. Technical report, Samsung Heavy Industries, december 2010. for DNV.

[25] MAN. 45000 m3 lng tanker engine application. Technical report, MAN Diesel Turbo, january 2013. rev0.

[26] MAN. Lng carrier propulsion by me engines and reliquefaction, 0.

[27] Gerd-Michael Wursig. Lng fuel tank, benefits and challenges. In *Small Scale LNG Norway*, June 2013. DNV.

[28] MAN. Me-gi dual fuel, a technical, operational and cost-effective solution for ships fuelled by gas. Copenhagen, Denmark, 0.

[29] Hamworthy. Lng systems for marine application, lng reliquefaction and lng regasification, 2014.

[30] Cryostar. The cryostar magazine, special report reliquefaction system ecorel, 2007.

[31] Geir Skaugen. Liquefaction of natural gas. how can fundamental rd help the industry? case studies from gts. In *6th Annual LNG TECH Global Summit*. SINTEF Energy Research, 2011.

[32] P. Neksa, E. Brendenga, M. Dreschera, and B. Norberg. Development and analysis of a natural gas reliquefaction plant for small gas carriers. *Journal of Natural Gas Science and Engineering*, 2:143–149, 2010.

[33] IM Skaugen. Small scale lng - multigas carriers, 0.

[34] Petter Neksa. Master thesis supervision. personal communication, 2014.

[35] MAN. Lng carriers with me-gi engine and high pressure gas supply system, 2007.

[36] Hyundai. Hhi-fgss for me-gi engine (for proposal). Technical report, Hyundai Heavy Industries Co., Ltd, Engine & Machinery Division, May 2012.

[37] Chansaem Park, Kiwook Song, Sangho Lee, Youngsub Lim, and Chonghun Han. Retrofit design of a boil-off gas handling process in liquefied natural gas receiving terminals. *Energy*, 44:69–78, 2012.

[38] Eirik Melaaen. Fuel gas handling system and bog reliquefaction for lng carrier. In *Two stroke debut of dual fuel engine*. Wartsila, 2013.

[39] Jorn Magnus Jonas. A plant comprising a tank for storing of liquid natural gas (lng) as marine fuel, 2011.

[40] Jorn Magnus Jonas. Master thesis supervision. personal communication, 2014.

[41] MAN. Basic principles of ship propulsion, 2004.

[42] Maritime Connector. Ship sizes, 2007.

[43] MAN. *Marine Engine IMO Tier II Programme 2014*. MAN Diesel Turbo, 2014.

[44] MAN. *MAN B&W 98-50 ME/ME-C-TII Type Engines Engine Selection Guide*. MAN Diesel Turbo, 1 edition, June 2010.

[45] Cryostar. The cryostar magazine, 2008.

[46] Christos Frangopoulos George Dimopoulos. A dynamic model for liquefied natural gas evaporation during marine transportation. *International Journal of Thermodynamics*, 11(3):123–131, September 2008.

[47] Jostein Pettersen. Tep 4185 natural gas technology - course compendium, 2013.

[48] Aspen. *Aspen HYSYS V8.3 User Guide*. Aspen Technology, Inc., August 2013.

[49] Eric C. Carlson. Don t gamble with physical properties for simulations. *Chemical Engineering Progress*, 1996. Aspen Technology, Inc.

[50] Gadhiraju Venkatarathnam. *Cryogenic Mixed Refrigerant Processes*. Springer, 2008.

[51] S. Mokhatab, J. Y. Mak, J. V. Valappil, and D. A. Wood. *Handbook of LNG*. Bostn Gulf Professional Publishing, 2014. Chapter 1 - LNG Fundamentals.

[52] Abdullah Alabdulkarema, Amir Mortazavia, Yunho Hwanga, Reinhard Radermachera, and Peter Rogers. Optimization of propane pre-cooled mixed refrigerant lng plant. *Applied Thermal Engineering*, 2011.

[53] J Sarkar, Souvik Bhattacharyya, and M Ram Gopal. Optimization of a transcritical co2 heat pump cycle for simultaneous cooling and heating applications. *International Journal of Refrigeration*, 2004.

[54] F Kauf. Determination of the optimum high pressure for transcritical co2 refrigeration cycles. *International Journal of Thermal Sciences*, 38, 1999.

[55] S M Liao, T S Zhao, and A Jakobsen. A correlation of optimal heat rejection pressures in transcritical carbon dioxide cycles. *Applied Thermal Engineering*, 20, 2000.

[56] D M Robinson and E A Groll. Efficiencies of transcritical co2 cycles with and without an expansion turbine. *International Journal of Refrigeration*, 21, 1998.

[57] Rush and Hall. Tutorial on cryogenic submerged electric motor pumps. In *Proceedings of the 18th International Pump Users Symposium*. EBARA International Corporation, 2001.

[58] Jeff Gumbrell. Application and adaptation of traditional lng pump technology for the growing small-scale lng market. In *8th annual LNG Tech global summit*. EBARA, 2013.

[59] Coyle and Patel. Processes and pump services in the lng industry. In *Proceedings of the Twenty-second International Pump User Symposium*. KBR, 2005.

[60] Peter Ernst. The lng bog labyrinth-piston compressor with flexible capacity control. In *Gastech Houston*. Sulzer-Burckhardt, 2000.

[61] unknown. internet search, 2014.

[62] Ohama, Kurioka, Tanaka, and Koga. Process gas applications where api 619 screw compressors replaced reciprocating and centrifugal compressors. In *Proceedings of the 35th turbomachinery symposium*, September 2006.

[63] Sven Erik Brink. Single shaft turbocompressors for bog recovery in lng terminals. Siemens AG Energy, 2010.

[64] Burckhardt. Laby compressors - contactless labyrinth sealing for highest availability, 2014.

[65] Mario Imberti. Personal comunication. reference person in SIAD, 2014.

[66] Nakoi Akamo. Process critical compressors. *LNG Industry*, 2008. Kobe Steel Ltd.

[67] EFRC. European forum of reciprocating compressors, 2014.

[68] Andreas Norberg. Master thesis supervision. personal communication, 2014.

[69] L Tavian. Large cryogenic systems at 1.8 k. In *European Particle Accelerator Conference*, 2000.

[70] Klaus D. Timmerhaus and Richard Reed. *Cryogenic Engineering: Fifty Years of Progress*. Springer, 2006.

[71] Warren D. Seider, J.D. Seader, and Daniel R. Lewin. *Product and Process Design Principles: Synthesis, Analysis, and Evaluation*. Wiley, 2004.

[72] V. Mulyandasari A. L. Ling. Heat exchanger selection and sizing (engineering design guideine). Technical report, KLM Technology Group, 2010.

[73] Lars Greitsch, Georg Eljardt, and Stefan Krueger. Operating conditions aligned ship design and evaluation. In *First International Symposium on Marine Propulsors, Trondheim*. Hamburg University of Technology (TUHH), June 2009.